1990-12

Robust path tracking of autonomous underwater vehicles using sliding modes

Chism, Steven R.

Monterey, California: Naval Postgraduate School

(2)

NAVAL POSTGRADUATE SCHOOL
Monterey, California

THESIS

Robust Path Tracking of Autonomous
Underwater Vehicles Using Sliding Modes

by

Steven R. Chism

December 1990

Thesis Advisor: Fotis A. Papoulias

UNCLASSIFIED
SECURITY CLASSIFICATION OF THIS PAGE

REPORT DOCUMENTATION PAGE

Form Approved
OMB No. 0704-0188

1a REPORT SECURITY CLASSIFICATION: UNCLASSIFIED	1b RESTRICTIVE MARKINGS
2a SECURITY CLASSIFICATION AUTHORITY	3 DISTRIBUTION / AVAILABILITY OF REPORT: APPROVED FOR PUBLIC RELEASE; DISTRIBUTION IS UNLIMITED.
2b DECLASSIFICATION / DOWNGRADING SCHEDULE	
4 PERFORMING ORGANIZATION REPORT NUMBER(S)	5 MONITORING ORGANIZATION REPORT NUMBER(S)
6a NAME OF PERFORMING ORGANIZATION: NAVAL POSTGRADUATE SCHOOL; 6b OFFICE SYMBOL (If applicable): ME	7a NAME OF MONITORING ORGANIZATION: NAVAL POSTGRADUATE SCHOOL
6c. ADDRESS (City, State, and ZIP Code): MONTEREY, CA 93943-5000	7b ADDRESS (City, State, and ZIP Code): MONTEREY, CA 93943-5000
8a NAME OF FUNDING SPONSORING ORGANIZATION; 8b OFFICE SYMBOL (If applicable)	9 PROCUREMENT INSTRUMENT IDENTIFICATION NUMBER
8c. ADDRESS (City, State, and ZIP Code)	10 SOURCE OF FUNDING NUMBERS: PROGRAM ELEMENT NO; PROJECT NO; TASK NO; WORK UNIT ACCESSION NO

11 TITLE (Include Security Classification)
ROBUST PATH TRACKING OF AUTONOMOUS UNDERWATER VEHICLES USING SLIDING MODES

12. PERSONAL AUTHOR(S) CHISM, STEVEN R.

13a TYPE OF REPORT	13b TIME COVERED	14 DATE OF REPORT (Year, Month, Day)	15 PAGE COUNT
MECHANICAL ENGINEER	FROM _____ TO _____	DECEMBER 1990	158

16 SUPPLEMENTARY NOTATION THE VIEWS EXPRESSED IN THIS THESIS ARE THOSE OF THE AUTHOR AND DO NOT REFLECT THE OFFICIAL POLICY OR POSITION OF THE DEPARTMENT OF DEFENSE OR THE U.S.

17 COSATI CODES			18 SUBJECT TERMS (Continue on reverse if necessary and identify by block number)
FIELD	GROUP	SUB-GROUP	AUTONOMOUS, UNDERWATER VEHICLES, AUV, GUIDANCE, CONTROL

19 ABSTRACT (Continue on reverse if necessary and identify by block number)

Accurate track keeping of auntonomous underwater vehicles is necessary for the autonomous navigation of a vehicle through confined spaces, and in the presence of obstacles and cross-current environments. Uncertainties in the force coefficients and environmental disturbances, as well as the required accuracy lead to the need for a robust sliding mode control for successful vehicle operations. This thesis investigates the use of a cross track error guidance law with a sliding mode compensator and presents results based on computer simulations using a nonlinear dynamic model of the Swimmer Delivery Vehicle. Steady state errors and stability requirements are evaluated analytically for a given current speed and direction, and are confirmed through numerical integrations. The use of integral control and disturbance estimation and compensation methods are developed in order to achieve the desired steady state accuracy. A leading track control monitoring technique is used to eliminate track overshoot during turning and reduce the rudder activity. Finally, the effects of measurement noise are evaluated and guidelines are developed for suppressing them.

20 DISTRIBUTION / AVAILABILITY OF ABSTRACT	21 ABSTRACT SECURITY CLASSIFICATION
☒ UNCLASSIFIED/UNLIMITED ☐ SAME AS RPT ☐ DTIC USERS	UNCLASSIFIED
22a NAME OF RESPONSIBLE INDIVIDUAL: Fotis A. Papoulias	22b TELEPHONE (Include Area Code): 408 646 3381; 22c OFFICE SYMBOL: MEPa

DD Form 1473, JUN 86 — Previous editions are obsolete — S/N 0102-LF-014-6603 — SECURITY CLASSIFICATION OF THIS PAGE: UNCLASSIFIED

Approved for public release; distribution is unlimited.

Robust Path Tracking of Autonomous
Underwater Vehicles Using Sliding Modes

by

Steven R. Chism
Lieutenant, United States Navy
B.S., University of Southern California

Submitted in partial fulfillment
of the requirements for the degree of

MASTER OF SCIENCE IN MECHANICAL ENGINEERING
and
MECHANICAL ENGINEER

from the

NAVAL POSTGRADUATE SCHOOL
December 1990

Author: [redacted]
Steven R. Chism

Approved by: [redacted]
Fotis A. Papoulias, Thesis Advisor

[redacted]
Anthony J. Healey, Chairman
Department of Mechanical Engineering

[redacted]
DEAN OF FACULTY
AND GRADUATE STUDIES

ABSTRACT

Accurate track keeping of auntonomous underwater vehicles is necessary for the autonomous navigation of a vehicle through confined spaces, and in the presence of obstacles and cross-current environments. Uncertainties in the force coefficients and environmental disturbances, as well as the required accuracy lead to the need for a robust sliding mode control for successful vehicle operations. This thesis investigates the use of a cross track error guidance law with a sliding mode compensator and presents results based on computer simulations using a nonlinear dynamic model of the Swimmer Delivery Vehicle. Steady state errors and stability requirements are evaluated analytically for a given current speed and direction, and are confirmed through numerical integrations. The use of integral control and disturbance estimation and compensation methods are developed in order to achieve the desired steady state accuracy. A leading track control monitoring technique is used to eliminate track overshoot during turning and reduce the rudder activity. Finally, the effects of measurement noise are evaluated and guidelines are developed for suppressing them.

TABLE OF CONTENTS

I. INTRODUCTION 1

A. BACKGROUND 1

B. OBJECTIVE OF THIS THESIS 2

C. THESIS OUTLINE 3

II. EQUATIONS OF MOTION AND SLIDING PLANE DEVELOPMENT . 5

A. INTRODUCTION 5

B. EQUATIONS OF MOTION 5

C. SLIDING PLANE AND GAIN COEFFICIENT DEVELOPMENT 8

1. Pole Placement Method 8

2. Coordinate Transformation with Pole Placement Method 12

3. Linear Quadratic Regulator Coordinate Transformation 17

III. TRACK DEVELOPMENT 19

A. INTRODUCTION 19

B. NOMINAL STRAIGHT LINE TRACK 19

1. Geometry of a Nominal Straight Line 20

2. Nomenclature of a Nominal Straight Line Track 22

C. STEADY STATE ERROR 23

IV. INTEGRAL CONTROL METHOD 37

A. INTRODUCTION 37

B. INTEGRAL CONTROL METHOD 37

C. STEADY STATE ERROR 38

D. MODIFIED INTEGRAL CONTROL 46

V. DISTURBANCE ESTIMATION AND COMPENSATION METHOD . . . 50

A. INTRODUCTION 50

B. DISTURBANCE COMPENSATION METHOD 51

C. STEADY STATE ERROR 52

D. CURRENT OBSERVER DEVELOPMENT 54

E. DISTURBANCE ESTIMATION AND COMPENSATION METHOD 63

F. MODIFIED DISTURBANCE ESTIMATION AND COMPENSATION 69

VI. LEADING TRACK CONTROL MONITORING TECHNIQUE 75

A. INTRODUCTION 75

B. LEADING TRACK CONTROL MONITORING DEVELOPMENT . 76

C. RESULTS 76

VII. ROBUSTNESS TESTS AND SENSOR NOISE EFFECTS 93

A. INTRODUCTION 93

B. ROBUSTNESS PROPERTIES 93

C. EFFECTS OF SENSOR NOISE 97

D. EFFECTS OF SENSOR DRIFT 105

E. NAVIGATIONAL UPDATES EFFECT 109

CONCLUSIONS AND RECOMMEDATIONS 116

A. CONCLUSIONS 116

B. RECOMMENDATIONS 120

APPENDIX A 121

APPENDIX B 134

LIST OF REFERENCES 148

INITIAL DISTRIBUTION LIST 150

I. INTRODUCTION

A. BACKGROUND

Autonomous underwater vehicles (AUV'S) are generating much interest in the U. S. Navy and major private defense corporations. As monetary and budgetary constraints dominate the force structure of the armed forces, intelligent unmanned underwater vehicles become a highly attractive alternative to manned submarines [Ref. 1]. The AUV can be downloaded with a myriad of unclassified missions, i.e., reconnaissance, ASW, decoy, survey, ocean engineering; for a fraction of the cost of a manned submarine for the same missions. In order for the AUV to carry out these missions, the AUV should be able to operate freely in the ocean environment with respect to speed, heading and depth. Such operational requirements have to be easily and reliably accomplished in the presence of environmental and physical uncertainties. Autopilot design becomes then an integral and important aspect of overall AUV design [Refs. 2, 3, 4 and 5].

The autopilot, which controls the AUV with regards to a commanded direction and/or depth, is subjugated to a global planner, which monitors and directs the AUV in a global sense. All information concerning the environment of the AUV is detected by the sensing instrumentation onboard the AUV and sent to the higher level intelligence systems, such as the global planner and the autopilot, so that its missions may be carried out. The dynamics of underwater vehicles are described by highly complex, nonlinear

systems of equations with uncertain coefficients and disturbances that are difficult to measure [Refs. 6, 7 and 8]. A complete six degree of freedom model for the underwater maneuvering of the AUV is utilized in which the hydrodynamic force coefficients are taken from previous studies of a swimmer delivery vehicle [Refs. 9 and 10]. Recently, the development of variable structure control in the form of sliding mode control has been shown to provide added robustness that is quite remarkable for AUV autopilot design [Ref. 11]. Robust control using sliding mode control provides accurate control of nonlinear systems despite unmodelled system dynamics, thus making it a highly likely prospect for designing the control laws and guidance methods that will govern the autopilot function of unmanned vehicles.

B. OBJECTIVE OF THIS THESIS

After developing the necessary sliding mode control theory, the objective of this thesis is to investigate the use of a cross track error guidance law with a sliding mode compensator and to present results based on computer simulations using a nonlinear dynamic model of a swimmer delivery vehicle. Various control methods will be investigated for use in the sliding mode based cross track error guidance law. In the development of one of the control methods, a current observer will be developed and shown to work well. This current observer is direly needed because the current will be used as a constant disturbance in this control law and must somehow be determined. Since the lateral current for each track is used and cannot be measured for every track for all times, then the current must be estimated or observed from parameters that can be measured.

After different control methods have been developed and their results presented, a leading track control monitoring technique will be developed. This technique can be used with each of the control methods presented. It will be shown that this technique will automatically initiate the turn onto the leading track, taking into account the environmental conditions, with no overshoot and optimal use of the rudder.

Finally, noise will be introduced into the measurable parameters and the effects will be evaluated. Guidelines will then be developed for suppressing the effects of measurement noise. From all this, conclusions will be made and recommendations will be developed for a highly robust and effective system for controlling the next generation of autonomous underwater vehicles under construction at the Naval Postgraduate School and elsewhere in private industry.

C. THESIS OUTLINE

In Chapter 2, the sliding plane and gain coefficients to be used as the basis for developing an AUV autopilot, using the sliding mode control theory, are developed. The equations of motion to be used only in the horizontal plane, or the path keeping aspect of the AUV, are presented.

Chapter 3 develops a straight line track that becomes the reference from which the cross track error is measured. The track nomenclature and geometry to regulate the error in deviation, or cross track distance, from the nominal straight line track is presented.

Chapter 4 develops the integral control method. The effects of adding integral control to eliminate the steady state error for a single way point and for multiple way

points are investigated. A modified integral control method is developed and results are presented.

Chapter 5 develops a disturbance compensation method, for perfect current input, and a disturbance estimation and compensation method, for estimated or observed current input. Since the lateral current to each track is used as a constant disturbance in the control law, then the lateral current must be able to be determined for each track. The only way to determine the lateral current for each track is to develop a current observer using measurable parameters from onboard sensors. This current observer is developed and results are presented in this chapter.

Chapter 6 investigates a technique referred to as leading track control monitoring, which utilizes the leading track to automatically initiate the turn onto the leading track, within the physical constraints of the AUV and taking into account the environmental conditions. This technique initiates the turn so as not to overshoot the leading track and to optimize the use of the rudder, within the vehicle contstraints. Results of this technique are presented.

Chapter 7 introduces noise into the measurable parameters and the effects are evaluated. Guidelines for suppressing the effects of measurement noise are put forth in this chapter.

II. EQUATIONS OF MOTION AND SLIDING PLANE DEVELOPMENT

A. INTRODUCTION

Prior to beginning a discussion on cross track error guidance control law, an in depth overview of the sliding plane and gain coefficients for use in regulating the steady state error in deviation from the nominal straight line track needs to be developed. Also, a development of the equations of motion used in this research will be conducted. The main assumption to be made, at the beginning, is that only the horizontal plane, or the steering aspect of the AUV, will be considered throughout this research. This assumption is based upon the previous work done on the Line of Sight (LOS) guidance control law by Lienard [Ref. 12], where it was established that heading, speed and depth sliding mode autopilots could be designed independently. The remaining part of this chapter will develop the equations of motion for the AUV used in this research and will also develop the sliding plane and gain coefficients to be used as the basis for developing an AUV autopilot using the sliding mode control theory.

B. EQUATIONS OF MOTION

Intead of an exact set of equations of motion for a rigid body moving in a fluid, a simplified linear set of equations of motion was chosen to be used for control design. The full sets of nonlinear equations of motion for the AUV were taken from the work done previously at NPS by Boncal [Ref. 2], who used the dynamic model as established

by Crane, Summey, et al [Ref. 10], as representative of the SDV Mark 9 vehicle. The SDV Mark 9 vehicle is different than the AUV currently being used at NPS, but it remains a useful vehicle for the study of dynamics and control issues. Since the current NPS AUV does not yet have validated hydrodynamic coefficients, the SDV Mark 9 vehicle serves our purpose in developing guidance control laws that can apply to the NPS AUV or any vehicle of choice.

It is too time consuming for an onboard computer to try and control an underwater vehicle using an exact set of equations of motion, therefore, a linearized set of equations of motion was developed. By restricting the motion of the vehicle to the horizontal plane, only the equations of motion in the horizontal plane will be developed. In fact, this research utilizes the assumptions and equations of motion done previously by Lienard [Ref 12]. The state space form that can be used for heading control is

$$\dot{\psi} = r \tag{2.1a}$$

$$\dot{v} = a_{11}uv + a_{12}ur + b_1u^2\delta \tag{2.1b}$$

$$\dot{r} = a_{21}uv + a_{22}ur + b_2u^2\delta \tag{2.1c}$$

with $a_{11} = -0.04538$, $a_{12} = -0.35119$, $a_{21} = -0.002795$, $a_{22} = -0.09568$, $b_1 = 0.011432$ and $b_2 = -0.04273$, upon which the control laws can be based utilizing

sliding mode control theory. To regulate the error in deviation from a nominal straight line track, the following equation is introduced

$$\dot{y} = v\cos\psi + u\sin\psi \tag{2.2}$$

and when linearized

$$\dot{y} = v + u\psi \qquad (no\ current), \tag{2.3}$$

where y denotes the cross track distance off the nominal track. So, the state space form to be used for cross track error control, with no current, is

$$\dot{\psi} = r \tag{2.4a}$$

$$\dot{v} = a_{11}uv + a_{12}ur + b_1u^2\delta \tag{2.4b}$$

$$\dot{r} = a_{21}uv + a_{22}ur + b_2u^2\delta \tag{2.4c}$$

$$\dot{y} = v + u\psi \tag{2.4d}$$

at any nominal u.

The system equations of (2.1) and (2.4) will be used for the controller design, whereas, the equations developed by Lienard [Ref. 12] for the nonlinear steering equations will be used to simulate the AUV in all trial runs.

C. SLIDING PLANE AND GAIN COEFFICIENT DEVELOPMENT

1. Pole Placement Method

Since the vehicle motion is based on linearized differential equations of motion, then the nature of the motion of the vehicle can at best be only approximated. Now, any control law based on an approximate plant model must be robust enough to ensure stability and acceptable transient response characteristics in the presence of parameter variations and/or unmodeled dynamics [Ref. 13]. Since the parameters and coefficients are valid for the nonlinear model of the SDV Mark 9 vehicle and a new set of parameters and coefficients has still to be verified for the NPS AUV, then there will definitely exist parameter variations, unmodelled dynamics, and disturbances. Sliding mode control laws provide effective and robust ways of controlling uncertain plants. Sliding mode control utilizes a high speed switching control law to drive the plant's state trajectory on to a sliding plane for all subsequent times. The control law will be based upon the linear model

$$\dot{x} = [A]x + [b]u \tag{2.5}$$

where

$$x^T = [\psi,v,r,y], \quad b^T = [0,0.4116,-0.1538,0], \quad u = \delta$$

and

$$[A] = \begin{bmatrix} 0 & 0 & 1 & 0 \\ 0 & -0.2723 & -2.1071 & 0 \\ 0 & -0.0168 & -0.1538 & 0 \\ 6 & 1 & 0 & 0 \end{bmatrix}.$$

For the four dimensional system (2.4), the sliding plane is the Euclidean space

$$\sigma(x) = 0 \quad \textit{where} \quad s_1x_1 + s_2x_2 + s_3x_3 + s_4x_4 = 0, \tag{2.6}$$

and the coefficient s_1 is arbitrary. Equation (2.6) can be written as

$$s^Tx = 0 \quad \textit{with} \quad s^T = [s_1, s_2, s_3, s_4]. \tag{2.7}$$

Determining s will determine the sliding plane uniquely. The control law has to be able to drive system (2.1) onto the sliding plane (2.6) for an arbitrary choice of initial conditions. By defining the Lyapunov function

$$V(x) = \frac{1}{2}[\sigma(x)]^2, \tag{2.8}$$

asymptotic stability of (2.8) is guaranteed provided $\dot{V}(x)$ is a negative definite function, or

$$\dot{V} = \sigma\dot{\sigma} = -\eta^2\sigma(x),$$

such that,

$$\dot{\sigma} = -\eta^2 sign(\sigma). \tag{2.9}$$

Since $\sigma(x) = s^Tx$, system (2.1) and equation (2.5) can be used to get

$$s^T(Ax + bu) = -\eta^2 sign(\sigma),$$

and solving for u

$$u = -(s^T b)^{-1} s^T Ax - \eta^2 (s^T b)^{-1} sign(\sigma),$$

or,

$$u = \hat{u} + \overline{u}. \tag{2.10}$$

It is important to recognize that the feedback control law u is composed of two parts. The first,

$$\hat{u} = -(s^T b)^{-1} s^T Ax \tag{2.11}$$

is a linear feedback law, whereas the second,

$$\overline{u} = -\eta^2 (s^T b)^{-1} sign(\sigma) \tag{2.12}$$

is a nonlinear feedback with its sign toggling between plus and minus according to which side of the sliding plane the system is located on. Since $\overline{u}$ has to change its sign as the system crosses $\sigma(x) = 0$, the sliding surface has to be a hyperplane (dimension of one less than the state space). It is $\overline{u}$ which is mainly responsible for driving and keeping the system onto the sliding plane, $\sigma(x) = 0$ (where $\overline{u} = 0$ as well). Provided the gain η^2 has been chosen large enough, $\overline{u}$ can provide the required robustness due to momentary disturbances and unmodelled dynamics without any compromise in stability.

The linear feedback law (2.11) is designed such that the system has the desired dynamics on the sliding plane. Since $\sigma(x) = 0$, then in this case

$$u = \hat{u} = -(s^T b)^{-1} s^T A x,$$

and the closed loop dynamics of (2.2) are given by

$$\dot{x} = [A - b(s^T B)^{-1} s^T A]x \tag{2.13}$$

or,

$$\dot{x} = (A - bk)x, \tag{2.14}$$

where the gain vector k can be found from standard pole placement methods. The closed loop dynamics matrix

$$A_c = A - bk \tag{2.15}$$

has eigenvalues specified for desirable response. One of the eigenvalues of A_c must be specified to be zero. This is consistent with the decomposition in (2.10). The linear feedback $\hat{u}$ provides the desired dynamics on the sliding plane only. Therefore, $\hat{u}$ has no effect in a direction perpendicular to $\sigma(x) = 0$. With A_c specified and k computed by pole placement, s can be determined from (2.13) and (2.14),

$$k = (s^T b)^{-1} s^T A,$$

and

$$s^T(A - bk) = 0, \tag{2.16a}$$

or,

$$s^T A_c = 0. \tag{2.16b}$$

Therefore, s is a left eigenvector of A_c that corresponds to the zero eigenvalue. With this choice of s, the sliding plane, $s^T = 0$, and the feedback control law (2.10) are completely determined. It should be pointed out that, in applications, the states x_1, x_2, x_3 and x_4 are to be interpreted as errors between the actual values of ψ, v, r, y and their set points.

There are two problems that arise from using this approach of pole placement in finding s. First, there is no guarantee that the eigenvector for s will always be real. Second, for multiple input systems, this approach will not work, since more than one pole can not be placed at the origin in order to find s reliably. For this research, these two problems did not play a major factor, however, other methods were investigated.

2. Coordinate Transformation with Pole Placement Method

An alternate approach that accounts for the two problems stated in the pole placement method is to perform a coordinate transformation and to find the corresponding transformation matrix [Refs. 14 and 15].

Define a coordinate transformation,

$$y = Tx \quad ,$$

where T is an orthogonal n by n transformation matrix such that

$$Tb = \begin{bmatrix} b_1 \\ 0 \end{bmatrix} \tag{2.17}$$

where b_1 is m by m and 0 is (n - m) by m. The number of states is n and the number of inputs is m. In this research m = 1. To determine T, use the QR factorization of b, where b is decomposed into the form

$$b = Q \begin{bmatrix} R \\ 0 \end{bmatrix} \tag{2.18}$$

and Q is orthogonal and R is the upper triangular. Now, from (2.17) and (2.18),

$$T = Q^T \quad .$$

From the coordinate transformation,

$$y = Tx \quad ,$$

then,

$$x = T^T y \quad ,$$

and,

$$\dot{y} = T\dot{x} \quad ,$$

and when substituted into (2.2), a linear model is obtained in the transformed variable y,

$$\dot{y} = TAT^T y + Tbu \quad . \tag{2.19}$$

The sliding condition,

$$s^T x = 0 \quad ,$$

becomes

$$s^T T^T y = 0 \quad ,$$

or

$$C^T y = 0 \quad , \tag{2.20}$$

with C = Ts. Performing a partition on y and C,

$$y = \begin{bmatrix} y_1 \\ y_2 \end{bmatrix}$$

where y_1 is one by one and y_2 is (n - 1) by one, and

$$C = \begin{bmatrix} C_1 \\ C_2 \end{bmatrix}$$

where C_1 is one by one and C_2 is (n - 1) by one, so that the state equations in the transformed variable become

$$\dot{y}_1 = A_{11} y_1 + A_{12} y_2 + b_1 u \tag{2.21a}$$

$$\dot{y}_2 = A_{21} y_1 + A_{22} y_2 \quad . \tag{2.21b}$$

The sliding plane (2.20) now becomes

$$C_1 y_1 + C_2^T y_2 = 0 \quad ,$$

or

$$y_1 + C_2^T y_2 = 0 \quad , \tag{2.22}$$

with C_1 normalized to one. For the sliding plane to be completely and uniquely defined, then C_2^T needs to be determined.

Again by defining the Lyapunov function

$$V(y) = \frac{1}{2}(\sigma(y))^2 \quad , \tag{2.23}$$

asymptotic stability of (2.23) is guaranteed provided $\dot{V}(y)$ is a negative definite function, or

$$\dot{V}(y) = \sigma\dot{\sigma} = -\eta^2\sigma(y) \quad ,$$

or

$$\dot{\sigma} = -\eta^2 sign(\sigma) \quad . \tag{2.24}$$

Differentiating the equation for the sliding plane (2.20) and equating to (2.24),

$$\dot{y}_1 + C_2^T \dot{y}_2 = -\eta^2 sign(\sigma) \quad . \tag{2.25}$$

Substituting (2.21a) and (2.21b) into (2.25) and solving for

$$u = \hat{u} + \bar{u} \quad ,$$

$$A_{11}y_1 + A_{12}y_2 + b_1 u + C_2^T(A_{21}y_1 + A_{22}y_2) = -\eta^2 sign \quad (\sigma)$$

$$\hat{u} = -b_1^{-1}[(A_{11} + C_2^T A_{21})y_1 + (A_{12} + C_2^T A_{22})y_2] \tag{2.26a}$$

$$\bar{u} = -\eta^2 b_1^{-1}\, sign(\sigma) \quad . \tag{2.26b}$$

From the sliding plane design, it is desired to have $\sigma(y) = 0$, which gives $\bar{u} = 0$ and $u = \hat{u}$. Solving (2.22) for y_1,

$$y_1 = -C_2^T y_2 \quad . \tag{2.27}$$

Equations on the sliding plane become

$$\dot{y}_1 = A_{11}y_1 + A_{12}y_2 + b_1\hat{u} \quad ,$$

and substituting for $\hat{u}$ from (2.26a),

$$\dot{y}_1 = -C_2^T(A_{21}y_1 + A_{22}y_2) \quad ,$$

and substituting once more for $\dot{y}_1$ by differentiating (2.27),

$$-C_2^T\dot{y}_2 = -C_2^T(A_{21}y_1 + A_{22}y_2) \quad ;$$

a linear combination of the second set

$$\dot{y}_2 = A_{21}y_1 + A_{22}y_2 \quad .$$

The (n - 1) independent equations on the sliding plane are

$$\dot{y}_2 = A_{21}y_1 + A_{22}y_2 \quad ,$$

and substituting for y_1 from (2.27)

$$\dot{y}_2 = (A_{22} - A_{21}C_2^T)y_2 \quad . \tag{2.28}$$

Again using pole placement of (n - 1) poles, C_2^T can be determined and thus the sliding plane is uniquely and completely determined.

The system matrix in the y equation has rank (n - 1) and is a singular matrix, therefore, one pole is already at the origin. Only (n - 1) poles need to be determined by pole placement and the two problems from the previous pole placement method have been resolved.

3. Linear Quadratic Regulator Coordinate Transformation

Instead of pole placement to determine the sliding plane and gain coefficients, the Linear Quadratic Regulator (LQR) with a coordinate transformation was investigated. This LQR method involves minimizing a cost functional in which the integrand is a quadratic function of the state $x(\cdot)$ [Refs 14 and 15], such as

$$J = \frac{1}{2}\int (x^T Q x)\, dt \quad . \tag{2.29}$$

Using the coordinate transformation, y = Tx,

$$J = \frac{1}{2}\int y^T (TQT^T) y\, dt \quad ,$$

and by partitioning

$$TQT^T = \begin{bmatrix} Q_{11} & Q_{12} \\ Q_{21} & Q_{22} \end{bmatrix}$$

the cost functional becomes

$$J = \frac{1}{2}\int (y_1^T Q_{11} y_1 + y_2^T Q_{21} y_1 + y_1^T Q_{12} y_2 + y_2^T Q_{22} y_2)\, dt \quad .$$

Now defining

$$Q^* = Q_{22} - Q_{21}Q_{11}^{-1}Q_{12} \tag{2.30a}$$

$$A^* = A_{22} - A_{21}Q_{11}^{-1}Q_{12} \tag{2.30b}$$

$$V = y_1 + Q_{11}^{-1}Q_{12}y_2 \quad , \tag{2.30c}$$

a new cost functional, I, is obtained

$$I = \frac{1}{2}\int (y_2^T Q^* y_2 + V^T Q_{11} V)\, dt$$

and

$$\dot{y}_2 = A^* y_2 + A_{21} V \quad . \tag{2.31}$$

The problem is now to minimize I subject to (2.31). However, in order to minimize I, an arbitrary choice of Q^* needs to be made. The choice of Q^* greatly influences whether tight control or soft control will be obtained, but it provides no easier a method to obtain the sliding plane and gain coefficients. For the remainder of this research, the pole placement method is chosen to determine the sliding plane and gain coefficients with closed loop poles as specified for the particular trial run.

III. TRACK DEVELOPMENT

A. INTRODUCTION

Now that the foundation in sliding mode control theory has been laid and the method for determining the sliding plane and gain coefficients is known, a straight line track needs to be developed. It will be the perpendicular distance off this straight line track that will be defined as the cross track distance, y. This cross track distance will be the object of the sliding mode control laws so that this cross track distance will be controlled to zero. When the cross track distance is zero, then the vehicle is on the directed track specified by the global planner. This chapter will develop the track nomenclature and geometry in order to regulate the error in deviation, or cross track distance, from the nominal straight line track. Also, this chapter will show that, at steady state conditions, a steady state error exists in the presence of a current and how the value of k_n affects the stability of the controller. It will be the elimination of this steady state error that the various guidance controls laws to be developed will concern themselves.

B. NOMINAL STRAIGHT LINE TRACK

In order to construct the nominal straight line track to be used to measure the cross track distance, the global planner needs to input two way points, a starting point and a destination point. For this research, the two way points must be in global coordinates

(X,Y) and in terms of ship lengths. The following equations determine the inertial position rates of the AUV

$$\dot{X} = U_c + u\cos\psi - v\sin\psi$$

$$\dot{Y} = V_c + u\sin\psi + v\cos\psi$$

where U_c and V_c are the absolute current velocities in the global reference frame. The angle α, measured from the horizontal, will define the track for the two way points of interest. The perpendicular distance y, in local coordinates, will be the cross track distance that will be controlled such that when the cross track distance is zero, then the vehicle is on the desired track. The cross track distance, for this research, will be designated, y, and the distance along the track will be designated, x. Both y and x are in local coordinates. The current position of the vehicle will be designated by, X and Y, both in global coordinates.

1. Geometry of a Nominal Straight Line

Figure 1 will be used to develop a nominal straight line track, and it will be repeated as the vehicle goes from way point to way point. The equations to transform the global coordinates into the local coordinates are

$$x = X\cos\alpha + Y\sin\alpha$$

$$y = Y\cos\alpha - X\sin\alpha \quad .$$

Also, the equations to translate global currents into local currents are

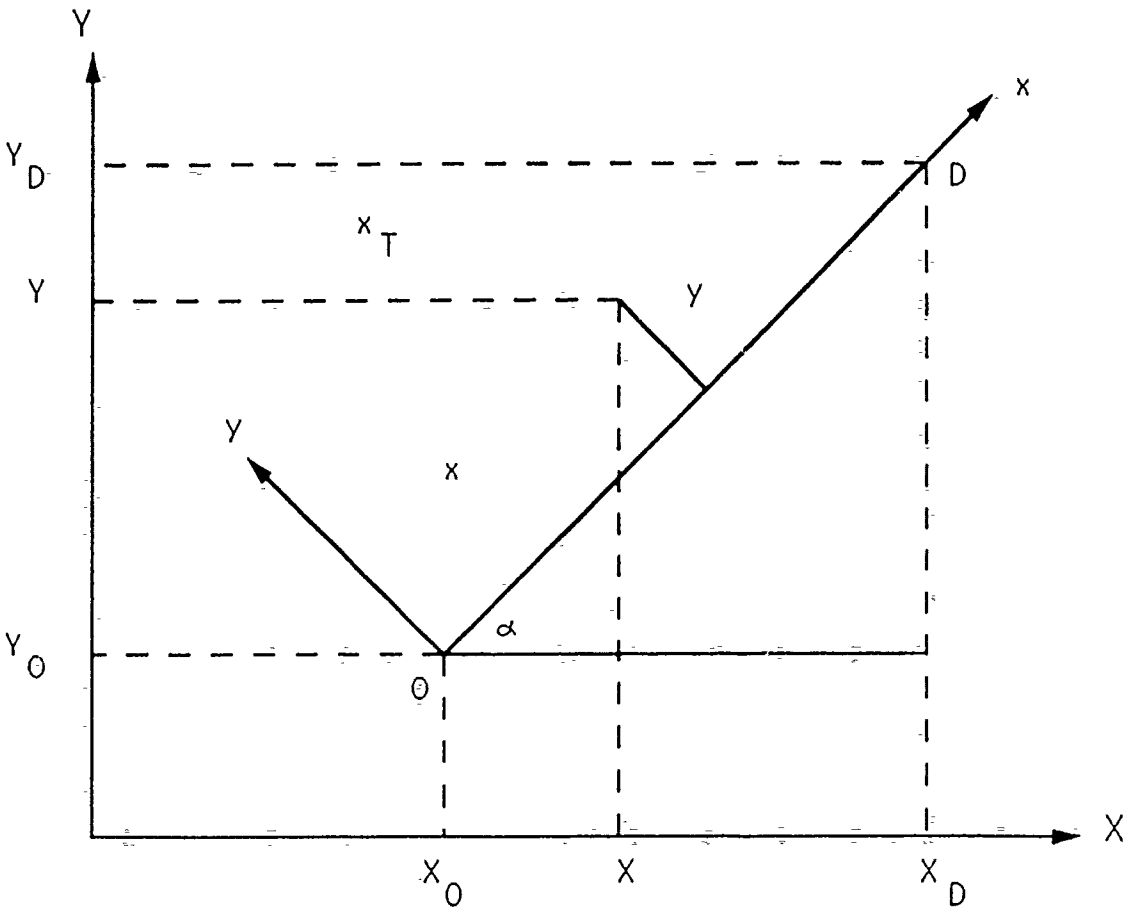

Figure 1. Geometry of the Nominal Straight Line Track.

$$u_c = U_c\cos\alpha + V_c\sin\alpha$$

$$v_c = V_c\cos\alpha - U_c\sin\alpha \quad .$$

2. Nomenclature of a Nominal Straight Line Track

The following nomenclature will be used in developing a nominal straight line track for this research:

- y: the perpendicular distance off the track, in local coordinates.
- x: the distance along the track, in local coordinates.
- XTIME: desired total time to go from the starting point to the destination point, in seconds.
- UREQ: the speed required to get from the starting point to the destination point in the desired time, in ft/sec.
- x_T: the total length of desired track, in feet.
- (X,Y): the current vehicle position, in global coordinates.
- (X_D, Y_D): the destination way point, in global coordinates and in ship lengths.
- (X_O, Y_O): the starting way point, in global coordinates and in ship lengths.
- α: the angle measured from the horizontal to the line between the starting point and the destination point.

From the geometry, the following parameters will be defined:

- $x_T = \dfrac{Y_D - Y_O}{\sin\alpha}$.

- $\alpha = \tan^{-1}\left(\dfrac{Y_D - Y_O}{X_D - X_O}\right)$.

- $y = (Y - Y_O)\cos\alpha - (X - X_O)\sin\alpha$.

- $x = (X - X_O)\cos\alpha + (Y - Y_O)\sin\alpha$.

- $UREQ = \dfrac{x_T}{XTIME}$.

C. STEADY STATE ERROR

In the presence of a current, it has been observed that a steady state error will occur, with no control, for the linearized set of equations of motion for the AUV at steady state conditions. The linearized set of equations of motion for the AUV, with no integral control, was developed in equation (2.1). To account for the current that is perpendicular to the track, v_c, equation (2.3) is modified to

$$\dot{y} = v + u\psi + v_c \quad . \tag{3.1}$$

At steady state,

$$\dot{\psi} = \dot{v} = \dot{r} = \dot{y} = 0 \tag{3.2}$$

so that

$$0 = r_s \tag{3.3a}$$

$$0 = a_{11} u v_s + b_1 u^2 \delta_s \tag{3.3b}$$

$$0 = a_{21} u v_s + b_2 u^2 \delta_s \tag{3.3c}$$

$$0 = v_s + u \sin\psi + v_c \tag{3.3d}$$

where a_{11}, a_{21}, b_1, b_2 and u are as defined in Chapter Two. The subscript s represents the value of the variable at steady state.

Since a_{11}, a_{21}, b_1 and b_2 are nonzero, then $v_s = \delta_s = 0$. Therefore,

$$\psi_s = \mp \sin^{-1}\left(\frac{v_c}{u}\right) \tag{3.4}$$

and when this is substituted into the sliding plane and rudder equations, a steady state error will develop. For rudder control,

$$\delta = k_1 \psi + k_2 v + k_3 r + k_n sat sgn(\sigma) \tag{3.5}$$

and for the sliding plane,

$$\sigma = s_1\psi + s_2 v + s_3 r + s_4 y \quad . \tag{3.6}$$

The coefficients of δ and σ are the gain coefficients and the sliding plane coefficients, respectively. At steady state,

$$\delta_s = 0 \quad ,$$

and when on the sliding plane, the following can be seen from (3.4) and (3.5)

$$satsgn(\sigma) = \frac{-k_1\psi_s}{k_n} = \frac{k_1}{k_n}\sin^{-1}\left(\frac{v_c}{u}\right) \tag{3.7}$$

and

$$\sigma = s_1\psi_s + s_4 y_s = -s_1\sin^{-1}\left(\frac{v_c}{u}\right) + s_4 y_s \quad . \tag{3.8}$$

Now,

$$satsgn(\sigma) = \frac{\sigma}{\phi} \quad , \tag{3.9}$$

therefore, from (3.7) and (3.9),

$$\frac{\sigma}{\phi} = \frac{k_1}{k_n}\sin^{-1}\left(\frac{v_c}{u}\right) \quad , \tag{3.10}$$

where

$$\frac{1}{\phi}\left[-s_1\sin^{-1}\left(\frac{v_c}{u}\right) + s_4 y_s\right] = \frac{k_1}{k_n}\sin^{-1}\left(\frac{v_c}{u}\right) \quad . \tag{3.11}$$

Now from (3.8) and (3.10) and solving for y_s,

$$s_4 y_s = \frac{\phi k_1}{k_n} \sin^{-1}\left(\frac{v_c}{u}\right) + s_1 \sin^{-1}\left(\frac{v_c}{u}\right) ,$$

and

$$y_s = \frac{1}{s_4}\left[\frac{\phi k_1}{k_n} + s_1\right] \sin^{-1}\left(\frac{v_c}{u}\right) . \tag{3.12}$$

Equation (3.12) represents the steady state error in the cross track distance that results in the presence of a lateral current. This steady state track error can be made smaller by increasing the value of the nonlinear gain k_n, but it can never become zero. For very large k_n, y_s is still bounded by

$$y_s = \frac{s_1}{s_4} \sin^{-1}\left(\frac{v_c}{u}\right) .$$

The above analysis is valid if

$$satsgn(\sigma) = \frac{\sigma}{\phi} ,$$

which requires that $| satsgn(\sigma) | \leq 1$. This requirement yields the necessary critical value of k_n for stability, from (3.10)

$$k_n \geq k_{crit} = \left| k_1 \sin^{-1}\left(\frac{v_c}{u}\right) \right| . \tag{3.14}$$

If the nonlinear gain is not selected large enough; i.e., if $k_n < k_{crit}$; then the controller cannot guarantee stability.

The above analytical results can be confirmed by numerical simulations of the full nonlinear, six degree of freedom model of the SDV. Closed loop poles on the sliding plane were selected at [-0.35,-0.36,-0.37], with ϕ = 0.5 and u = 6 ft/sec. This gives

$$\delta = 0.9556\psi - 0.1085v + 1.2286r + k_n sat sgn(\sigma) \tag{3.15}$$

$$\sigma = 2.9805\psi + 0.2199v + 3.4445r + 0.0700y \quad . \tag{3.16}$$

Figure 2 shows how the controller works with no current. The way point is selected at (X,Y) = (20,20) ship lengths. In Figure 2 and all subsequent similar figures, the following variables are displayed: X vs Y position, rudder angle vs time, the cross track error (YLCASE) vs time, the heading $\psi - \alpha$ (HEAD) vs time, the integral of the cross track error (YINTGR) vs time and the sliding surface σ (SS2) vs time. It can be seen that the vehicle achieves the desired track with no error. Figures 3 and 4 show how the controller works with a current and how the larger the k_n, the smaller the steady state cross track error. Figure 4 and (3.12) also show that as k_n gets infinitely large, a steady state error will still exist and the rudder will be cycled excessively. The current was U_c = 0.0, V_c = 2.0 ft/sec, which means that v_c = 1.4142 ft/sec, and using (3.14), k_{crit} = 0.2274. It can be seen that the steady state error, as predicted by (3.12), is in accordance with what was obtained through the numerical simulations. Finally, Figure 5 shows that for $k_n < k_{crit}$, the controller cannot guarantee stability and the controller starts to deviate in a linear manner in the presence of a current.

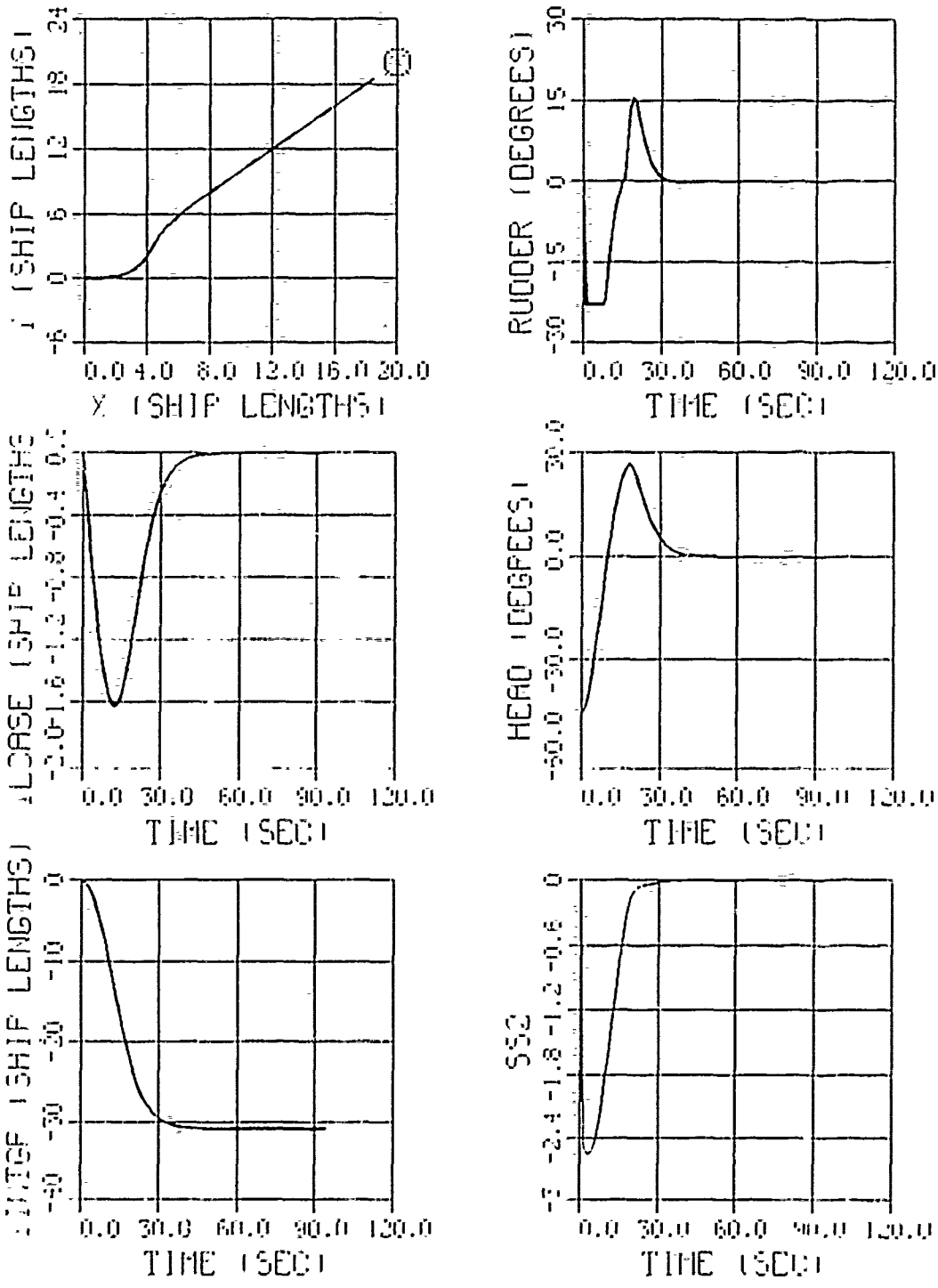

Figure 2. Cross Track Error Control with k_n = 0.5 and V_c = 0.

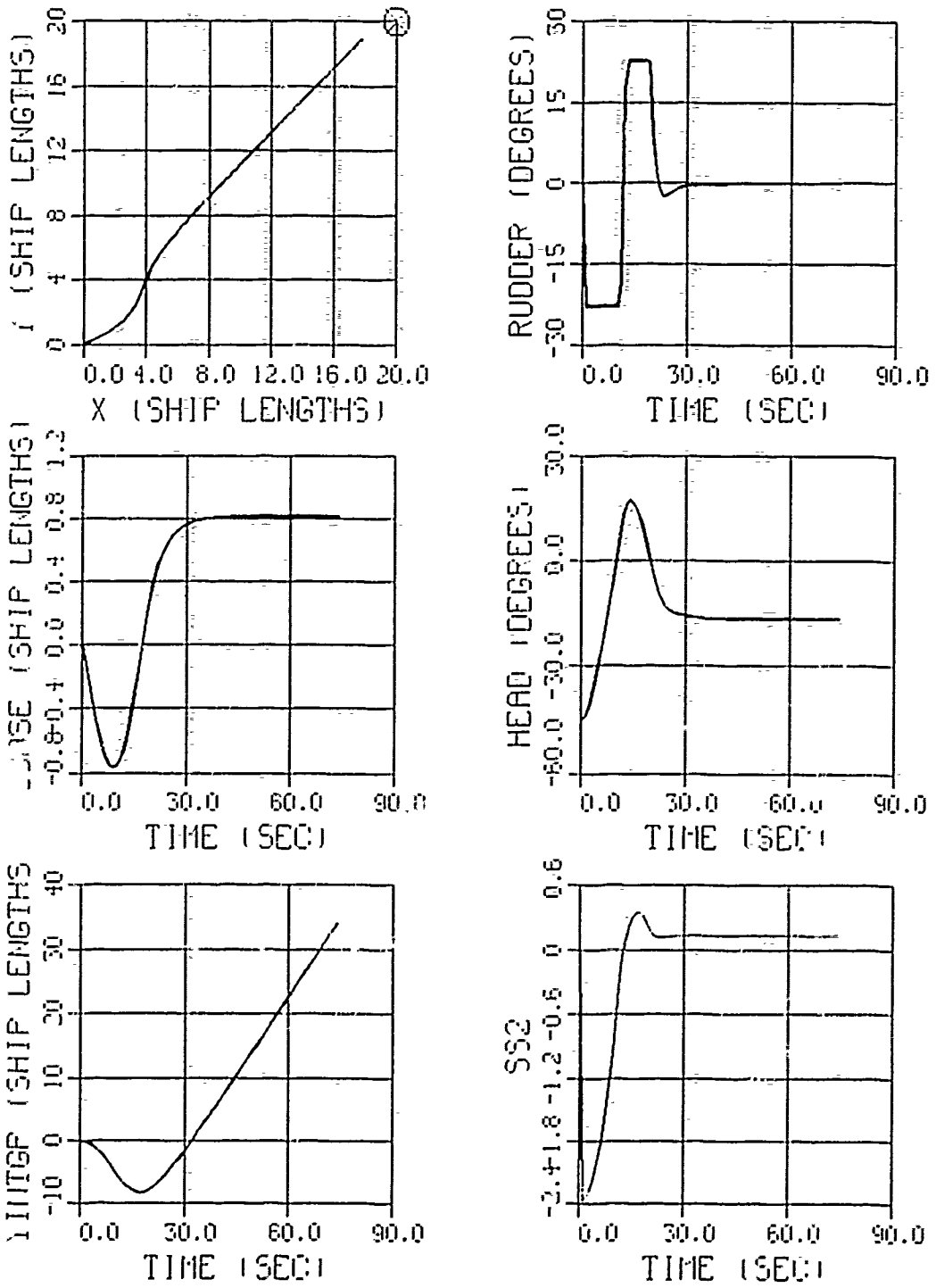

Figure 3. Cross Track Error Control with k_a = 1.0 and V_c = 2.

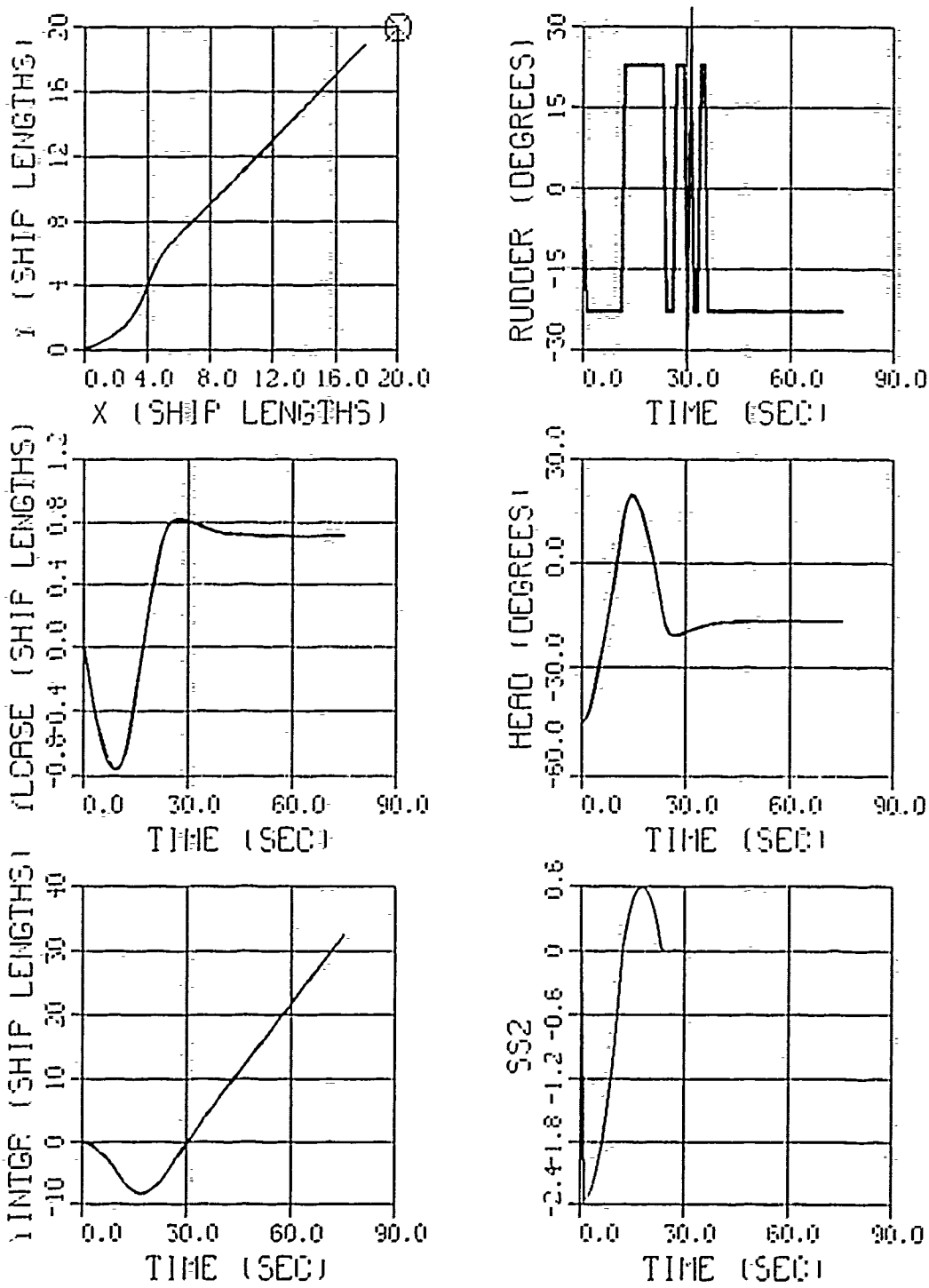

Figure 4. Cross Track Error Control with k_a = 1000 and V_c = 2.

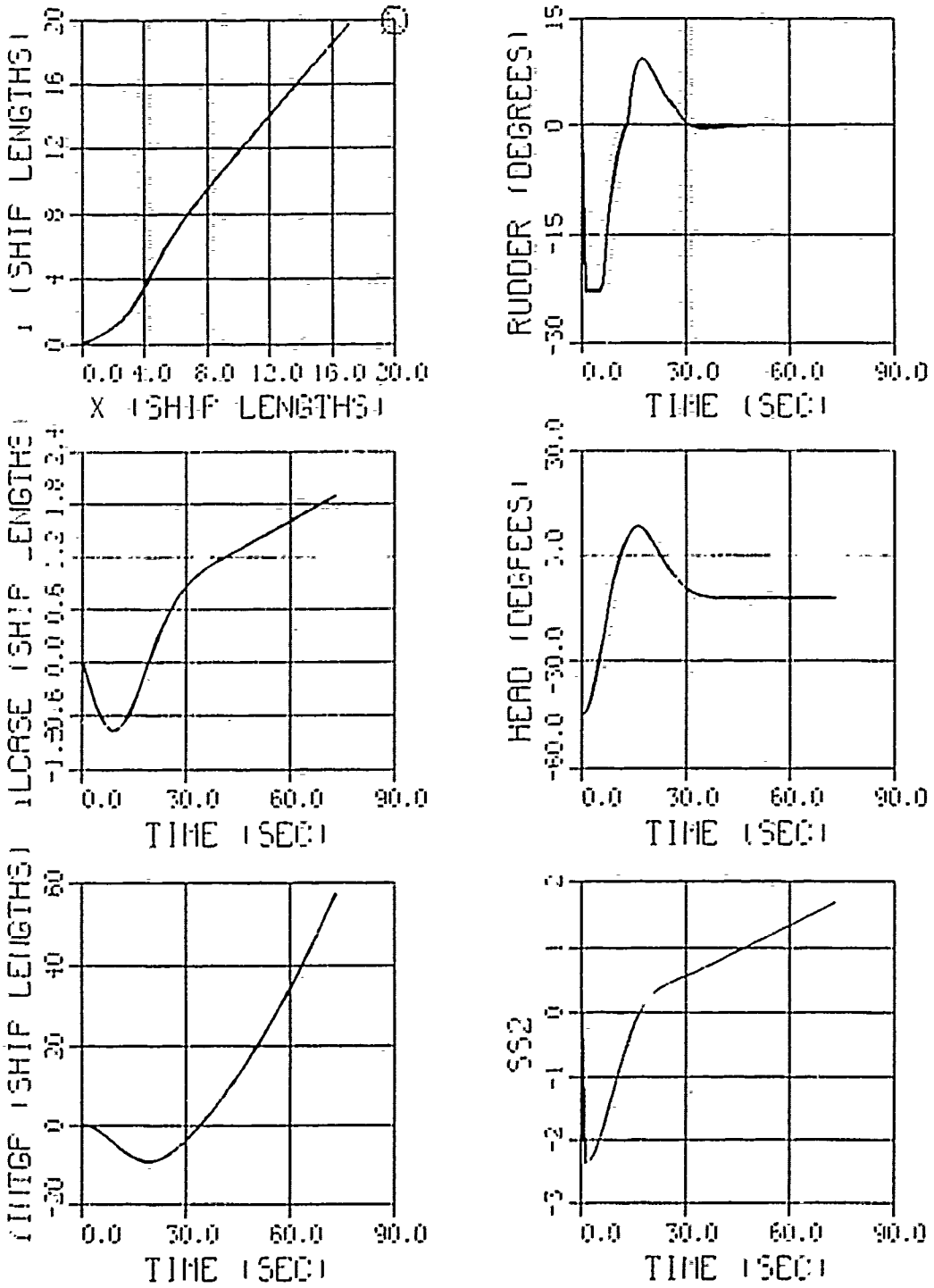

Figure 5. Cross Track Error Control with k_A = 0.2 and V_c = 2.

Results for multiple way points are presented in Figures 6 through 9. The way points were selected at (X,Y) = (10,0), (20,5) and (30,5). This corresponds to a lane changing maneuver, the change from the original track to a second parallel track. The local coordinate system is rotated every time a way point is reached. The criterion for reaching a way point is based on the distance from the way point along the local x direction, or target distance. Results for various values of the target distance are shown in Figures 6, 7 and 8, where the target distances are 0.5, 2 and 7 vehicle lengths, respectively. It can be seen that if the target distance is very small, the vehicle overshoots the desired track with significant rudder activity. On the other hand, if the target distance is very large, the vehicle turns in the wrong direction prior to completing the turn. The best target distance depends on the turn, vehicle response characteristics, and environmental conditions; and in this case it appears that a value of 2 causes minimal rudder and track overshoot.

Finally, the attempted lane changing maneuver in a current V_c = 2.0 is shown in Figure 9, where the existence of a significant steady state track error is evident. The following chapters will explore the use of an integral control method and the use of a disturbance estimation and compensation method to control the steady state error in the presence of a current, such that the vehicle remains on the desired track. These methods of control will utilize the above development of the desired track. Once the desired track has been defined, these methods of control will attempt to control the cross track distance to zero, so that the AUV will be on the desired track as consistently as possible.

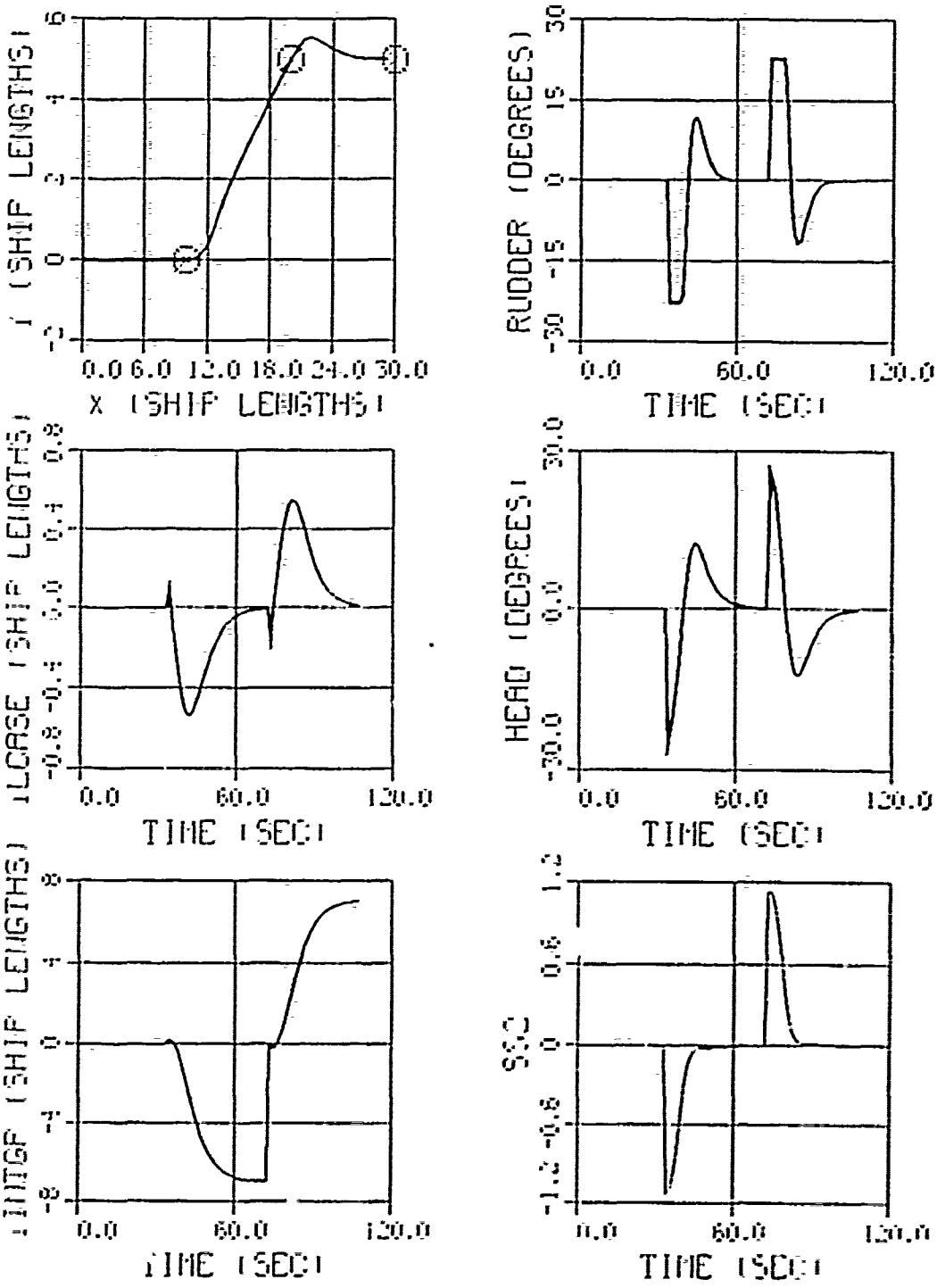

Figure 6. Lane Changing Maneuver, Target Distance 0.5 Vehicle Lengths.

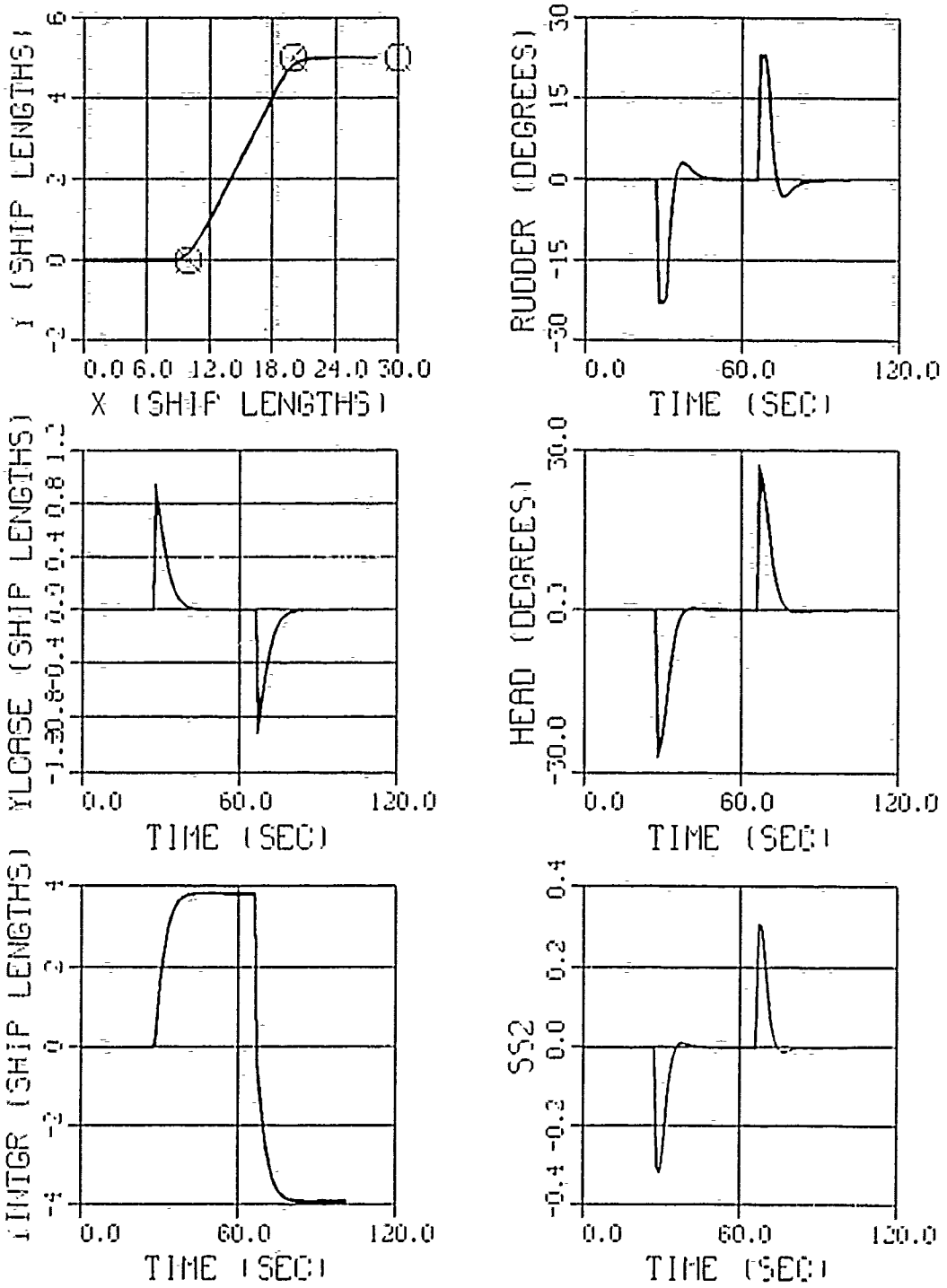

Figure 7. Lane Changing Maneuver, Target Distance 2 Vehicle Lengths.

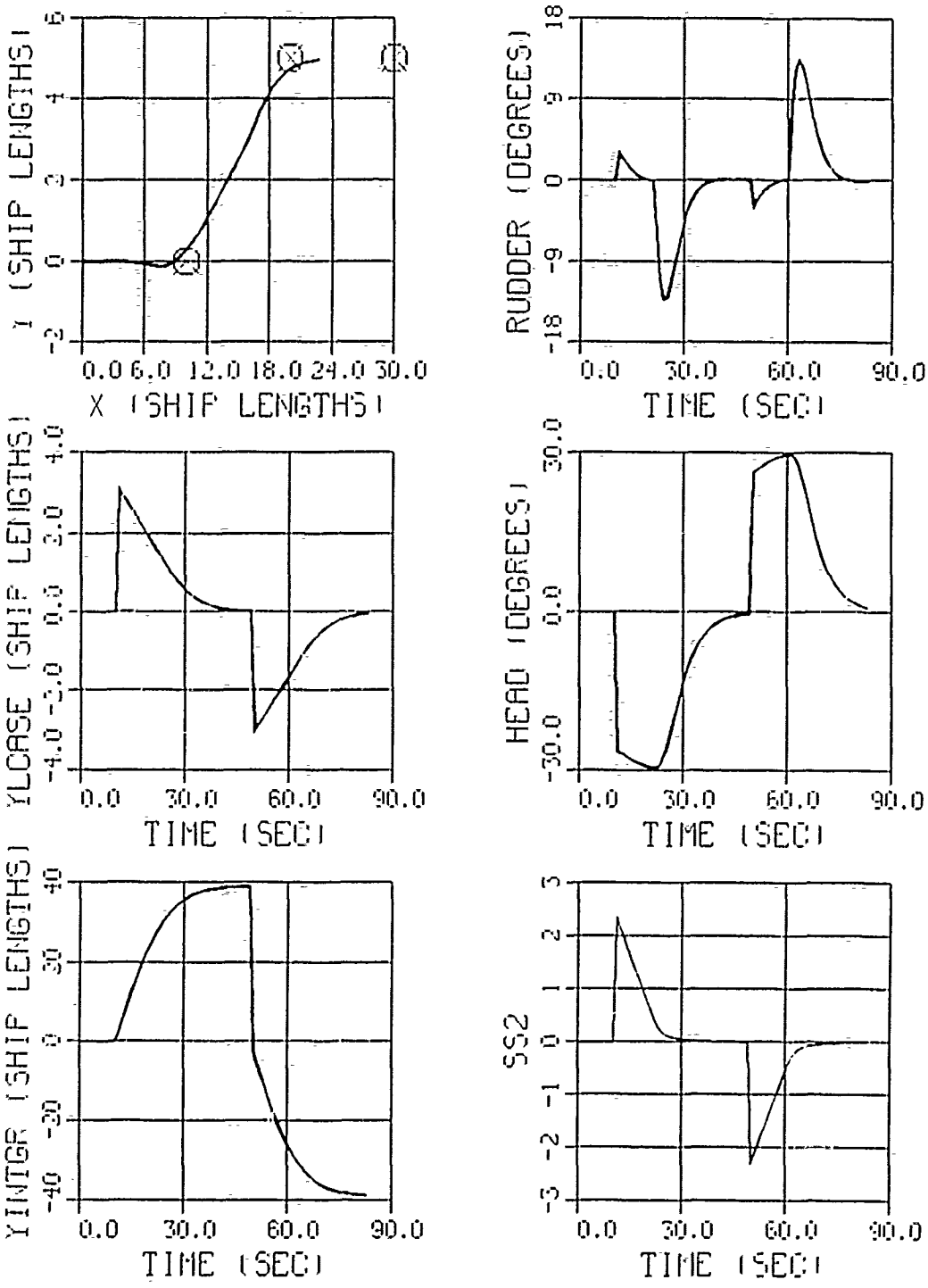

Figure 8. Lane-Changing Maneuver, Target Distance 7 Vehicle Lengths.

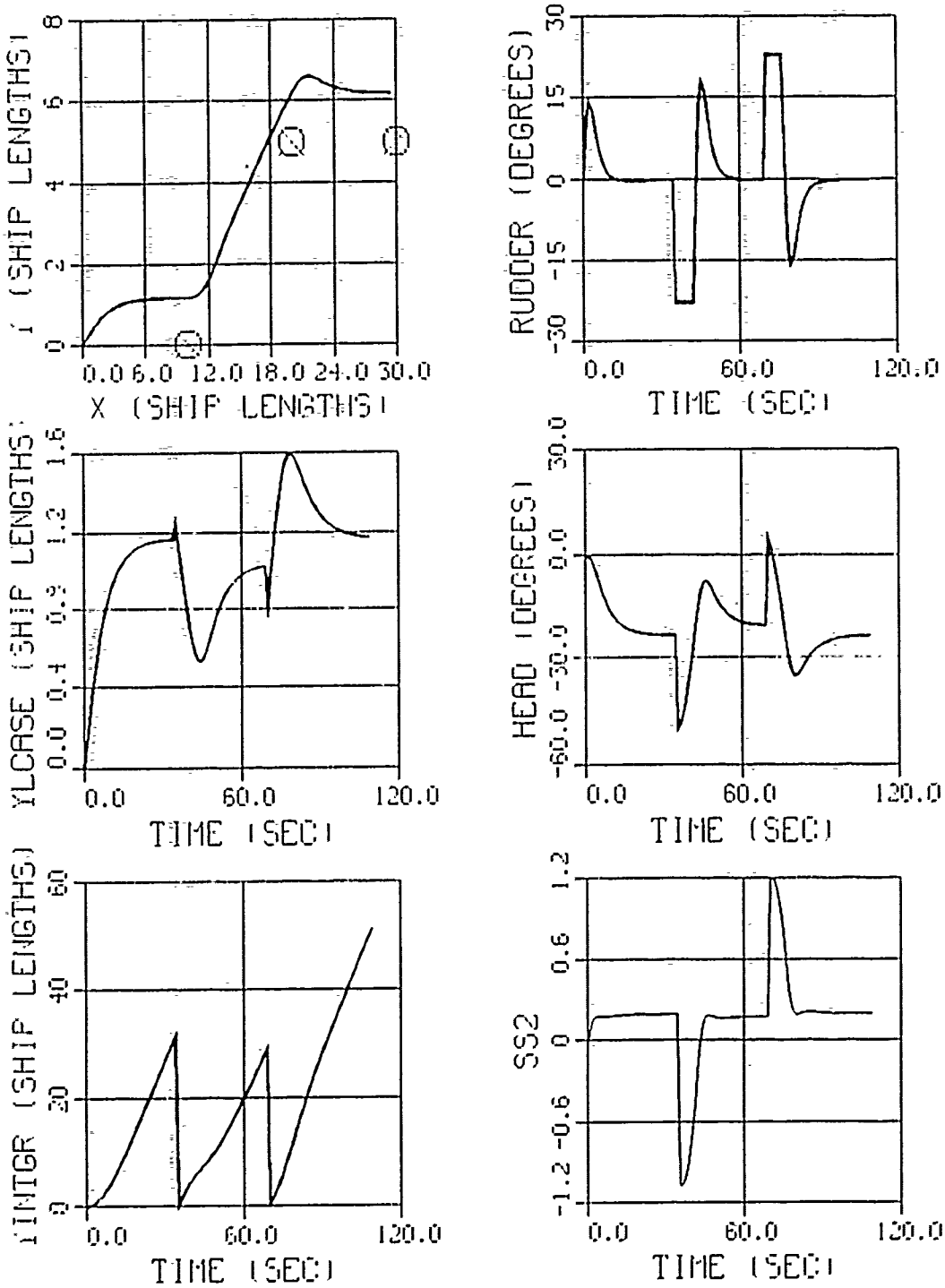

Figure 9. Lane Changing Maneuver in a Current.

IV. INTEGRAL CONTROL METHOD

A. INTRODUCTION

In the previous two chapters, the sliding mode control development, along with the nominal straight line track and the steady state error in the presence of a current, for a cross track error controller, have been developed. The first method to be used to eliminate this steady state error is the integral control method. This is the first logical choice, since traditionally, integrators have been used to eliminate steady state errors. However, in general, as more integrators are added to the system, then the chances increase for the system to become unstable due to the poles being added to the system. Also, when the integral action is introduced, the linearized equations for the system have to be modified, which will be seen in this chapter. This chapter will also show the effects of adding integral control to eliminate the steady state error for a single way point and for multiple way points, as in Chapter Three. A modified integral control method will also be investigated in this chapter with results to show how well the modified method works.

B. INTEGRAL CONTROL METHOD

Before proceeding with the method of integral control, the linearized system equations must be modified. If the cross track error y needs to reach zero at steady state

conditions in the presence of constant disturbances, then the state equations are augmented by

$$\dot{y}_I = y \quad . \tag{4.1}$$

Feedback of y_I then brings in the desired integral action. The augmented linear control law becomes

$$\delta = k_1\psi + k_2 v + k_3 r + k_4 y + k_n satsgn(\sigma) \quad , \tag{4.2}$$

$$\sigma = s_1\psi + s_2 v + s_3 r + s_4 y + s_5 y_I \quad . \tag{4.3}$$

Then at steady state,

$$r_s = v_s = \delta_s = 0$$

and (3.4) still holds with the additional $y_s = 0$ from (4.1).

C. STEADY STATE ERROR

The requirement of $\delta_s = 0$ and (4.2) with (3.4) yield

$$-1 \le satsgn(\sigma) = \frac{k_1}{k_n} \sin^{-1}\left(\frac{v_c}{u}\right) \le 1 \quad , \tag{4.4}$$

which establishes the lowest limit, $k_n \ge k_{crit}$, with k_{crit} given by (3.14). As long as this inequality is satisfied, then the integral control method will drive the cross track offset y to zero. The closed loop poles on the sliding plane were selected at [-0.35,-0.36,-0.37,-0.05], with $\phi = 0.5$ and $u = 6$ ft/sec. This gives

$$\delta = 1.2948\psi - 0.0834v + 1.6206r + 0.0080y + k_n sat sgn(\sigma) \qquad (4.5)$$

$$\sigma = 3.3118\psi + 0.2635v + 3.5612r + 0.0948y + 0.0035y_I \quad . \qquad (4.6)$$

Figure 10 shows how the integral control method works in the presence of a constant disturbance, a current. The current was U_c = 0.0, V_c = 2.0 ft/sec, which means that v_c = 1.4142 ft/sec for the chosen way point of (X,Y) = (20,20) ship lengths. Using (3.14), k_{crit} = 0.3081. Figure 10 was conducted using k_n = 2.0, which is larger than k_{crit}. From (4.4),

$$\frac{k_1}{k_n} \sin^{-1}\left(\frac{v_c}{u}\right) = 0.1540 \quad ,$$

thus the inequality of (4.4) is satisfied; and as seen in Figure 10, the integral control method drives the cross track offset y to zero, with some overshoot. As k_n is increased, the cross track error is brought to zero quicker, but the rudder is cycled much more excessively. Figure 11 was conducted with k_n = 0.2, which is smaller than k_{crit}, and the same current conditions as in Figure 10. From (4.4),

$$\frac{k_1}{k_n} \sin^{-1}\left(\frac{v_c}{u}\right) = 1.5404 \quad ,$$

thus the inequality of (4.4) is <u>not</u> satisfied and a steady state error developed. As seen in Figure 11, if the nonlinear gain is not selected large enough; i.e., if $k_n < k_{crit}$; then the integral controller cannot guarantee zero steady state error. In this case,

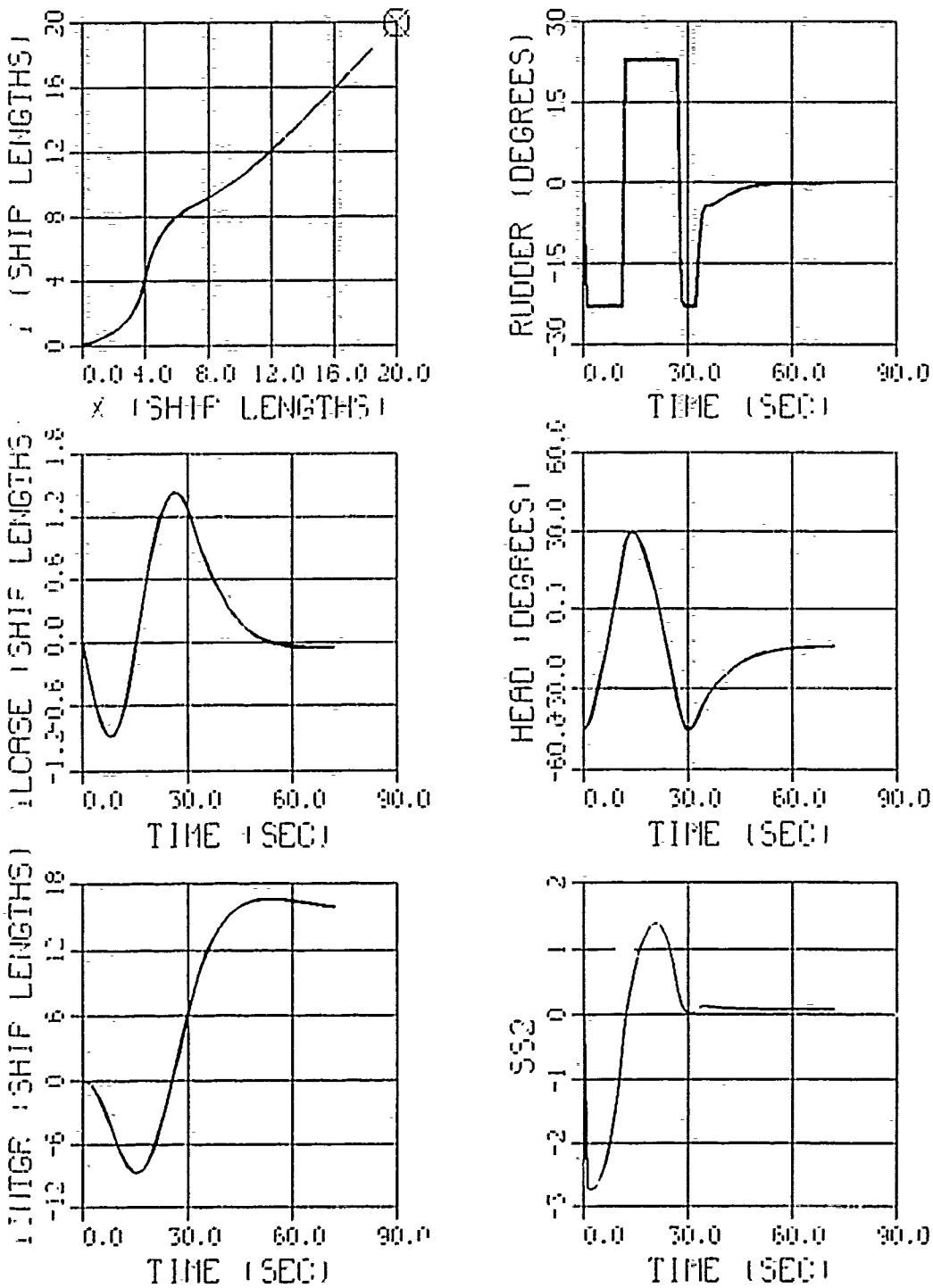

Figure 10. Integral Control with $V_c = 2$ and for $k_a > k_{crit}$.

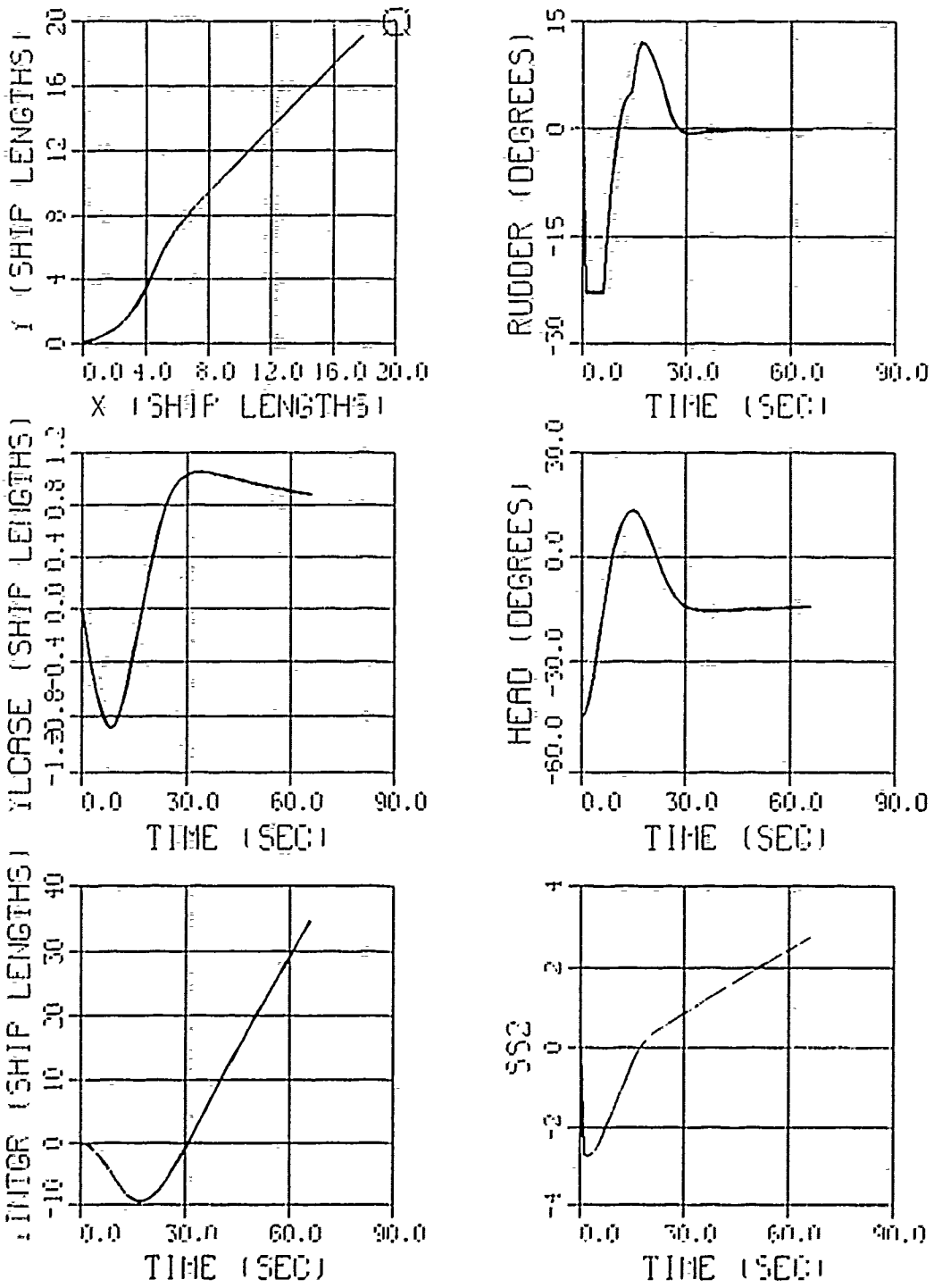

Figure 11. Integral Control with $V_c = 2$ and for $k_A < k_{crit}$.

$$satsgn(\sigma) = 1 \quad ,$$

which means $\sigma \geq \phi$, and using $\delta_s = 0$ and (3.4),

$$y_s = \frac{1}{k_4}\left[k_1 \sin^{-1}\left(\frac{v_c}{u} \right) - k_n \right] . \tag{4.7}$$

Equation (4.7) yields the steady state cross track error of the integral controller for small k_n. This was seen in Figure 11, where the integral control design developed a constant track deviation, unlike the cross track error controller which was unstable. Using (4.7), with the given values, $y_s = 0.7765$, as seen in the YLCASE vs TIME graph of Figure 11. This unique characteristic of the sliding mode track controller - the existence of a nonzero steady state error - is attributed to the lack of a linear feedback gain in y_l in (4.2). The term y_l appears only in the sliding surface equation (4.3), and if the nonlinear gain k_n does not possess the necessary strength, it cannot guarantee steady state accuracy. A modified integral control method will be developed later to solve this problem with the integral control method. In the case where the integral controller is operating in the environment with no current, Figure 12 shows that the vehicle achieves the desired track with zero steady state error.

Results for multiple way points are presented in Figures 13 and 14. The way points were again selected at (X,Y) = (10,0), (20,5) and (30,5), for comparison. The target distance for both figures was two vehicle lengths. Figure 13 shows the integral controller not having enough time, for the given current, to drive the vehicle onto the desired track.

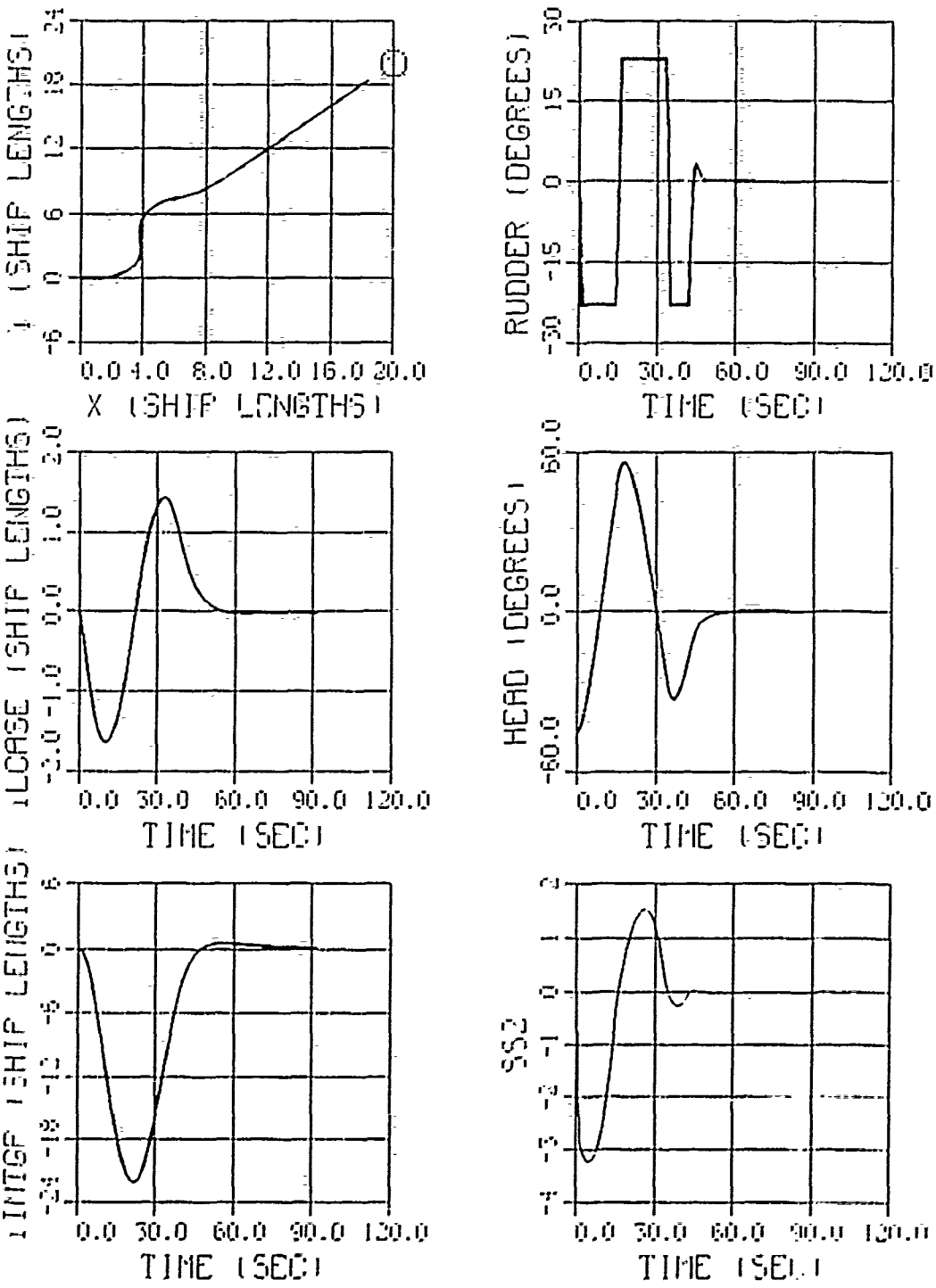

Figure 12. Integral Control with No Current.

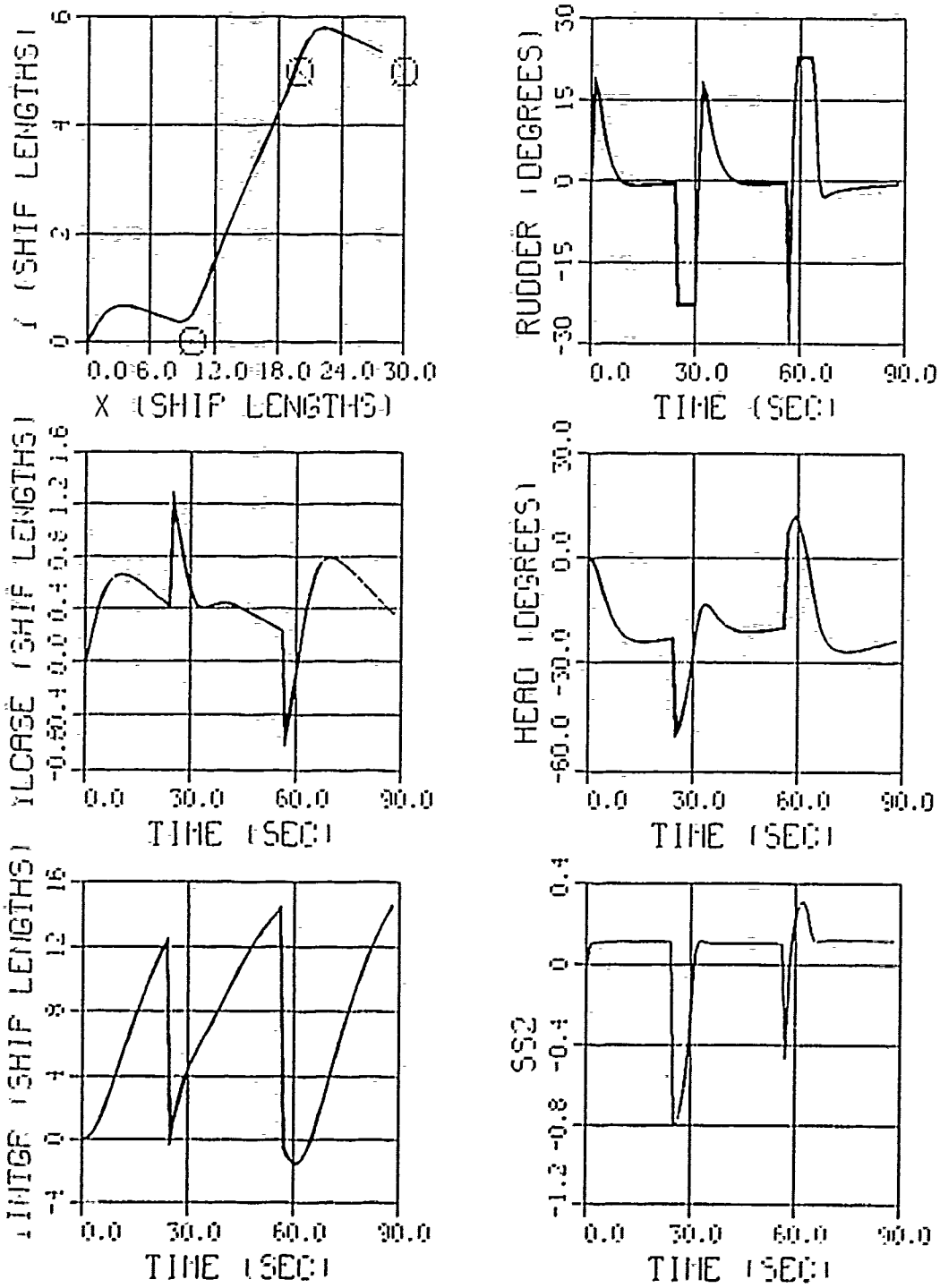

Figure 13. Lane Changing Maneuver Under Integral Control in a Current.

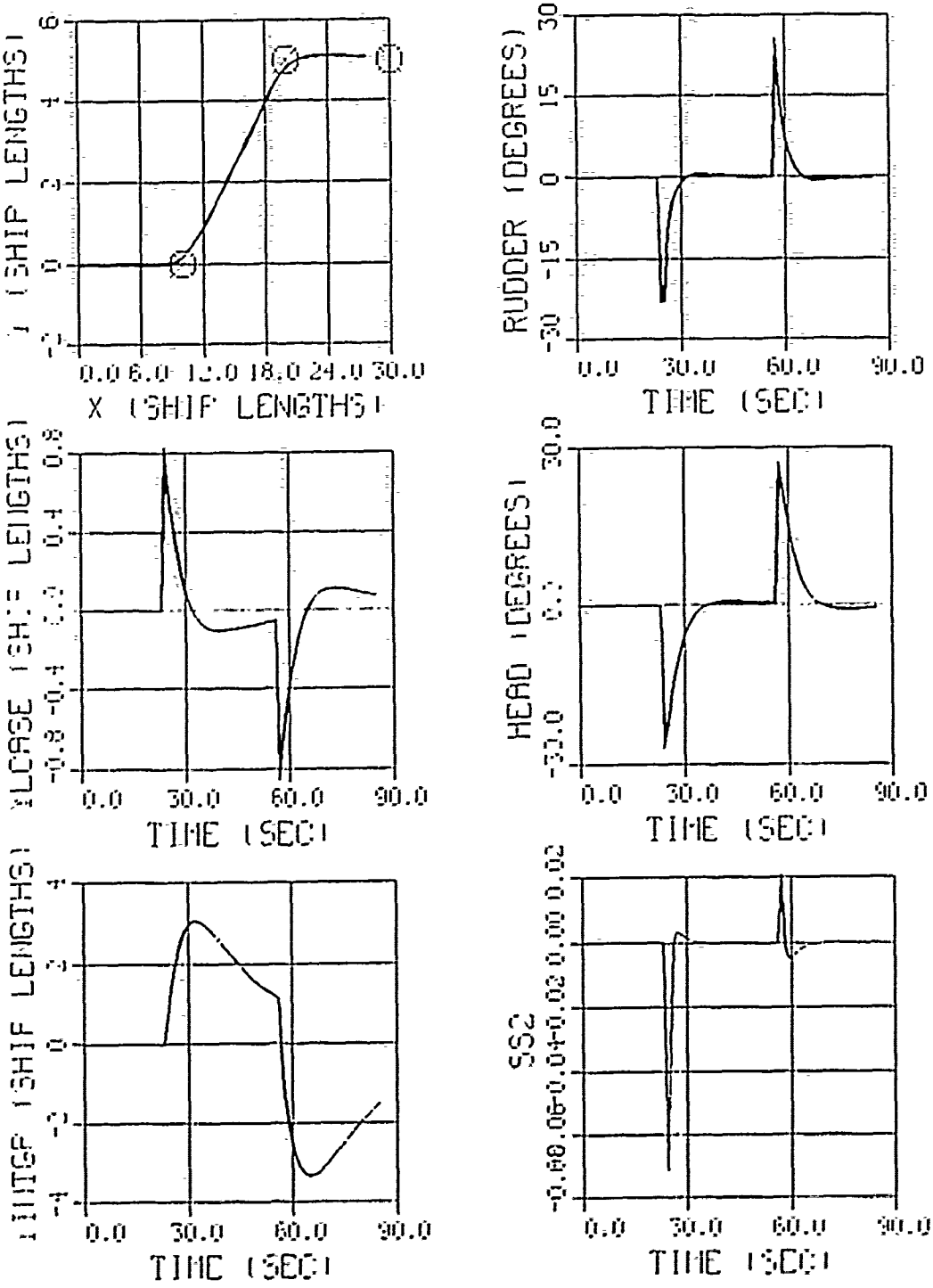

Figure 14. Lane Changing Maneuver Under Integral Control with No Current.

The current conditions for Figures 13 and 14 were as in Figure 10 with $k_n = 2.0$. Figure 14 shows how well the integral controller works for multiple way points with no current.

D. MODIFIED INTEGRAL CONTROL

An alternate design procedure that can eliminate the problem of the existence of a nonzero steady state track error, using integral control, is the modified integral control. Consider the linear system

$$\dot{x} = Ax + bu \tag{4.8}$$

and the sliding surface

$$\sigma = s^T x \quad . \tag{4.9}$$

The sliding condition $\sigma\dot{\sigma} < 0$ is met by

$$\dot{\sigma} = -\eta^2 sign(\sigma) \quad , \tag{4.10}$$

which gives the control law

$$u = -(s^T b)^{-1} s^T A x - \eta^2 (s^T b)^{-1} sign(\sigma) \quad . \tag{4.11}$$

Then, s can be found as a left eigenvector of the closed loop dynamics matrix which corresponds to the zero eigenvalue, as developed in Chapter Two. If, instead of (4.10), it is required that $\sigma\dot{\sigma} < 0$ be met by

$$\dot{\sigma} + \xi\sigma = -\eta^2 sign(\sigma) \quad ; \quad \xi > 0 \quad , \tag{4.12}$$

then the control law becomes

$$u = -(s^T b)^{-1} s^T (A + \xi I)x - \eta^2 (s^T b)^{-1} sign(\sigma) \quad , \tag{4.13}$$

and s can be found as a left eigenvector of the closed loop dynamics matrix which corresponds to the eigenvalue $-\xi$. Provided ξ is chosen small enough, (4.12) satisfies a "near" sliding condition and a sliding condition in the limit, $t \rightarrow \infty$. In this case of track control, (4.13) becomes

$$\delta = (k_1 + \xi s_1)\psi + (k_2 + \xi s_2)v + (k_3 + \xi s_3)r + (k_4 + \xi s_4)y + \xi s_5 y_I$$

$$+ k_n satsgn(\sigma) \quad . \tag{4.14}$$

Results are presented in Figure 15 for v_c = 1.4142 ft/sec lateral current, ξ = 0.1 and k_n = 0.2. It can be seen that the presence of the ξ - term in (4.14) eliminates the steady state error that is otherwise present. For k_n values higher than k_{crit}, the response characteristics of the two integral control laws (4.2) and (4.14) are very similar, as seen in Figure 16. Figure 16 used k_n = 2.0 and when compared to Figure 15 and Figure 10, all figures show similar results for $k_n > k_{crit}$.

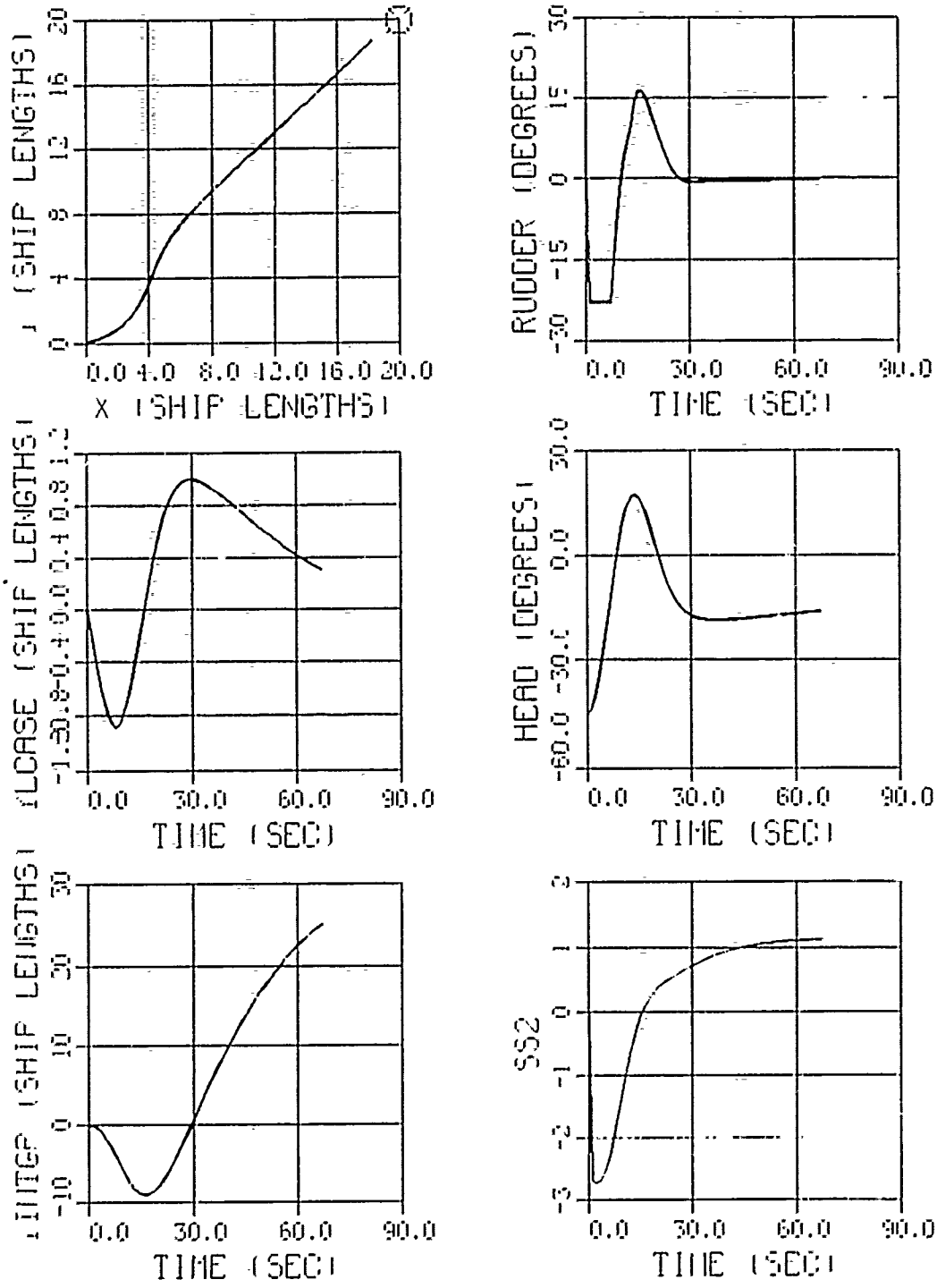

Figure 15. Modified Integral Control, $V_c = 2$, $k_n < k_{cnt}$, $\xi = 0.1$.

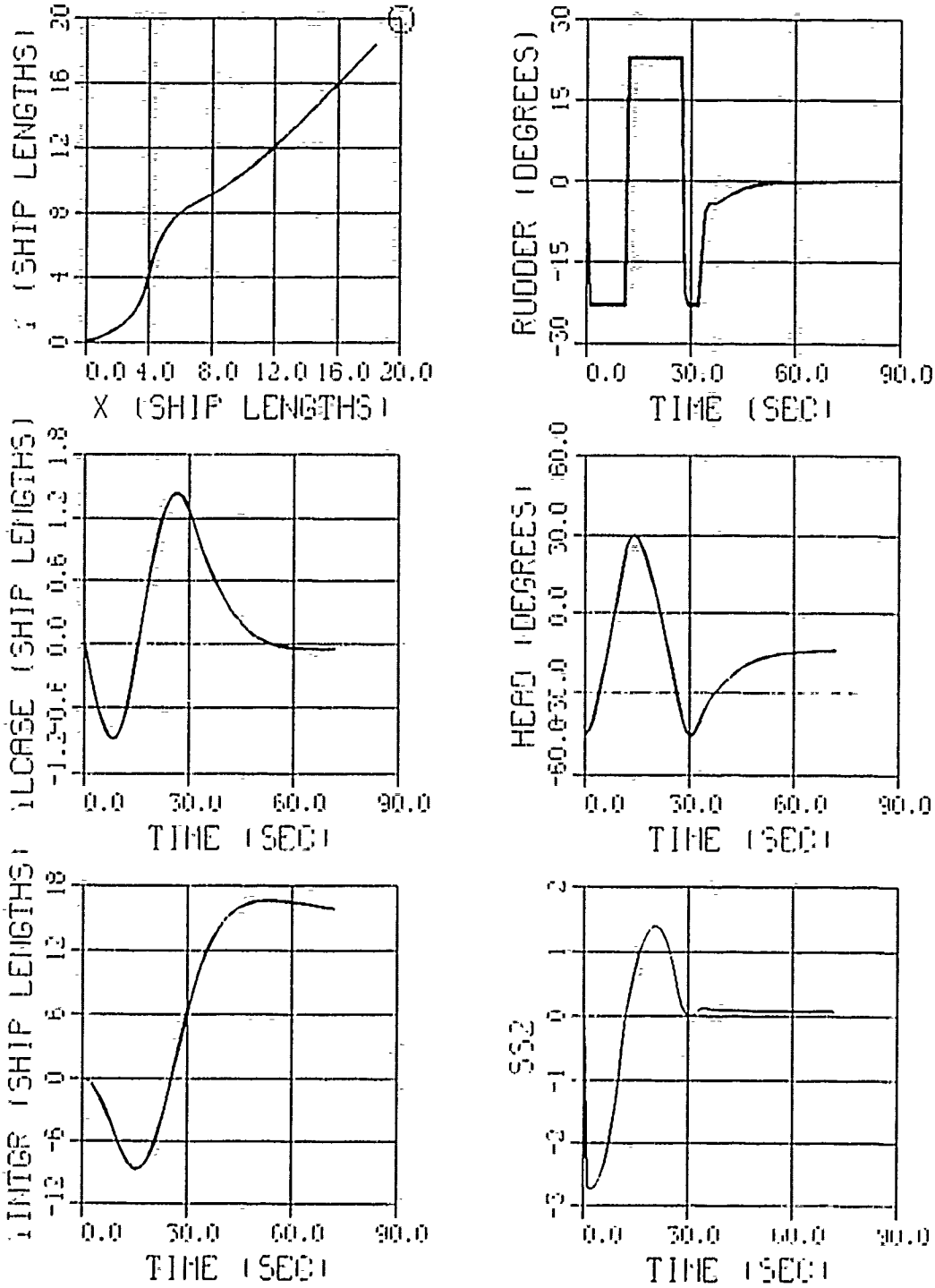

Figure 16. Modified Integral Control, $V_c = 2$, $k_n > k_{crit}$, $\xi = 0.1$.

V. DISTURBANCE ESTIMATION AND COMPENSATION METHOD

A. INTRODUCTION

The integral control methods of the previous section will ensure zero steady state error, for $k_n > k_{crit}$ and for $k_n < k_{crit}$, especially when using the modified integral control method. To improve on the transient response and to achieve the desired steady state, a disturbance estimation and compensation can be introduced in the cross track error design of the controller. This chapter will investigate the disturbance estimation and compensation method, which formulates the current as a disturbance to be included directly into the control law. In this chapter, the disturbance compensation method will first be developed with a perfect current input and then the disturbance estimation and compensation method will be developed with an estimate of the current using a current observer. This method will follow the same development as for the integral control. First, a single way point will be investigated with current and then without current, to see how well both methods control the AUV onto the desired track. Multiple way points will next be investigated and results will be given to show how well both methods handle these multiple way points. This methodology will be followed for the perfect current input as well as for the estimated current input.

B. DISTURBANCE COMPENSATION METHOD

The sliding surface (3.6) is modified to

$$\sigma = s_1\psi + s_2 v + s_3 r + s_4 y + \left(\phi \frac{k_1}{k_n} + s_1 \right) \sin^{-1}\left(\frac{v_c}{u}\right) , \tag{5.1}$$

with δ as in (3.5). At steady state, $r_s = v_s = \delta_s = 0$ and (3.4) is valid with $y_s = 0$, as dictated by (5.1) and

$$satsgn(\sigma) = \frac{\sigma}{\phi} .$$

If $k_n < k_{crit}$, then the disturbance compensation controller, with the cross track error, cannot guarantee stability. The steady state response in such a case is characterized by

$$r_s = v_s = \delta_s = 0 \tag{5.2}$$

and by

$$\psi_s = -\sin^{-1}\left(\frac{k_n}{k_1}\right) , \tag{5.3}$$

with y_s linearly increasing in time with the rate of change given by

$$\dot{y}_s = \frac{v_c}{u} - \sin\left(\frac{k_n}{k_1}\right) . \tag{5.4}$$

Equation (5.3) is obtained from (3.5) for $\delta_s = 0$ with $satsgn(\sigma) = 1$.

C. STEADY STATE ERROR

Again the requirement of $\delta_s = 0$ and (4.2) with (3.4) yields (4.4), which establishes the lowest limit, $k_n \geq k_{crit}$, with k_{crit} given by (3.14). Again, as long as this inequality is satisfied, the disturbance compensation method will drive the cross track offset y to zero. The closed loop poles on the sliding plane were again selected at [-0.35, -0.36, -0.37], with $\phi = 0.5$ and u = 6 ft/sec. This gives

$$\delta = 0.9556\psi - 0.1085v + 1.2286r + k_n sat sgn(\sigma) \tag{5.5}$$

$$\sigma = 2.9805\psi + 0.2199v + 3.4445r + 0.0700y + \left(\frac{0.4778}{k_n} + 2.9805\right) \sin^{-1}(0.2357). \tag{5.6}$$

Figure 17 shows how the disturbance compensation method works in the presence of a current, $U_c = 0.0$, $V_c = 2.0$ ft/sec, which means that $v_c = 1.4142$ ft/sec for the chosen way point (X,Y) = (20,20) ship lengths. Using (3.14), $k_{crit} = 0.3081$, as for the integral control method. Figure 17 was conducted using a perfect current input and $k_n = 2.0$, which is larger than k_{crit}. As seen in Figure 17, the disturbance compensation method brings the steady state error to zero with no overshoot and with a quicker response than the integral control method. In Figure 17 and all subsequent similar figures for the disturbance compensation and the disturbance estimation and compensation methods, the following variables are displayed: X vs Y position, rudder angle vs TIME, the cross track error (YLCASE) vs TIME, the heading $\psi - \alpha$ (HEAD) vs TIME, v_c (VCUR) vs TIME

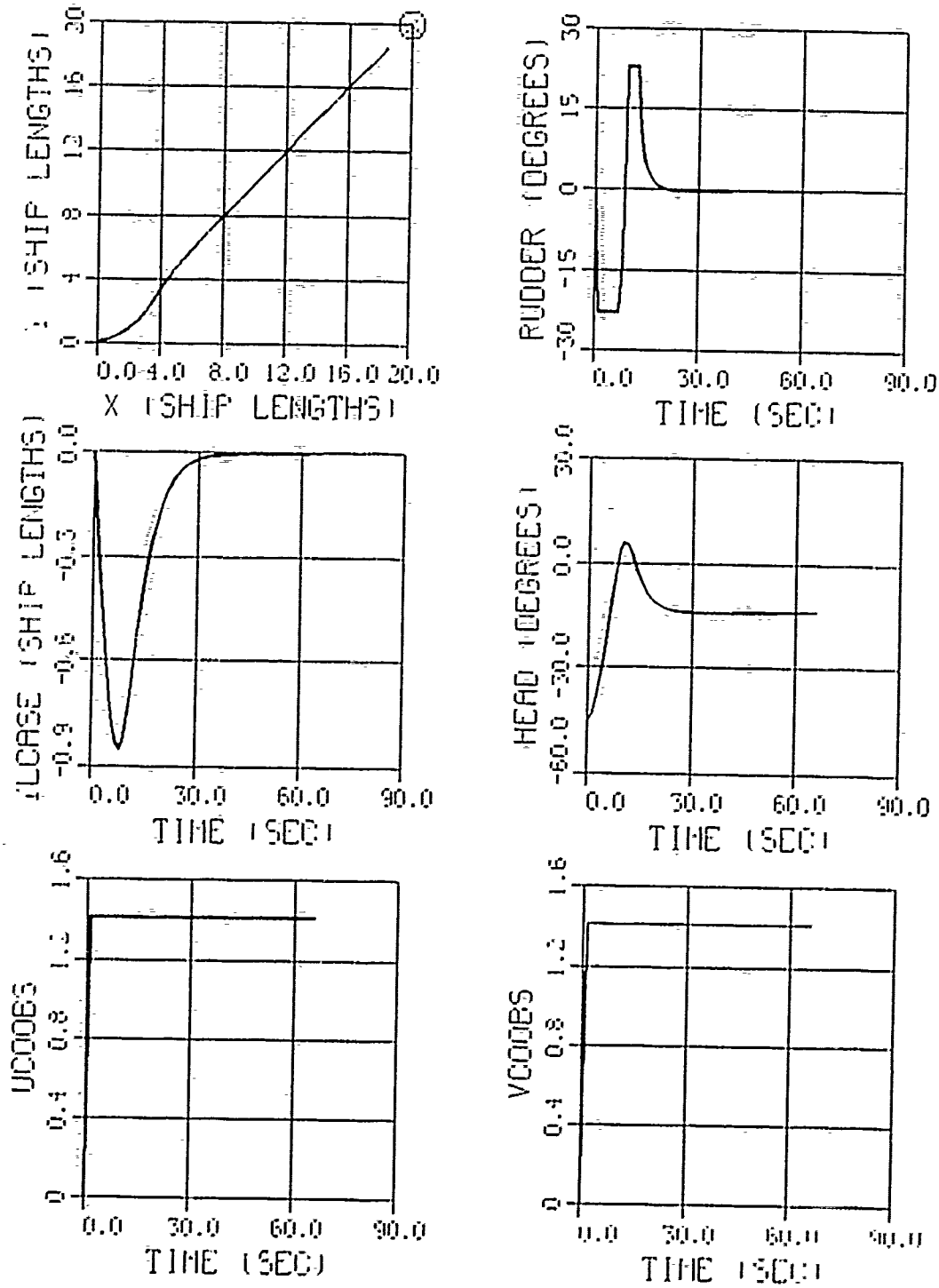

Figure 17. Disturbance Compensation, $V_c = 2$, $k_n > k_{crit}$.

and u_c (UCUR) vs TIME, for the perfect current input; and $\hat{v}_c$ (VCOOBS) vs TIME and $\hat{u}_c$ (UCOOBS) vs TIME, for the estimated current input. Figure 18 shows how the disturbance compensation method works in the presence of the same current conditions as in Figure 17 for k_n = 0.2, which is less than k_{crit}. As seen in Figure 18, the disturbance compensation method design gives rise to unstable behavior.

Results for multiple way points are presented in Figure 19. The way points were selected at (X,Y) = (10,0), (20,5) and (30,5) ship lengths, for comparison. Again, the target distance was selected at 2 vehicle lengths. Figure 19 was conducted with the same current conditions as in Figure 17.

D. CURRENT OBSERVER DEVELOPMENT

As seen in the previous section, the disturbance compensation method works well with absolute knowledge of the current. However, in reality, the current is never absolutely known at every location, so a current observer must be developed. A reduced order observer can be designed based on y, ψ and r measurements to estimate the lateral current velocity v_c and the current velocity along the track u_c. The observer design is based on the linear equations (2.1a), (2.1b), (2.1c) and

$$\dot{y} = v_c + u\psi + v \tag{5.7}$$

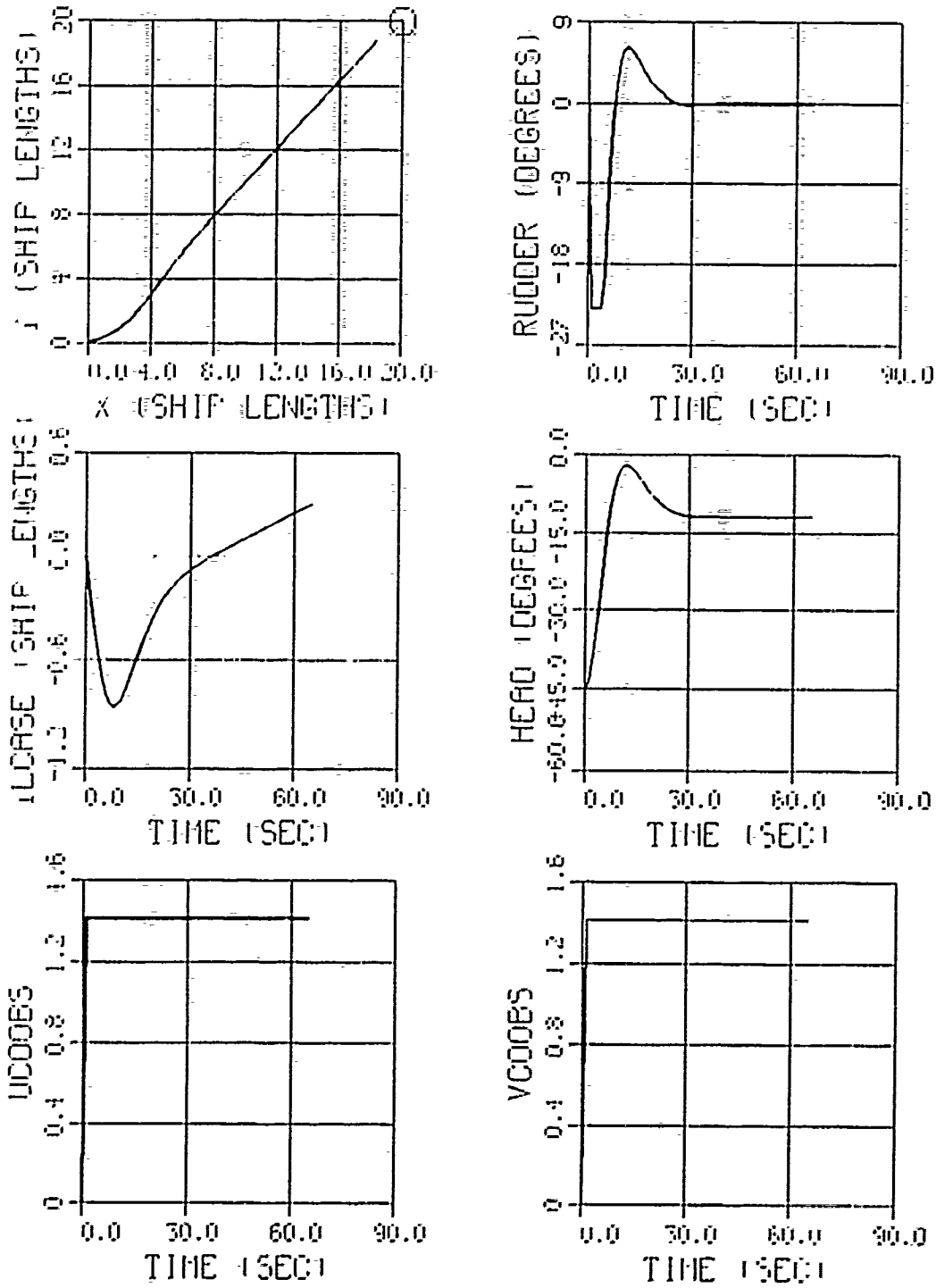

Figure 18. Disturbance Compensation, $V_c = 2$, $k_n < k_{cnt}$.

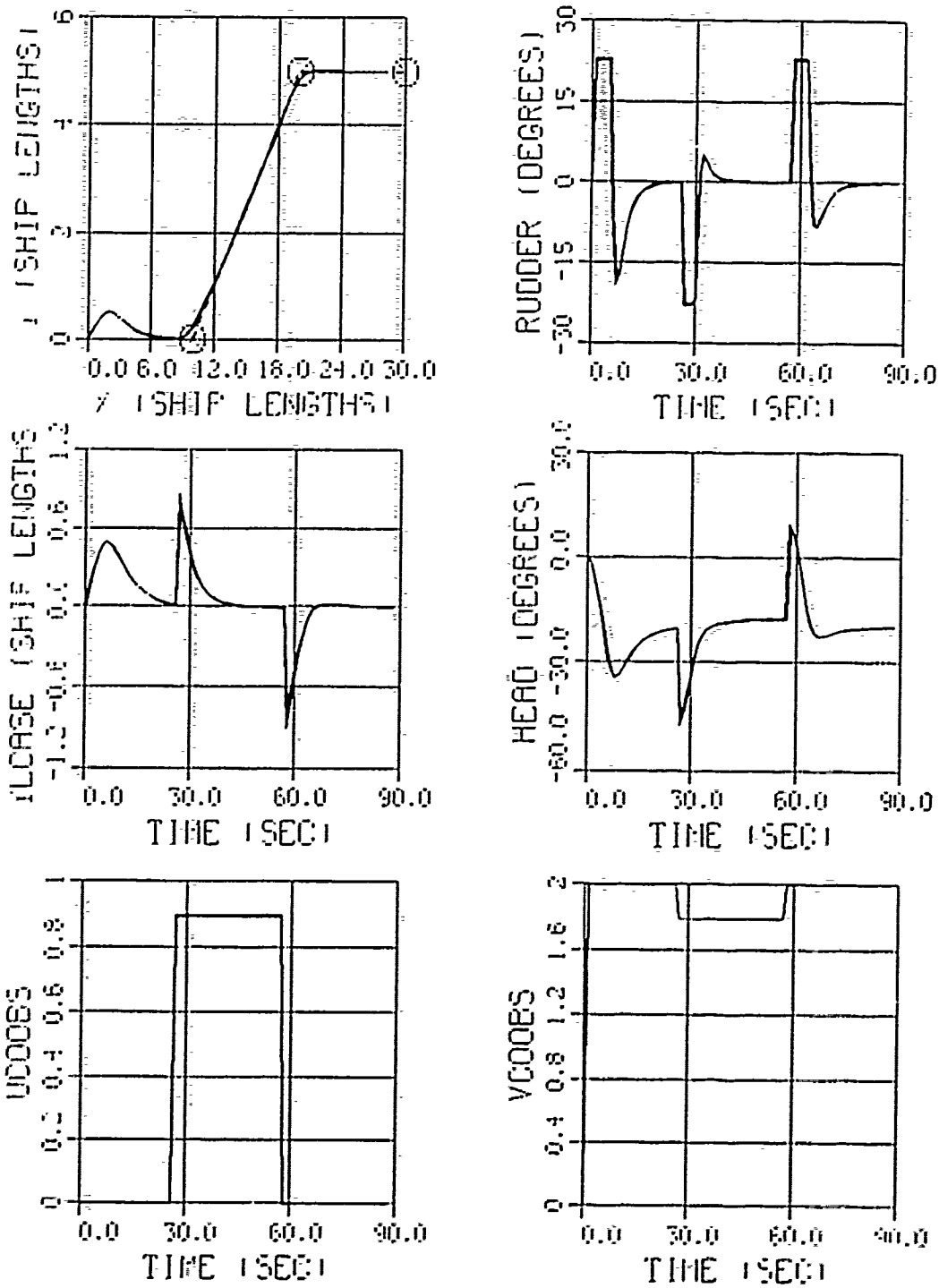

Figure 19. Lane Changing Maneuver Under Disturbance Compensation in a Current.

$$\dot{x} = u_c + u = u_c' \tag{5.8}$$

$$\dot{v}_c = 0 \tag{5.9}$$

$$\dot{u}_c = 0 \quad . \tag{5.10}$$

Rewriting these equations into matrix form,

$$\frac{d}{dt}\begin{bmatrix} x_1 \\ x_2 \end{bmatrix} = \begin{bmatrix} A_{11} & A_{12} \\ A_{21} & A_{22} \end{bmatrix}\begin{pmatrix} x_1 \\ x_2 \end{pmatrix} + \begin{bmatrix} B_1 \\ B_2 \end{bmatrix}\delta \tag{5.11}$$

where

$$x_1{}^T = [\psi \; r \; y \; x] \quad ,$$

$$x_2{}^T = [v \; v_c \; u_c] \quad ,$$

$$A_{11} = \begin{bmatrix} 0 & 1 & 0 & 0 \\ 0 & a_{22}u & 0 & 0 \\ 1 & 0 & 0 & 0 \\ 0 & 0 & 0 & 0 \end{bmatrix} \quad ,$$

$$A_{12} = \begin{bmatrix} 0 & 0 & 0 \\ a_{21}u & 0 & 0 \\ 1 & 1 & 0 \\ 0 & 0 & 1 \end{bmatrix} ,$$

$$A_{21} = \begin{bmatrix} 0 & a_{12}u & 0 & 0 \\ 0 & 0 & 0 & 0 \\ 0 & 0 & 0 & 0 \end{bmatrix} ,$$

$$A_{22} = \begin{bmatrix} a_{11}u & 0 & 0 \\ 0 & 0 & 0 \\ 0 & 0 & 0 \end{bmatrix} ,$$

$$B_1^T = [0, b_2u^2, 0, 0] \quad ,$$

and

$$B_2^T = [b_1u^2, 0, 0] \quad .$$

Equation (5.11) takes on the state space form of

$$\dot{x} = Ax + B\delta \tag{5.12a}$$

$$y = Cx \quad , \tag{5.12b}$$

where

$$C = I \quad ,$$

x_1^T are the measurable states and x_2^T are the states to be estimated or observed.

Expanding (5.12a),

$$\dot{x}_1 = A_{11}x_1 + A_{12}x_2 + B_1\delta$$

$$\dot{x}_2 = A_{21}x_1 + A_{22}x_2 + B_2\delta \quad .$$

From the Luenberger reduced order observer development for $\hat{x}_2$, the estimated or observed states are

$$\hat{x}_2 = Lx_1 + z_1 \quad , \tag{5.13}$$

and

$$\dot{z} = Fz + Gx_1 + H\delta \quad , \tag{5.14}$$

where

$$F = A_{22} - LA_{12} \quad , \tag{5.15}$$

$$G = A_{21} - LA_{11} \quad , \tag{5.16}$$

and

$$H = B_2 - LB_1 \quad . \tag{5.17}$$

In the above equations, the L matrix needs to be determined. The MATRIX_x software package is unable to determine the L matrix directly because more than one output is measurable. Therefore, the L matrix will be determined manually. Let

$$L = \begin{bmatrix} l_{11} & l_{12} & l_{13} & l_{14} \\ l_{21} & l_{22} & l_{23} & l_{24} \\ l_{31} & l_{32} & l_{33} & l_{34} \end{bmatrix}$$

and choose everything zero, except l_{12}, l_{23} and l_{34}, so that

$$L = \begin{bmatrix} 0 & l_{12} & 0 & 0 \\ 0 & 0 & l_{23} & 0 \\ 0 & 0 & 0 & l_{34} \end{bmatrix} .$$

From (5.15),

$$F = A_{22} - LA_{12} = \begin{bmatrix} a_{11}u - l_{12}a_{21}u & 0 & 0 \\ -l_{23} & -l_{23} & 0 \\ 0 & 0 & -l_{34} \end{bmatrix} . \qquad (5.18)$$

Now choose the observer poles of s_1, s_2 and s_3 to be at -1.0, -1.1 and -1.2, respectively, which are at least two times faster than the controller poles, defined in the above section, as required by a good observer design. Placing the observer poles in matrix form and equating to (5.18),

$$s_1 = a_{11}u - l_{12}a_{21}u \quad , \qquad (5.19a)$$

$$s_2 = -l_{23} \qquad (5.19b)$$

and

$$s_3 = -l_{34} \quad . \qquad (5.19c)$$

Solving (5.19) for l_{12}, l_{23} and l_{34},

$$l_{12} = \frac{a_{11}u - s_1}{a_{21}u} \quad , \tag{5.20a}$$

$$l_{23} = -s_2 \tag{5.20b}$$

and

$$l_{34} = -s_3 \quad . \tag{5.20c}$$

From (5.20), the L matrix is now determined, therefore, F, G and H are also determined.

From (5.14), the reduced order observer equations become

$$\dot{z}_1 = s_1 z_1 + (a_{12}u - l_{12}a_{22}u + s_1 l_{12})r + (b_1 u^2 - l_{12}b_2 u^2)\delta \tag{5.21a}$$

$$\dot{z}_2 = s_2 z_1 + s_2 z_2 - l_{23}u\sin(\psi - \alpha) + s_2 l_{23} y + s_2 l_{12} r \tag{5.21b}$$

$$\dot{z}_3 = s_3 z_3 + s_3 l_{34} x \quad . \tag{5.21c}$$

From (5.13), the equations for the estimated or observed quantities become

$$\hat{v} = z_1 + l_{12}r \quad , \tag{5.22a}$$

$$\hat{v}_c = z_2 + l_{23}y \tag{5.22b}$$

and

$$\hat{u}'_c = z_3 + l_{34}x \quad . \tag{5.22c}$$

Due to the way $\hat{u}'_c$ was defined in (5.8),

$$\hat{u}_{c_{obs}} = \hat{u}'_c - u\cos(\psi - \alpha) \tag{5.23}$$

and

$$\hat{v}_{c_{obs}} = \hat{v}_c \quad . \tag{5.24}$$

The sine and cosine terms are not linearized in (5.21b) and (5.23) to eliminate steady state errors in the observer when the angle $\psi - \alpha$ becomes significant at steady state in the presence of strong currents. Since the current perpendicular to the track and the current along the line of each track will be different locally every time the AUV drives onto a new track, the current observer quantities of z_2 and z_3 need to be reset every time a new way point is called for by the autopilot. The quantities z_2 and z_3 are used to determine $\hat{v}_c$ and $\hat{u}'_c$ which determine $\hat{v}_{c_{obs}}$ and $\hat{u}_{c_{obs}}$. The equations used to reset z_2, z_3, $\hat{v}_c$ and $\hat{u}'_c$ are

$$\hat{v}_{c_1} = \hat{v}_c\cos\alpha - \hat{u}'_c\sin\alpha \quad , \tag{5.25}$$

$$\hat{u}'_{c_1} = \hat{u}'_c\cos\alpha - \hat{v}_c\sin\alpha \quad , \tag{5.26}$$

$$z_2 = \hat{v}_{c_1} - 1.1y \quad , \tag{5.27}$$

and

$$z_3 = \hat{u}'_{c_1} - 1.2y \quad . \tag{5.28}$$

These equations are used as the new way point is asked for and prior to entering the observer for the first time on the new track.

E. DISTURBANCE ESTIMATION AND COMPENSATION METHOD

With the development of a current observer, reality can now be better incorporated into the controller design. The sliding surface (5.1) is now modified to

$$\sigma = s_1\psi + s_2 v + s_3 r + s_4 y + \left(\frac{\phi k_1}{k_n} + s_1\right) \sin^{-1}\left(\frac{\hat{v}_{c_{est}}}{u}\right) \quad , \tag{5.29}$$

with δ as in (3-5). The rest of the development for the disturbance estimation and compensation method is exactly the same as for the disturbance compensation method. Figure 20 shows how well the disturbance estimation and compensation method works in the presence of the same environmental conditions as in Figure 17. Also the response of Figure 20 is virtually the same as for the disturbance compensation method in Figure 17. Figure 20 used a k_n = 2.0, which is larger than k_{crit}. Again for k_n = 0.2, which is less than k_{crit}, unstable behavior results, as seen in Figure 21. Figure 22 shows the results of the disturbance estimation and compensation method with no current.

Results for multiple way points, using the disturbance estimation and compensation method, are presented in Figures 23 and 24, with a target distance of 2 vehicle lengths. Figure 23 was conducted using the same current as in Figure 17. It can be seen that the disturbance estimation and compensation method works as well as the disturbance

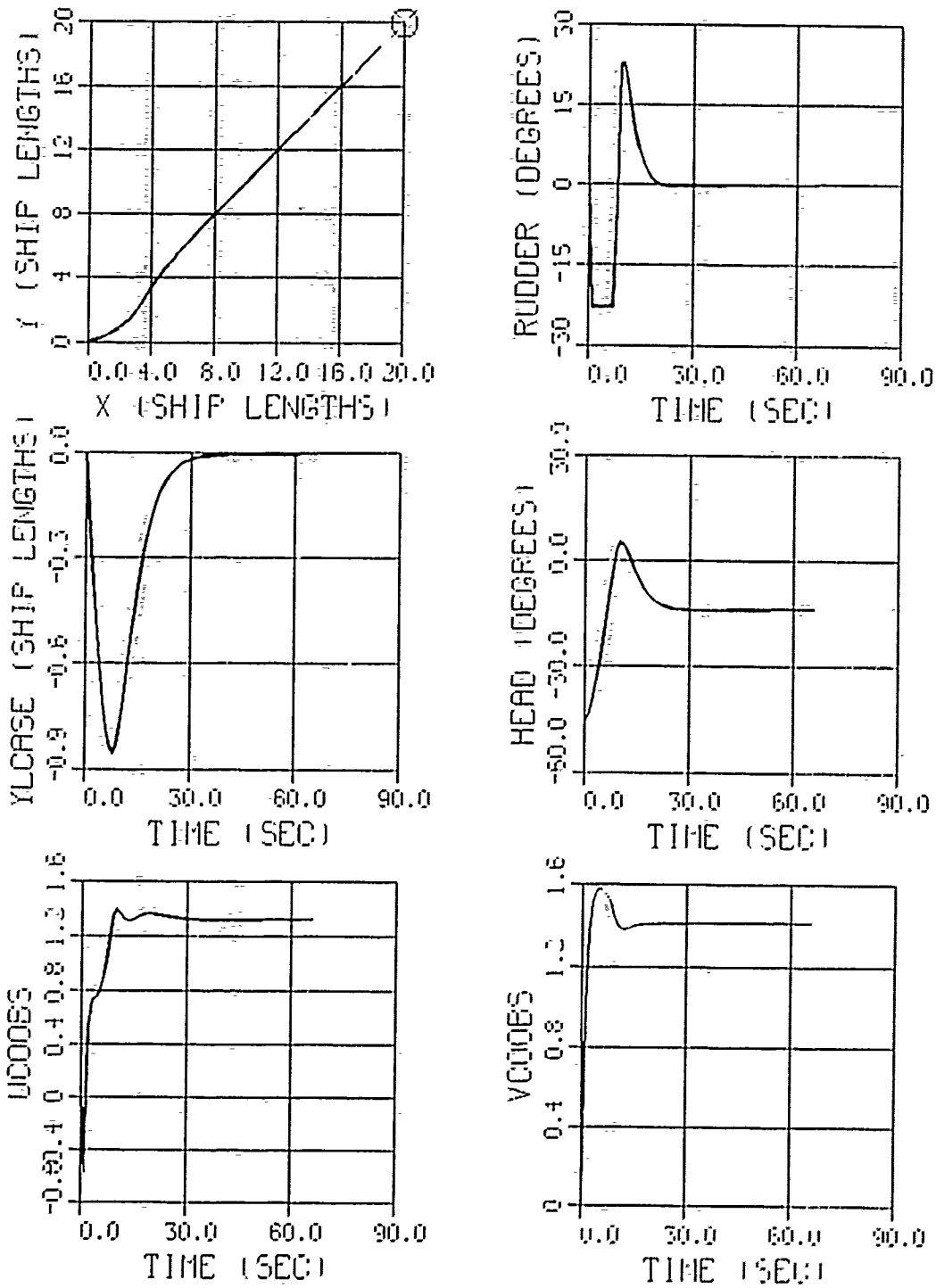

Figure 20. Disturbance Estimation and Compensation, $V_c = 2$, $k_n > k_{crit}$.

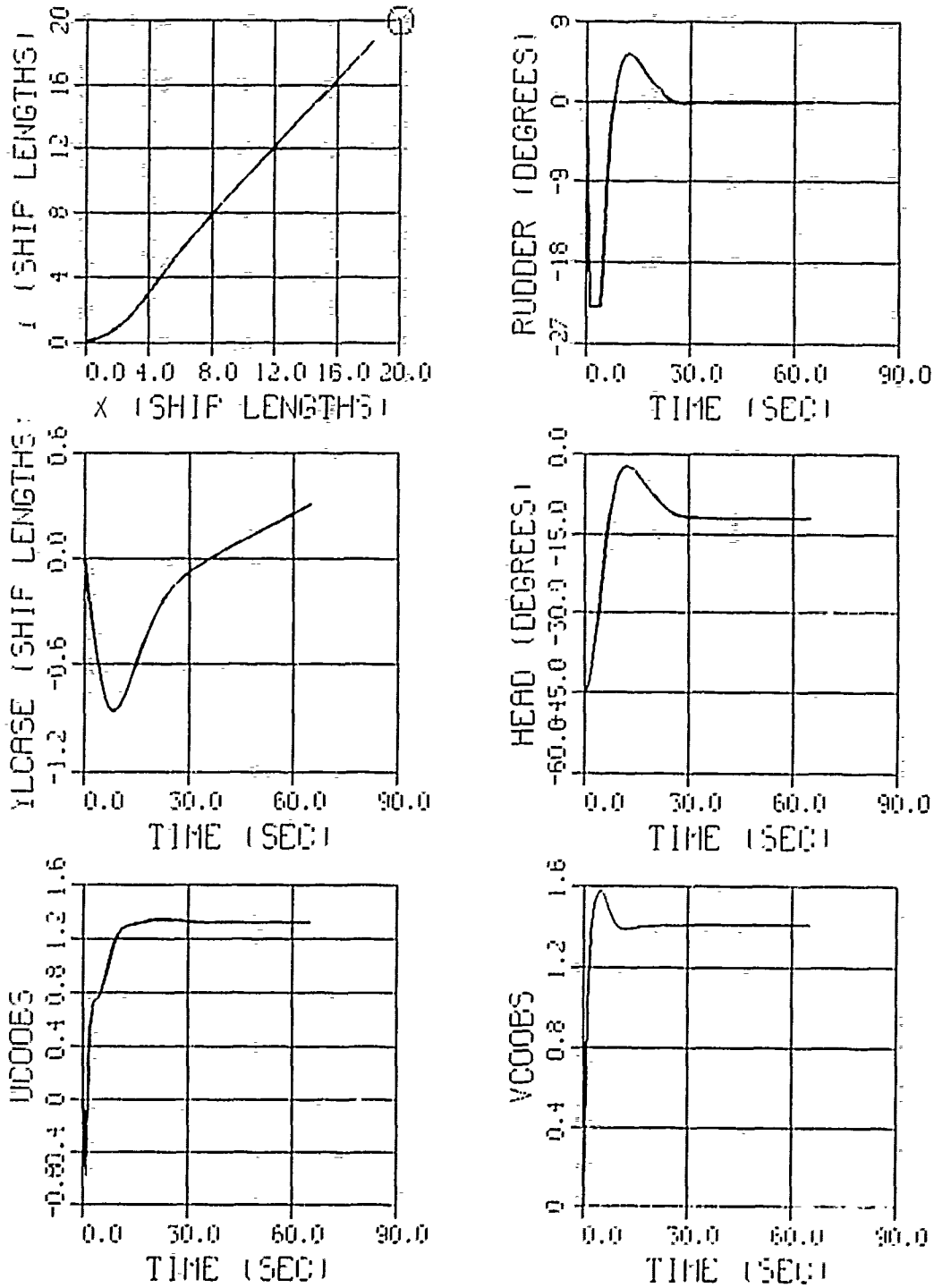

Figure 21. Disturbance Estimation and Compensation, $V_c = 2$, $k_n < k_{crit}$.

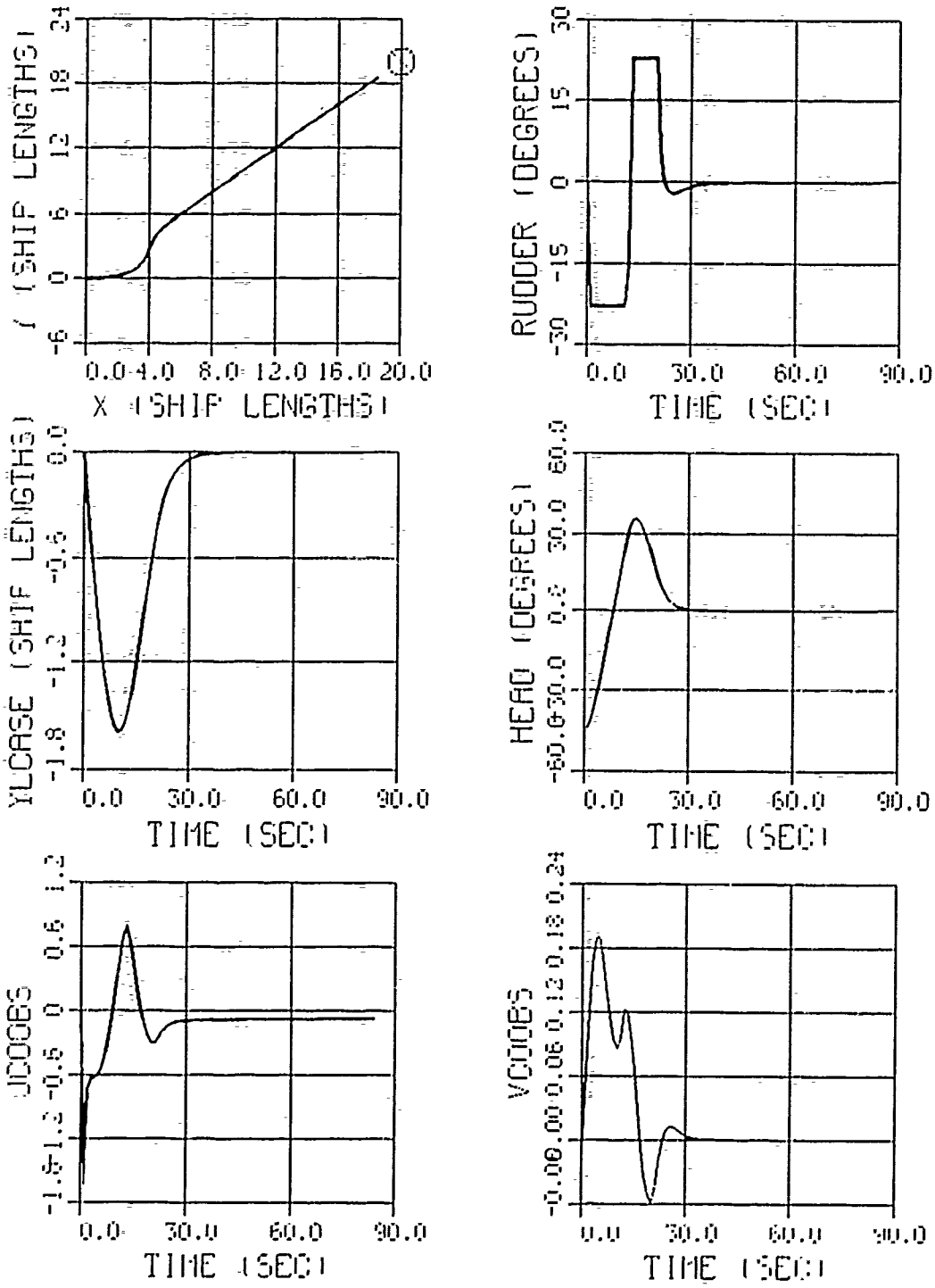

Figure 22. Disturbance Estimation and Compensation with No Current.

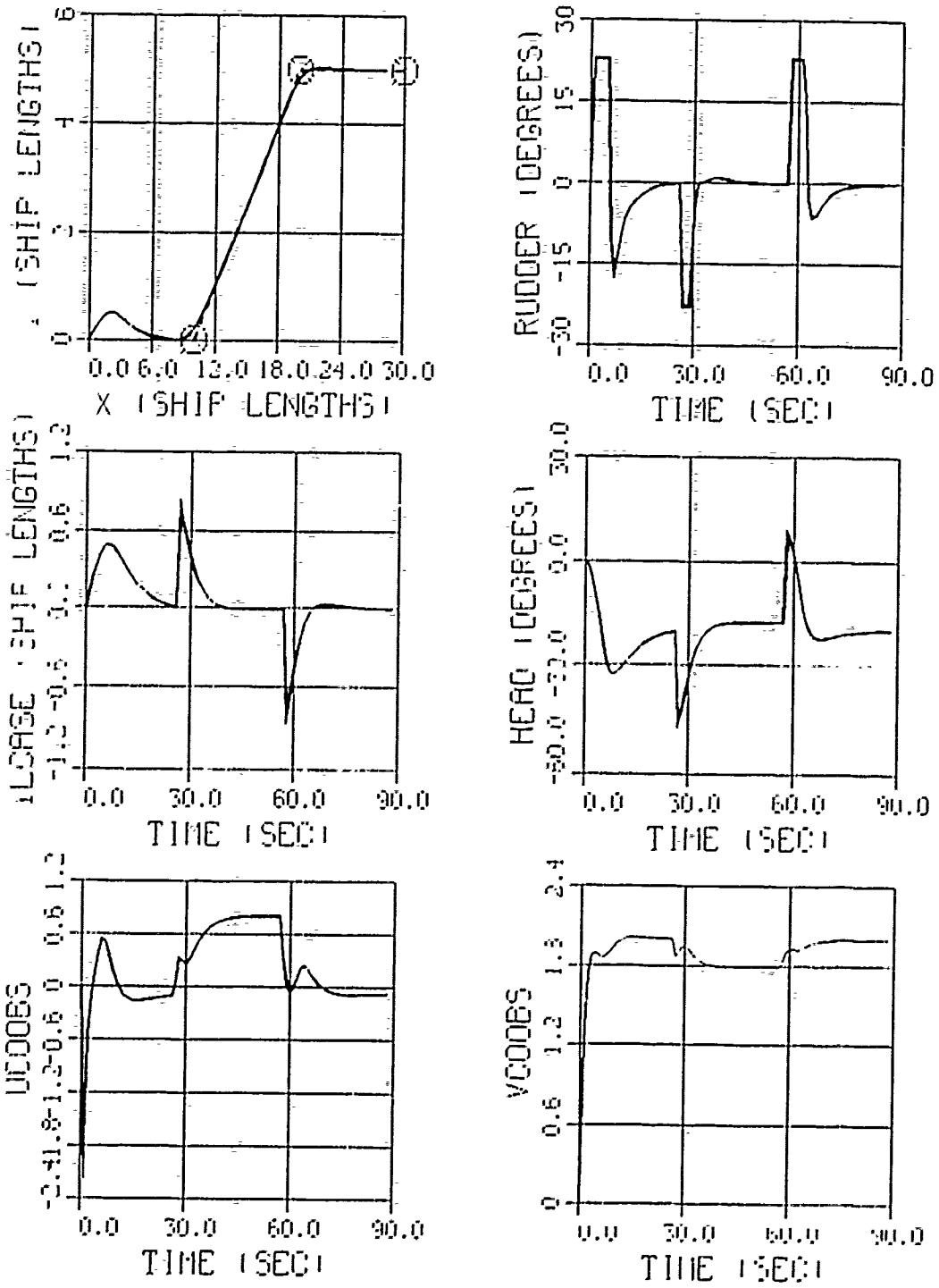

Figure 23. Lane Changing Maneuver Under Disturbance Estimation and Compensation in a Current.

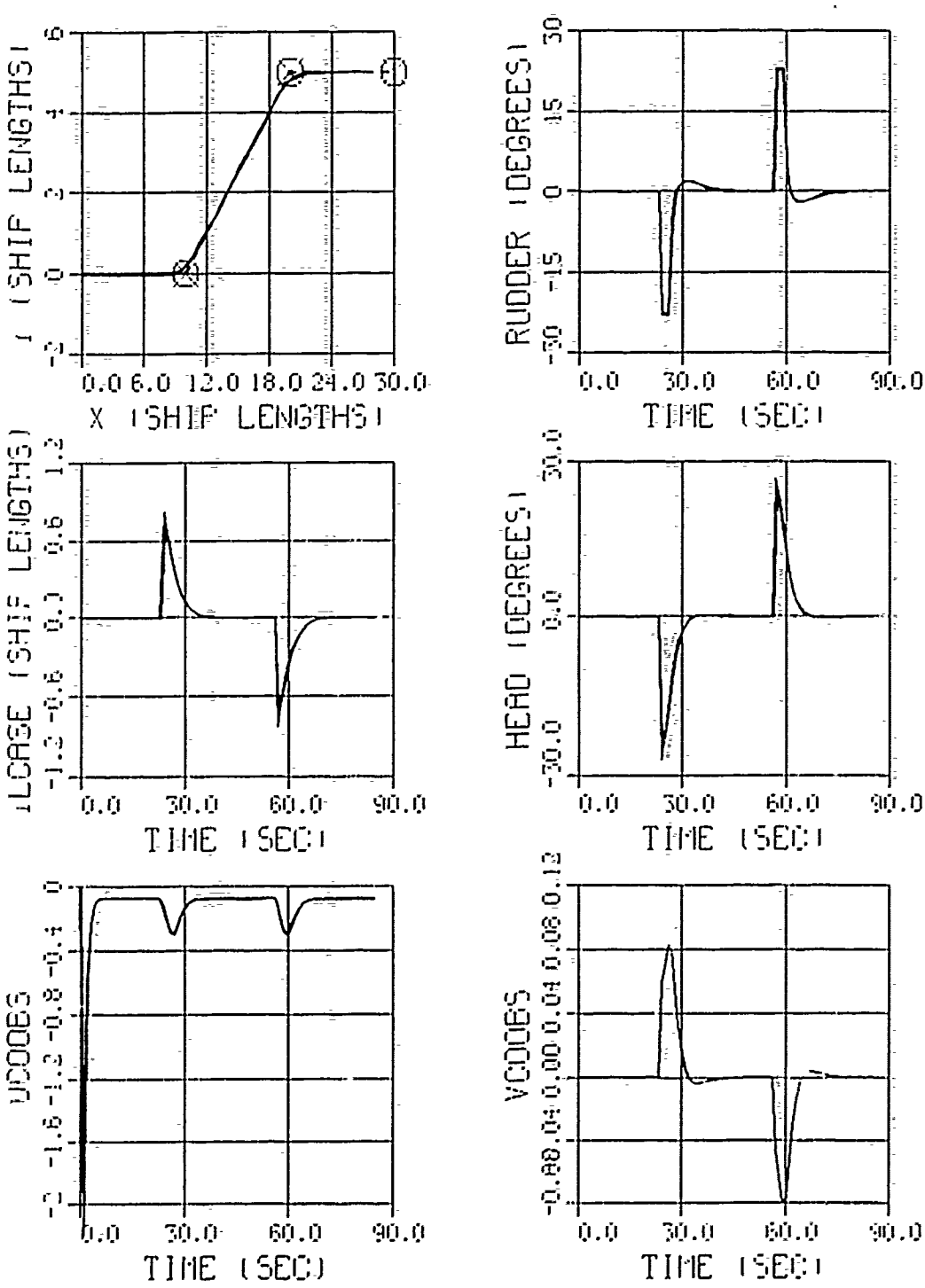

Figure 24. Lane Changing Maneuver Under Disturbance Estimation and Compensation with No Current.

compensation method, with perfect current input. Figure 24 shows how well the disturbance estimation and compensation method works for multiple way points with no current. In Figures 21 and 23 for zero estimated current in the track, it can be seen that there is a small nonzero current in the graph of UCOOBS vs TIME. This small nonzero current is a result of the integration time step not being small enough. Figures 20 through 24 were all run at a 0.01 second time step. As the time step decreases, the time to run the program increased dramatically.

F. MODIFIED DISTURBANCE ESTIMATION AND COMPENSATION

In order to overcome the instability of the disturbance estimation and compensation method for $k_n < k_{crit}$, a modified design will be considered. Similarly to the integral control method of Chapter IV, condition (4.12) will be required to be satisfied instead of (4.10), and the control law then becomes

$$\delta = (k_1+\xi s_1)\psi+(k_2+\xi s_2)v+(k_3+\xi s_3)r+\xi s_4 y+k_n satsgn(\sigma) \quad , \tag{5.30}$$

$$\sigma = s_1\psi+s_2 v+s_3 r+s_4 y+\left(\frac{\phi(k_1+\xi s_1)}{k_n}+s_1 \right) \sin^{-1}\left(\frac{v_c}{u} \right) \quad . \tag{5.31}$$

Then, at steady state $y_s = 0$ provided

$$k_n \geq k_{crit}' = \left| (k_1 + \xi s_1) \sin^{-1}\left(\frac{v_c}{u}\right) \right| \quad . \tag{5.32}$$

In this case, s can be found as the left eigenvector of the closed loop dynamics matrix that corresponds to the eigenvalue $-\xi$. For small values of ξ, the same s and k can be

used as before. If $k_n < k_{crit}'$, this modified design develops a finite steady state error, y_s, computed from $\delta_s = 0$ and $\sigma_s \geq \phi$. Results are presented in Figure 25 for the same conditions as in Figure 21, with $\xi = 0.5$. It can be seen that the nonzero value of ξ stabilized the vehicle and reduced the path error. This, however, is not always the case. The explanation lies in the fact that nonzero values of ξ raise the critical k_n as shown in (5.32). The steady state cross track errors versus ξ and k_n are shown in perspective views in Figures 26, 27 and 28, for u = 6 ft/sec and v_c = 1, 2.5 and 4 ft/sec, respectively. It can be seen that for $k_n < k_{crit}$, y_s is reduced by increasing ξ, although beyond a certain point the corresponding reduction in y_s is insignificant. For $k_n > k_{crit}$, the value of ξ should not be increased beyond the value that renders $k_n = k_{crit}'$ in (5.32), unless the vehicle is expected to operate in high current environments that would increase the value of k_{crit} in (3.14).

Chapters 3, 4 and 5 have dealt with methods to control the cross track error, due to a constant disturbance, to zero. Now that the methods have been developed and shown to work well, the next chapter will devise a technique to help optimize the time to turn, so that the turn is initiated and conducted in the most efficient manner given any environmental conditions. This technique will be referred to as the leading track control monitoring technique.

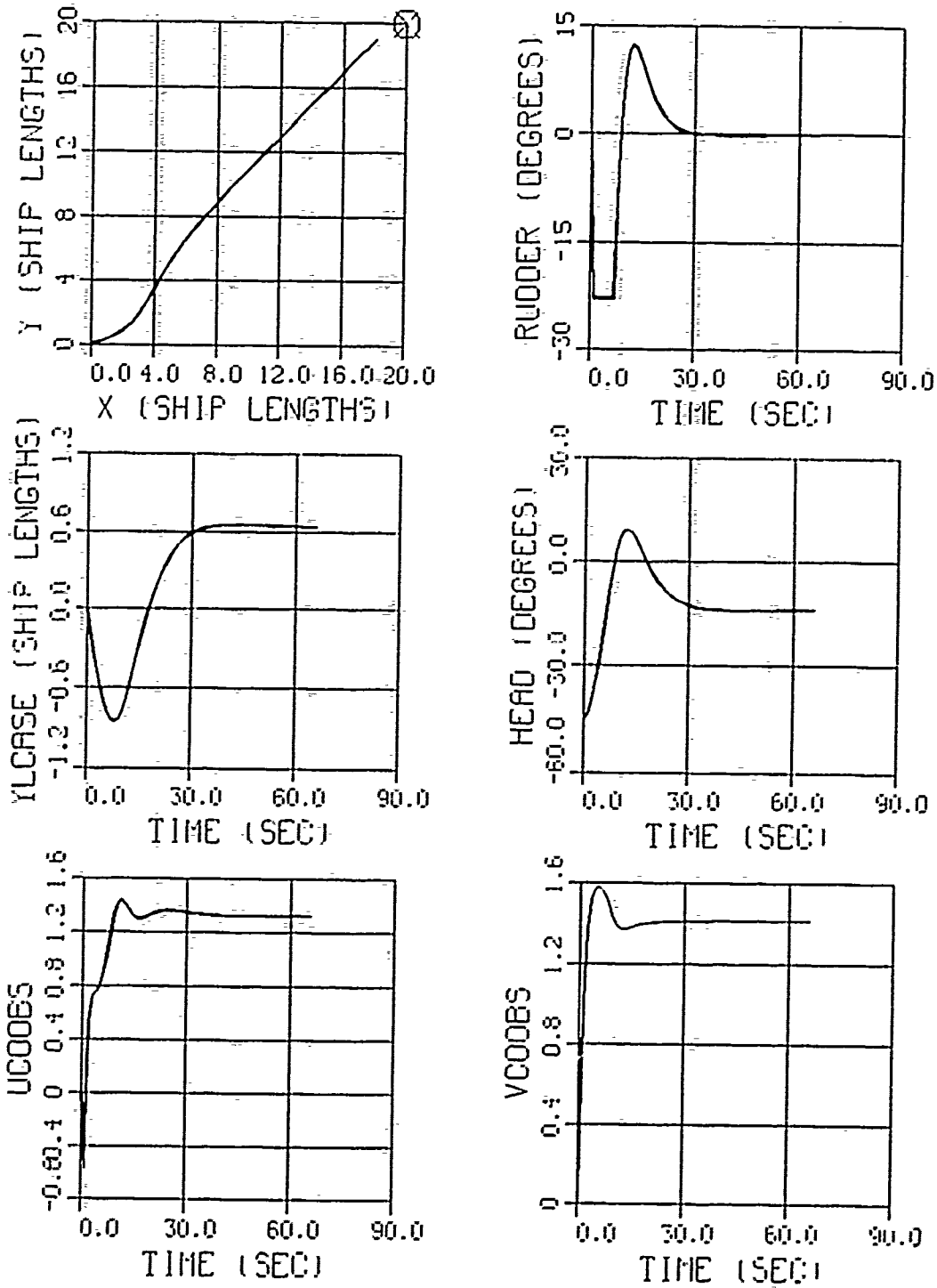

Figure 25. Modified Disturbance Estimation and Compensation, $V_c = 2$, $k_n < k'_{crit}$, $\xi = 0.5$.

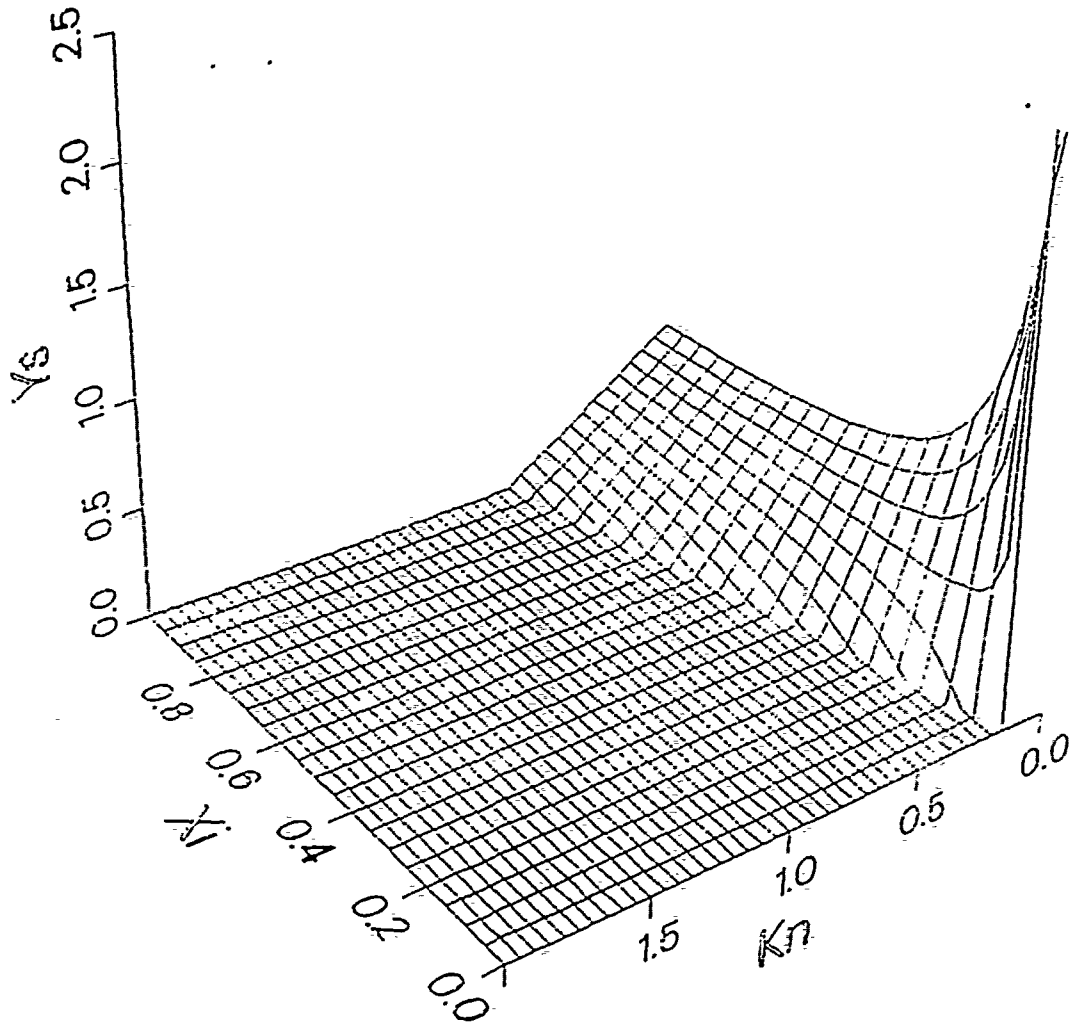

Figure 26. Steady State Track Errors of the Modified Disturbance Estimation and Compensation versus k_n and ξ for $V_c \equiv 1$.

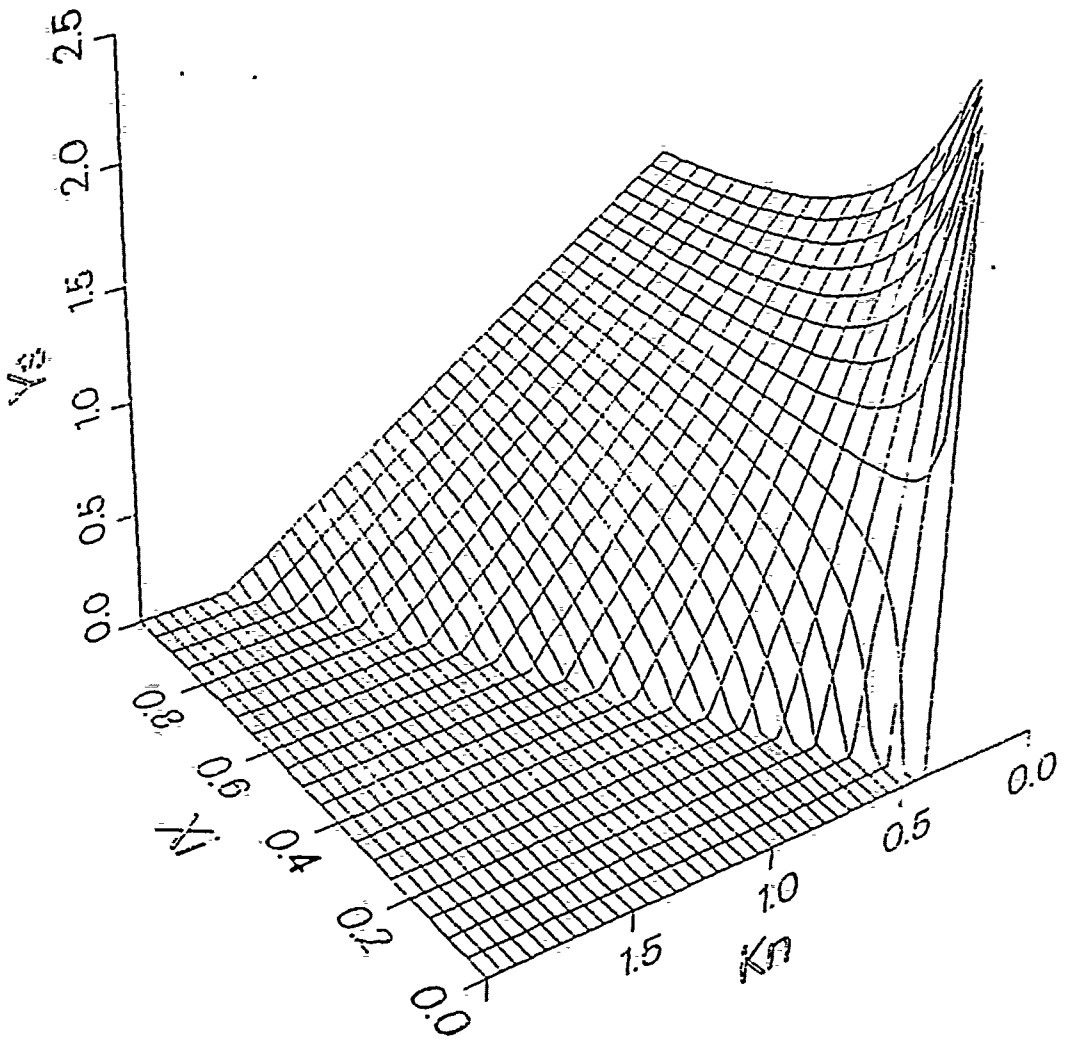

Figure 27. Steady State Track Errors of the Modified Disturbance Estimation and Compensation versus k_a and ξ for V_c = 2.5.

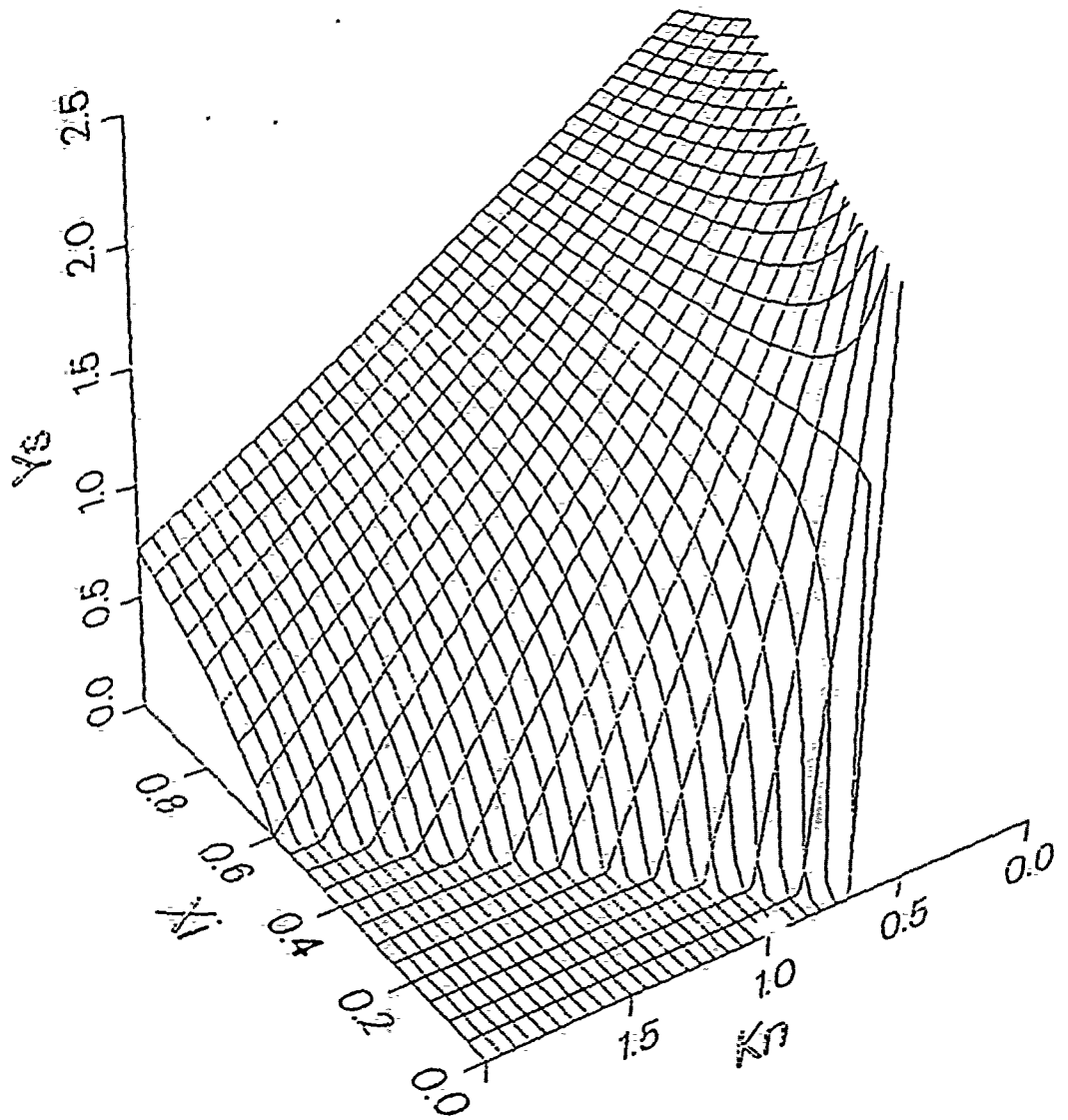

Figure 28. Steady State Track Errors of the Modified Disturbance Estimation and Compensation versus k_a and ξ for $V_c = 4$.

VI. LEADING TRACK CONTROL MONITORING TECHNIQUE

A. INTRODUCTION

Methods for controlling a cross track error, due to a constant disturbance, have been developed in Chapters 3, 4 and 5. In each method, it was seen that the desired track was attained within the limits of the theory, with the appropriate values of $k_p \geq k_{crit}$. It was also seen that, for multiple way points, the target distance played a major role on how well the AUV initiated the turn so as to attain the next track. The ability of the AUV to turn depends on the environmental conditions, the vehicle response characteristics and the turning angle, as discussed in Chapter III. This chapter will develop a technique that monitors the leading track, in order to determine the correct time for the AUV to initiate the turn with no overshoot and minimal rudder use. This technique is referred to as leading track control monitoring.

The concept of leading track control monitoring is to use two legs, the current leg to control the cross track error, or track deviation; and the second leg, to control course deviation, or to determine the correct time to initiate the turn onto the new track [Ref. 16]. This chapter will also show results on how well the leading track control monitoring technique works as compared to using the previous control methods; i.e., disturbance compensation, disturbance estimation and compensation and integral control; with various target distances.

B. LEADING TRACK CONTROL MONITORING DEVELOPMENT

A simple technique to automatically initiate the turn onto the new track at the proper time will be used for the course change from the current track to the leading track. The vehicle is assumed originally to be sailing on the current track. Now consider the application of the control law for the leading track, simultaneously, which will order the rudder command to drive the vehicle onto that track. Two control laws are constructed: one control law for the current track, which is used to reduce the track deviation; and one control law for the leading track, which is used to monitor course deviation. To make a smooth connection from the current track to the leading track, the control law for the leading track will be monitored in addition to the present control law for the current track, simultaneously. In the beginning, the track deviation is much larger than the course deviation. However, in the mean time, the track deviation will be decreased and the course deviation will become dominant. Therefore, a smooth connection can be attained by switching the actual control from the current track to the leading track as soon as the monitored leading track control reaches zero. The leading track control that reaches zero is the point the rudder for the leading track changes sign from positive to negative or vice versa.

C. RESULTS

Figures 29 through 34 show the results of the leading track control monitoring technique, which automatically determines the point to initiate the turn onto the next

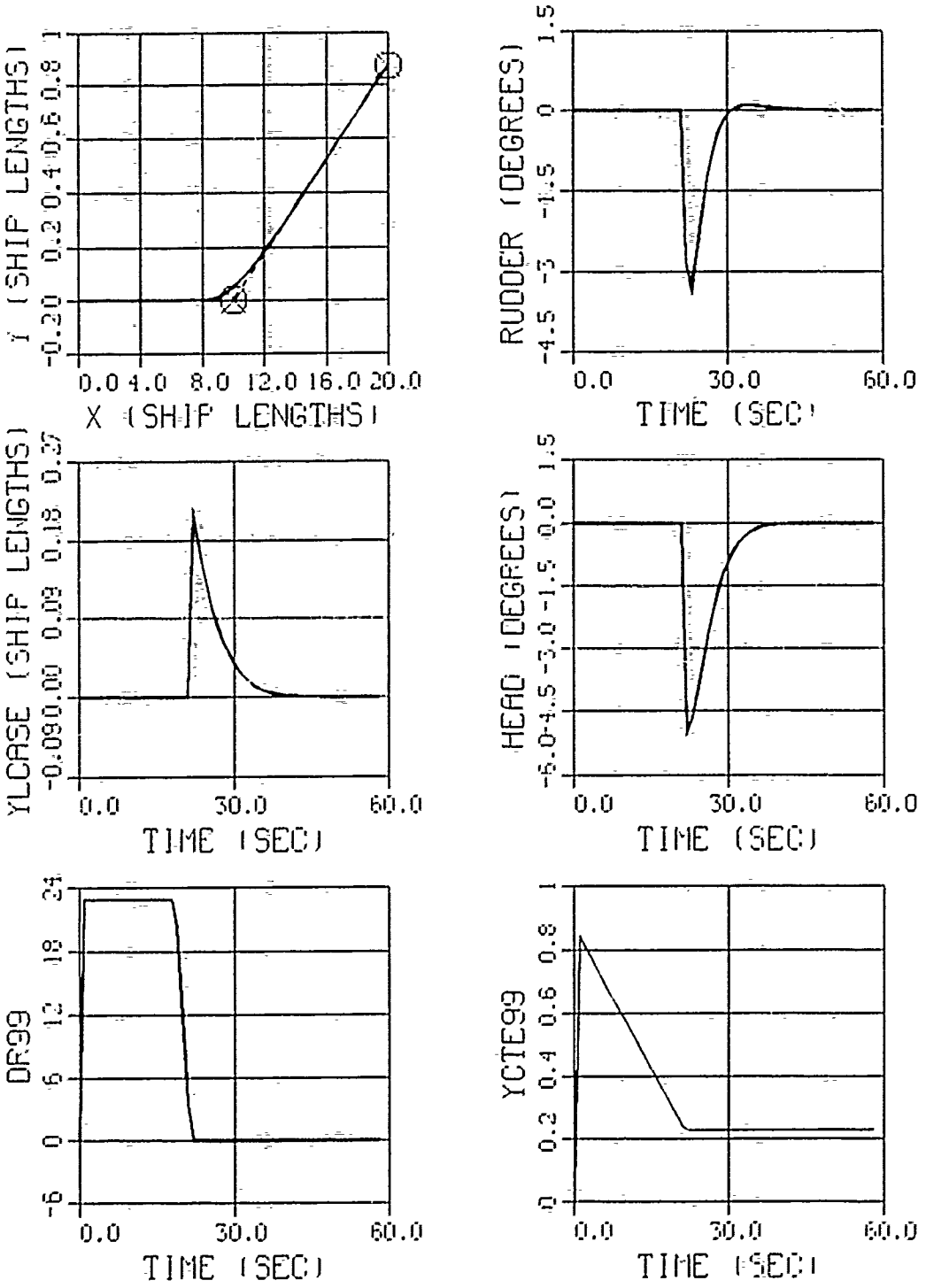

Figure 29. Leading Track Monitoring Technique: 5° Course Change.

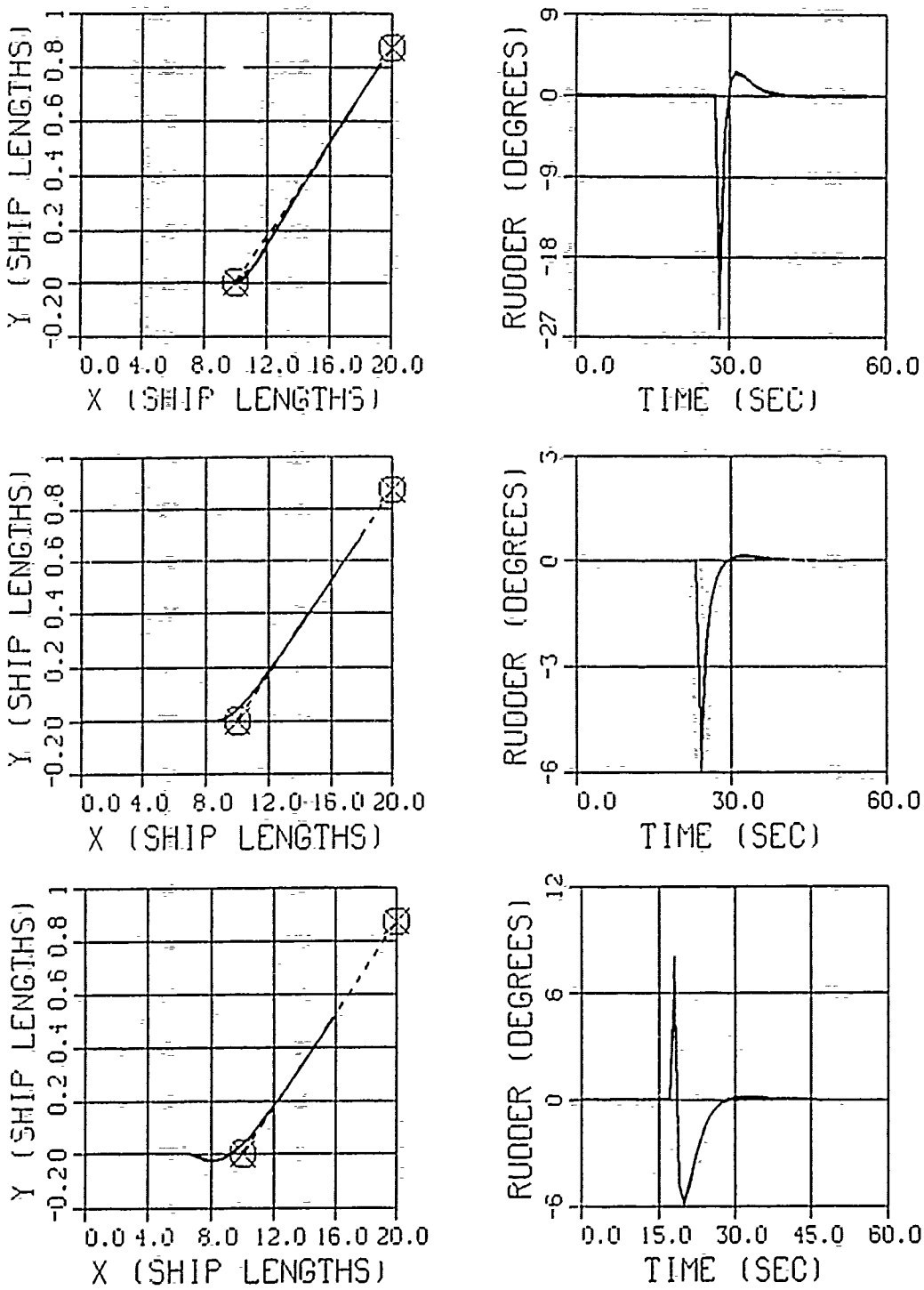

Figure 30. 5° Course Change: Fixed Target Distances of 0.5, 2 and 4 Vehicle Lengths.

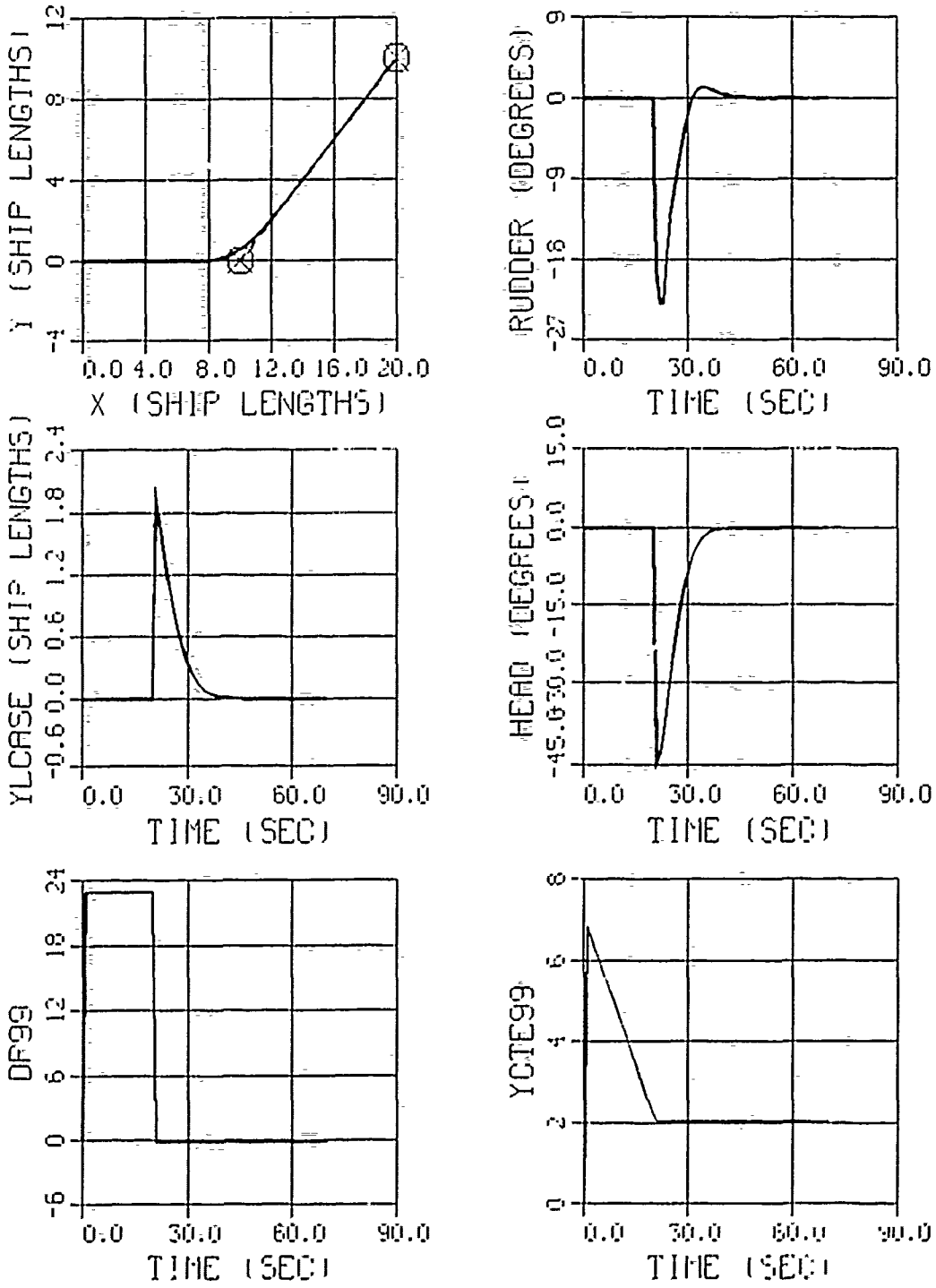

Figure 31. Leading Track Monitoring Technique: 45° Course Change.

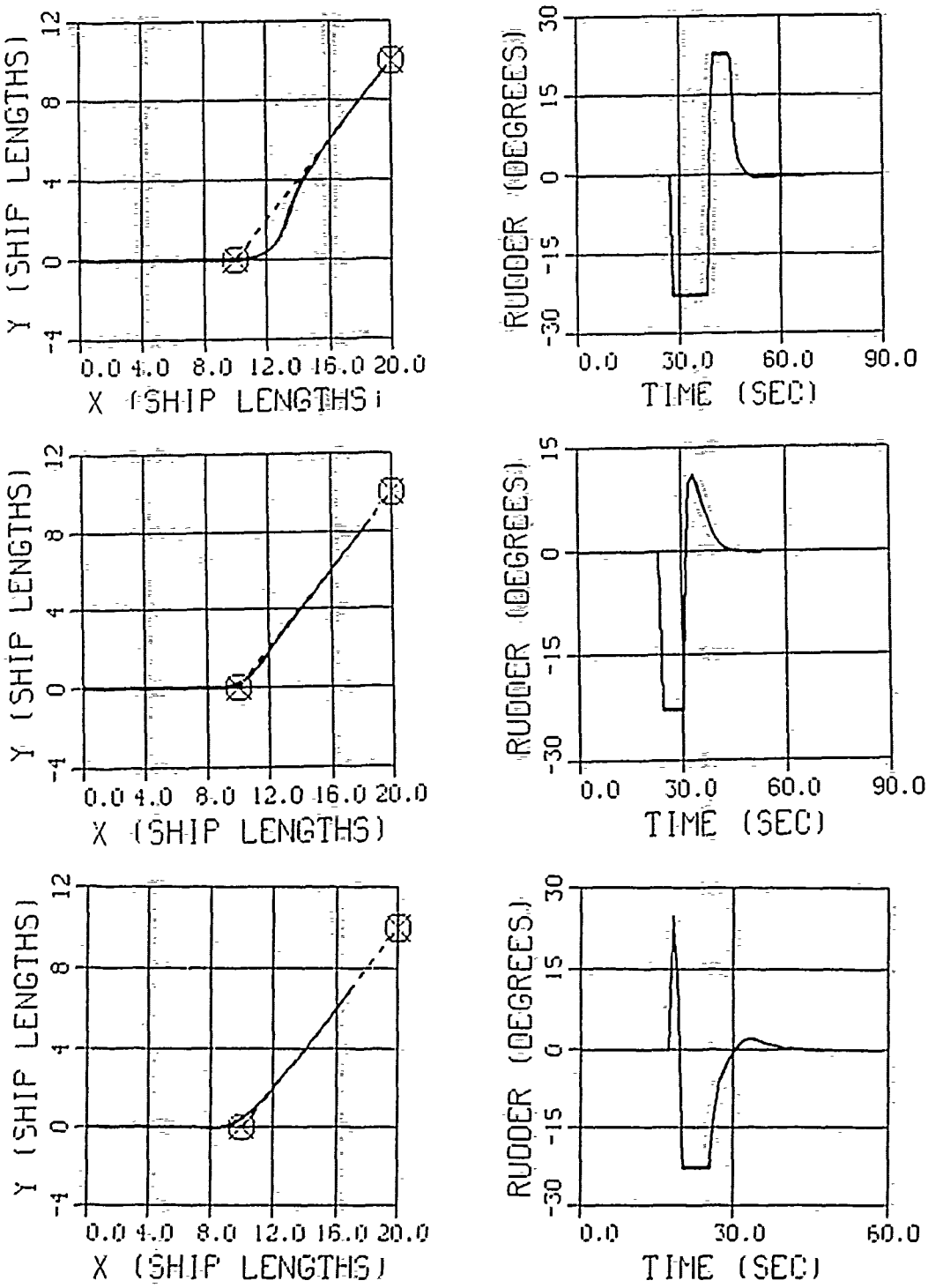

Figure 32. 45° Course Change: Fixed Target Distances of 0.5, 2 and 4 Vehicle Lengths.

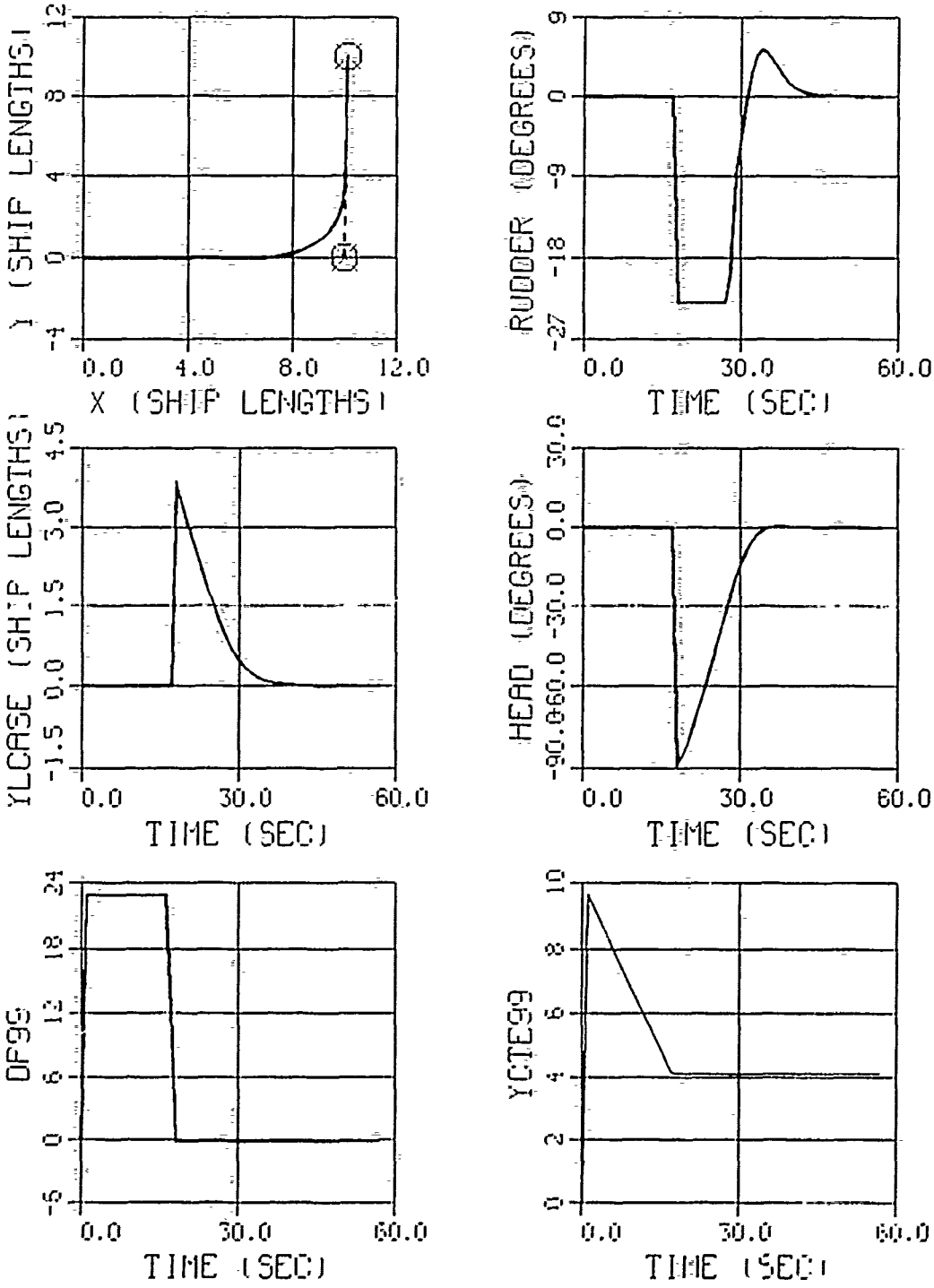

Figure 33. Leading Track Monitoring Technique: 90° Course Change.

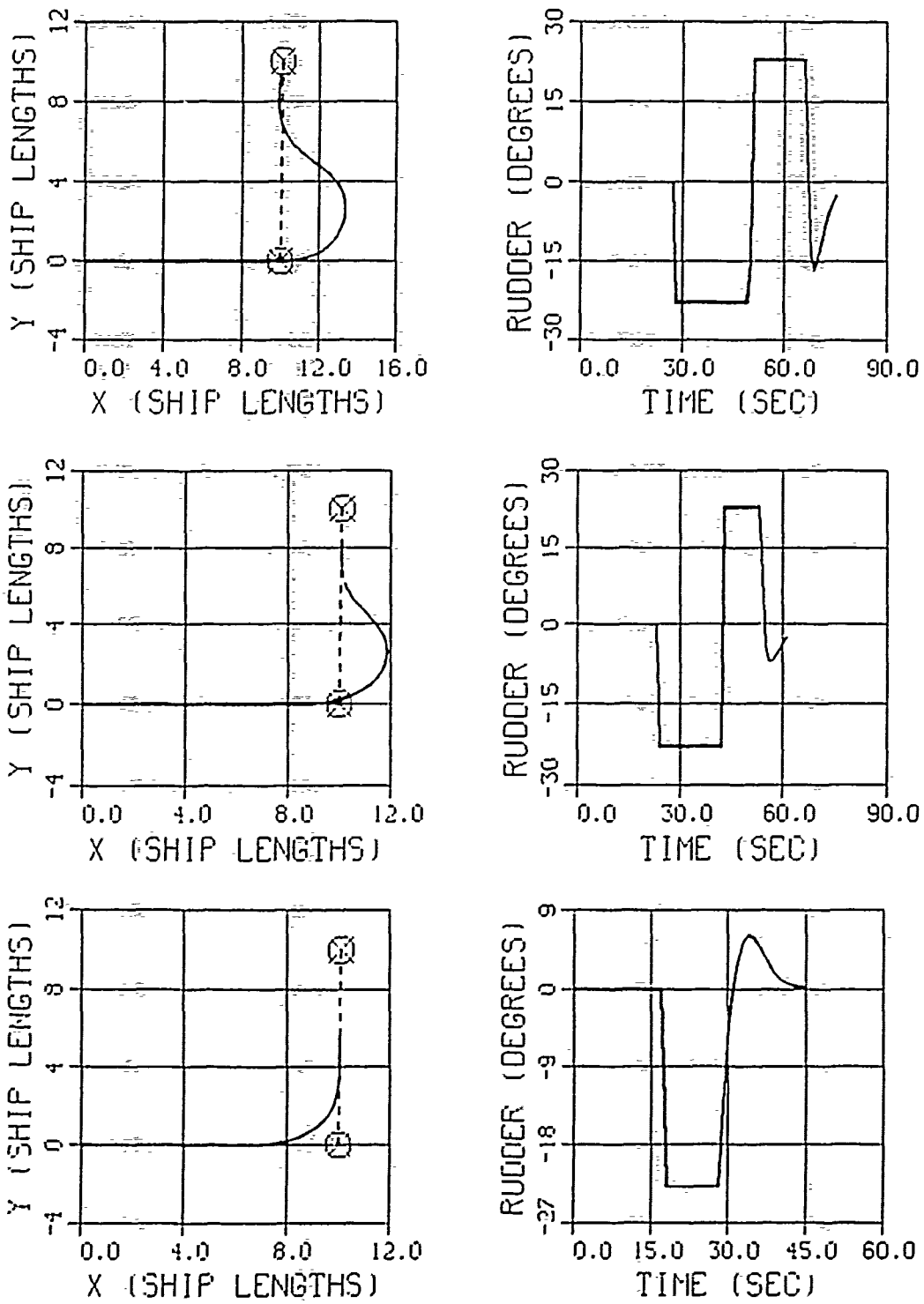

Figure 34. 90° Course Change: Fixed Target Distances of 0.5, 2 and 4 Vehicle Lengths.

track, applied to the disturbance estimation and compensation method and compared to fixed target distances of 0.5, 2 and 4 vehicle lengths, respectively, for no current. Figures 29, 31 and 33 show the results of the leading track control monitoring technique, with the disturbance estimation and compensation method, for course changes of 5°, 45° and 90°, respectively. The leading track monitored rudder angle and course deviation are referred to as DR99 and YCTE99 in the graphs, respectively. The leading track control monitoring technique can also be used with the other control methods discussed in the previous chapters, however, for Figures 29 through 34, the disturbance estimation and compensation method is utilized. Figures 30, 32 and 34 show the results of the disturbance estimation and compensation method for target distances of 0.5, 2 and 4 vehicle lengths, from top to bottom respectively. For each course change of 5°, 45° and 90°, there is one target distance that is best for that course change, and it will not necessarily be the best for the other course changes. For example, Figure 30 shows that a target distance of 2 vehicle lengths is best for a course change of 5°. However, for the course changes of 45° and 90°, target distances of 2 to 3 and 4 vehicle lengths, respectively, are best for these course changes. The leading track control monitoring technique eliminates the need to worry about what target distance is required because the technique automatically determines the distance required to initiate the turn onto the next track without any overshoot and minimal rudder use.

Figures 35 through 39 show the performance of the leading track monitoring control technique in the presence of a current for the multiple way points used in the previous

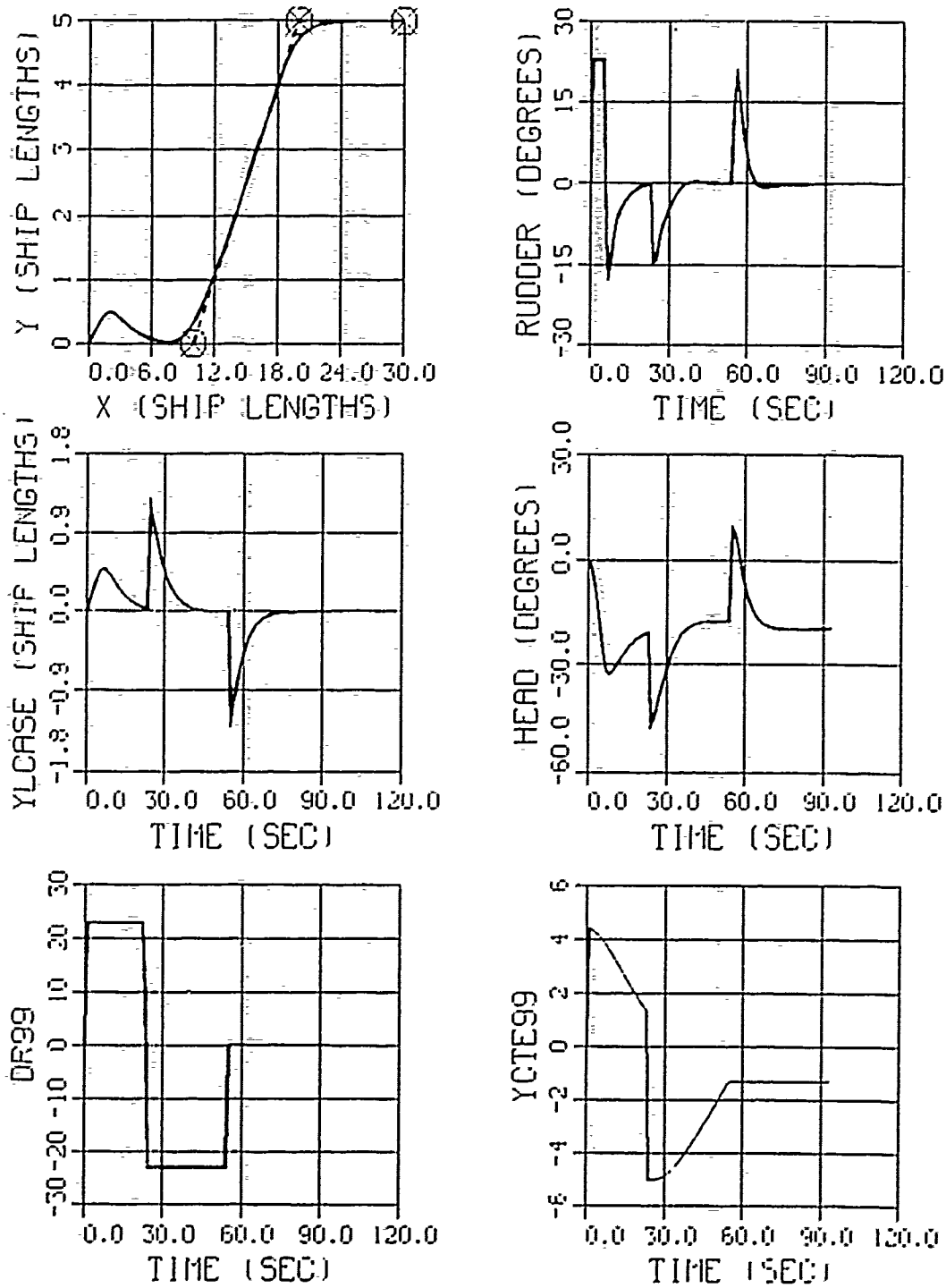

Figure 35. Lane Changing Maneuver, Disturbance Estimation and Compensation, Leading Track Monitoring Technique: Current $U_c = 0$, $V_c = 2$, Course Change 5 : 10.

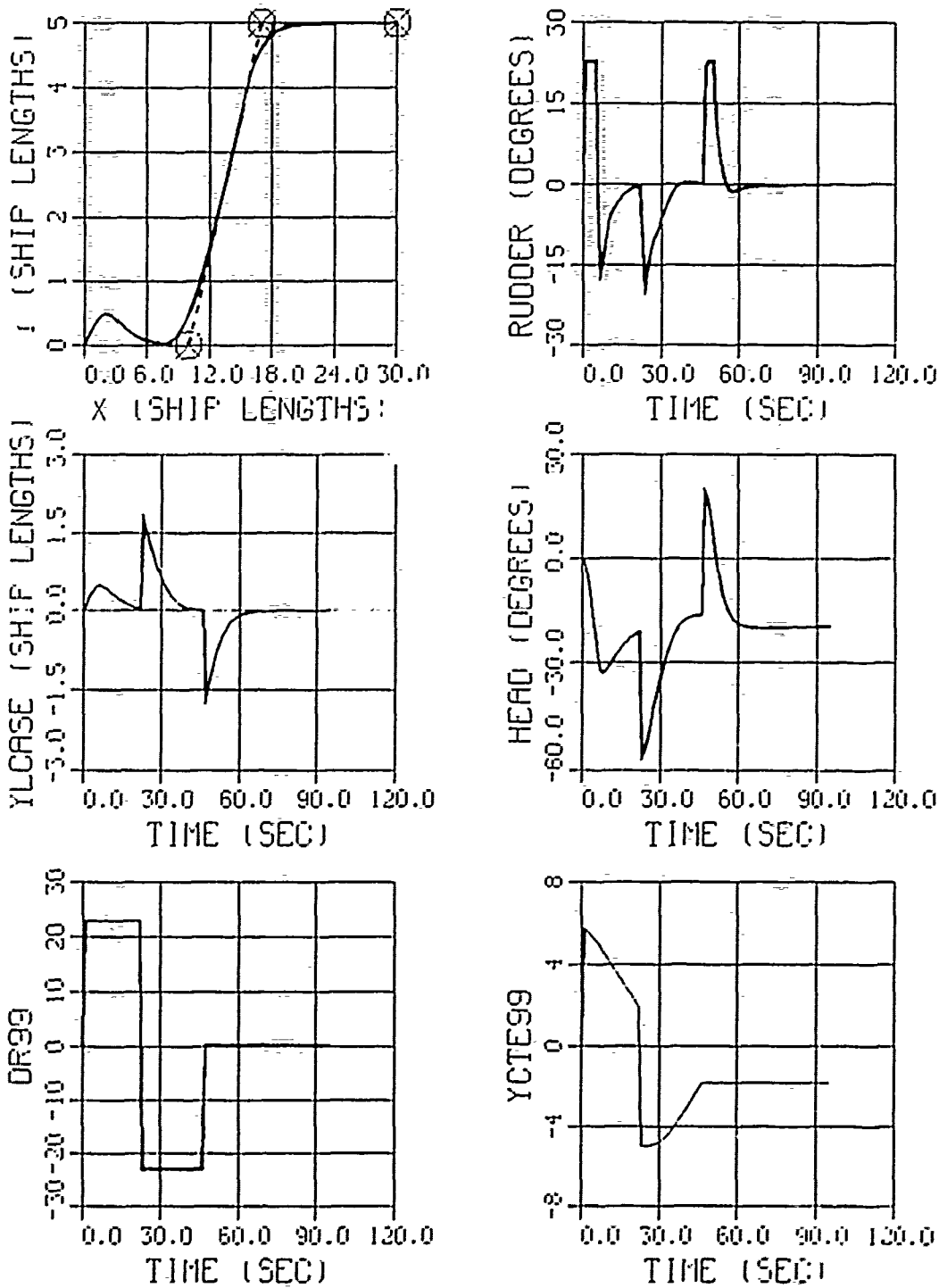

Figure 36. Same As Figure 35 with Course Change 5 : 7.

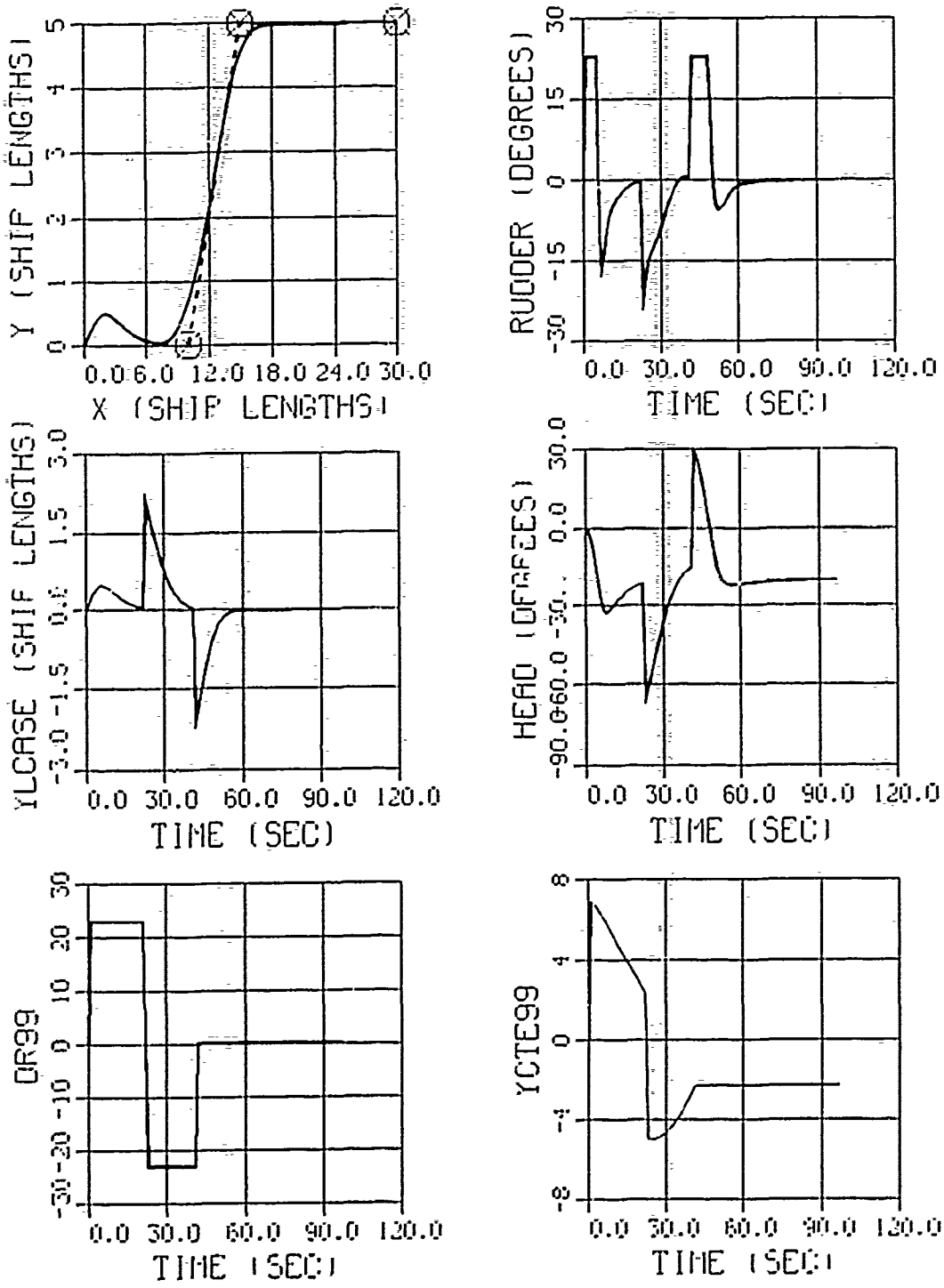

Figure 37. Same As Figure 35 with Course Change 5 : 5.

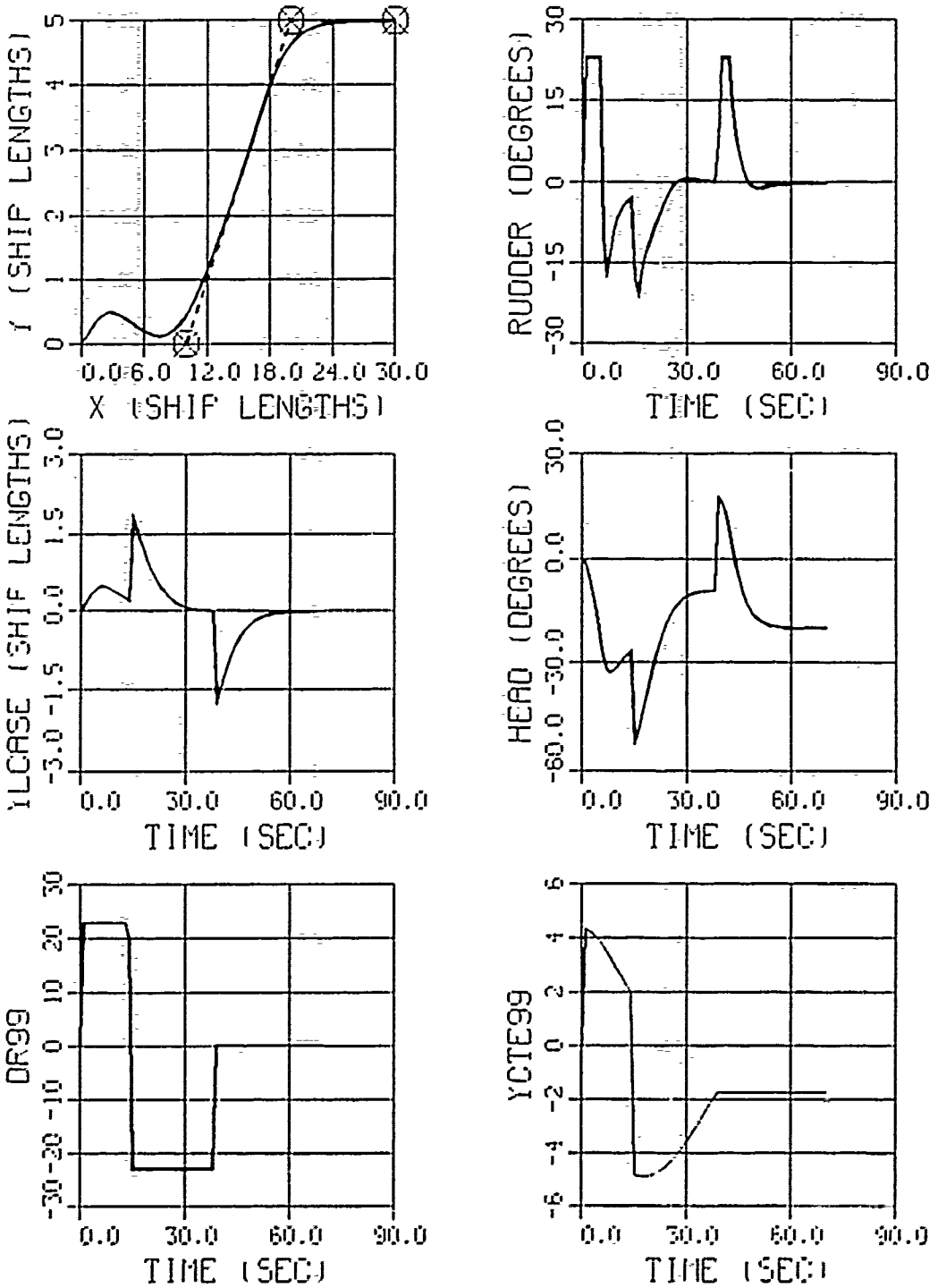

Figure 38. Lane Changing Maneuver, Disturbance Estimation and Compensation, Leading Track Monitoring Technique: Current $U_c = V_c = 2$, Course Change 5 : 10.

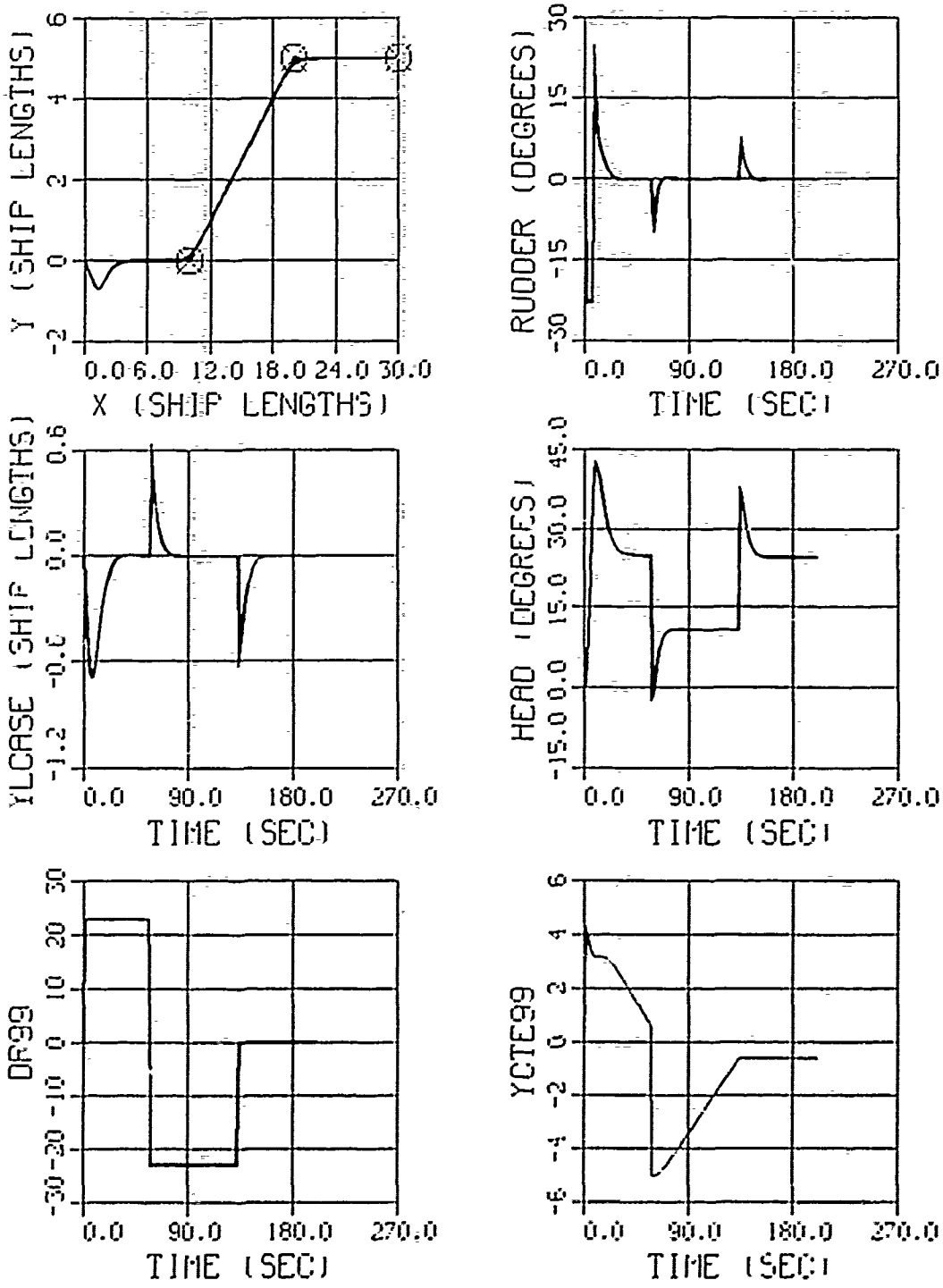

Figure 39. Lane Changing Maneuver, Disturbance Estimation and Compensation, Leading Track Monitoring Technique: Current $U_c = V_c = -2.5$, Course Change 5 : 10.

chapters. Figures 35 through 37 were conducted at U_c = 0.0 and V_c = 2.0 ft/sec for increasing course changes. It can be seen that the leading track control monitoring technique works superbly in the presence of a current for increasing course changes with no overshoot for each turn onto the leading track, with minimal use of the rudder. Figures 38 and 39 show the leading track control monitoring technique for currents other than that used in Figures 35 through 37. Figure 38 used a current of $U_c = V_c$ = 2.0 ft/sec and Figure 39 used a current of $U_c = V_c$ = −2.5 ft/sec. Both of these figures reveal that the leading track control monitoring technique can handle very large currents, within the physical constaints of the vehicle, very well.

The automatically selected target distance d (in vehicle lengths), by this technique, is plotted in Figure 41 for different current magnitudes and directions (the symbols are explained in Figure 40) and u ≡ 6 ft/sec. It can be seen that d depends on both the strength v and orientation θ of the current and the turning angle α. As the angle α is increased, d is also increased, as expected. The same is true for increasing current speed. For very small changes in vehicle path α, the leading track control monitoring technique tends to be conservative; i.e., it initiates the turn early with very little rudder usage. If the technique is modified such that the actual switching occurs when the monitored rudder angle reaches a specified value (such as its saturation limit) after the zero crossing, then smaller target distances can be achieved for small α. Also, the technique in its current application, cannot handle turning angles more than 90°. Although such turns are rarely

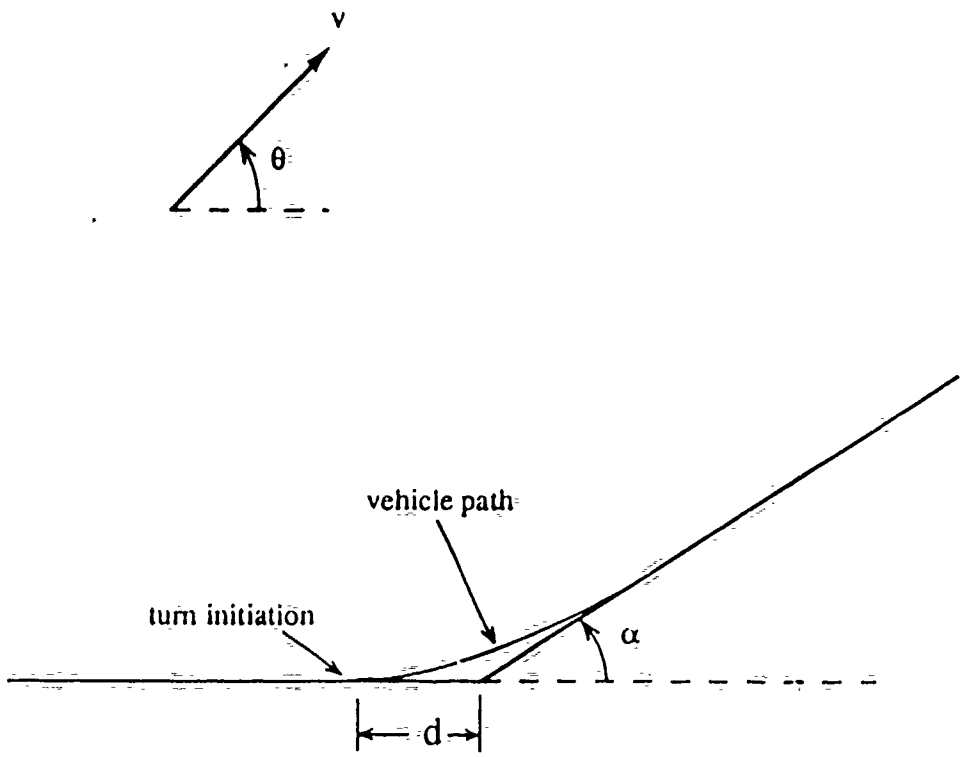

LEGEND

d	target distance (automatically selected)
α	course change (commanded turning angle)
θ	current direction
v	current resultant speed

Figure 40. Nomenclature for Leading Track Monitoring Technique.

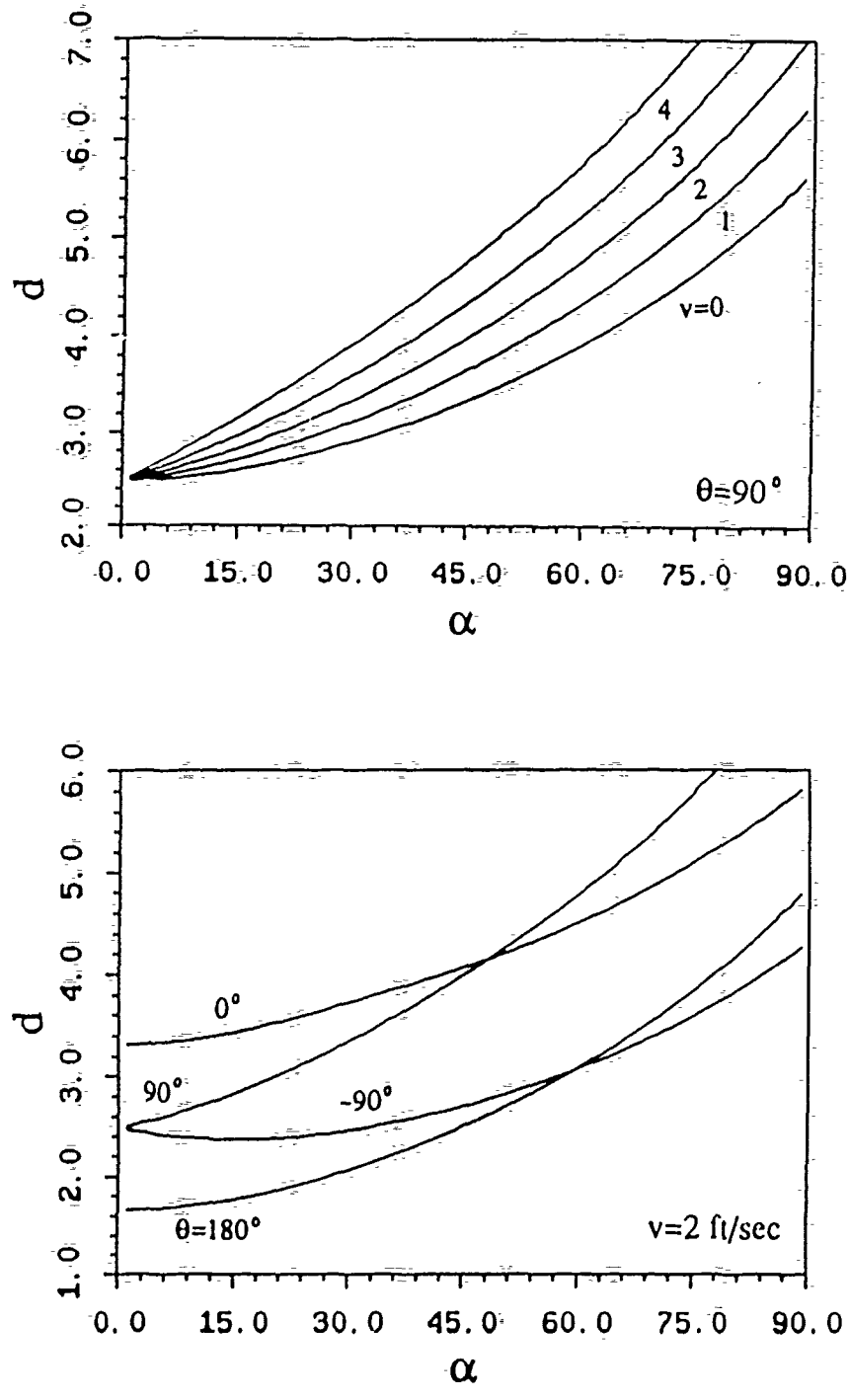

Figure 41. Automatically Selected Target Distances for Different Current Magnitudes and Directions.

demanded for by the path planner, the technique can be modified to allow for these drastic turns if desired.

In the final chapter, noise will be introduced into the measureable parameters; i.e., ψ, r, y or x; and the effects will be evaluated. Also, guidelines will be developed for suppressing the effects of measurement noise.

VII. ROBUSTNESS TESTS AND SENSOR NOISE EFFECTS

A. INTRODUCTION

The characteristics of the controllers that were designed in the previous chapters are analyzed here with a view to their robustness properties with respect to unmodelled dynamics and actual/mathematical model mismatch. For the sake of brevity, emphasis is placed on the disturbance estimation and compensation design. The effects of sensor noise and sensor drift are also evaluated through a series of digital simulations. This brings another level of realism into the design.

B. ROBUSTNESS PROPERTIES

The effect of the sway velocity observer is evaluated in Figure 42. Curve 1 is obtained by using the observed value of the sway velocity v, whereas, Curve 2 is obtained by assuming that $\hat{v} = 0$. The vehicle speed u was kept constant at u = 6 ft/sec, and the lateral current was $v_c = 2$ ft/sec. Disturbance estimation and compensation was used with $k_n = 5$ and $\phi = 0.5$. It can be seen that the response of the two curves is almost identical. It can be, therefore, concluded that the sway velocity does not appear to be very significant for track control design. This result is analogous to the Line of Sight navigation case [Ref. 12].

Results for different forward speeds are shown in Figure 43, for the same conditions as in the previous test. Curve 2 was obtained for u = 6 ft/sec (nominal design), while

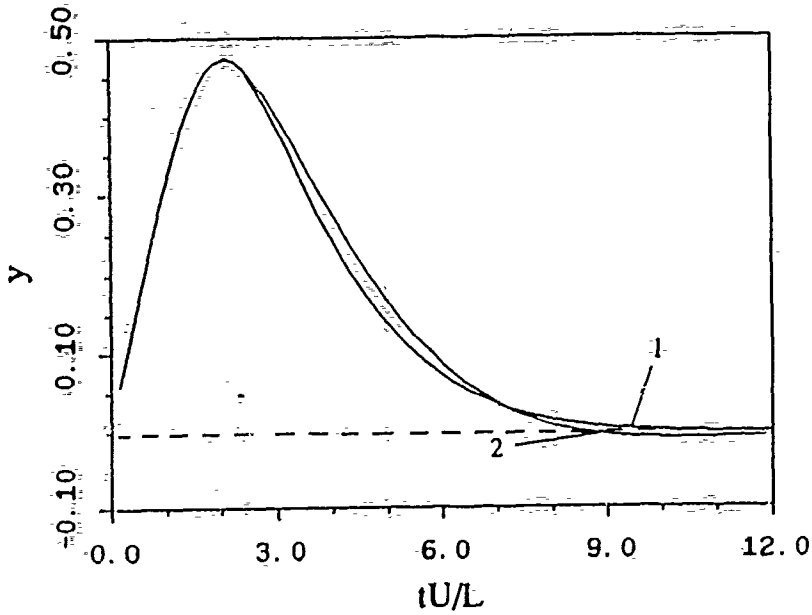

Figure 42. Robustness Test: Sway Velocity Effect.

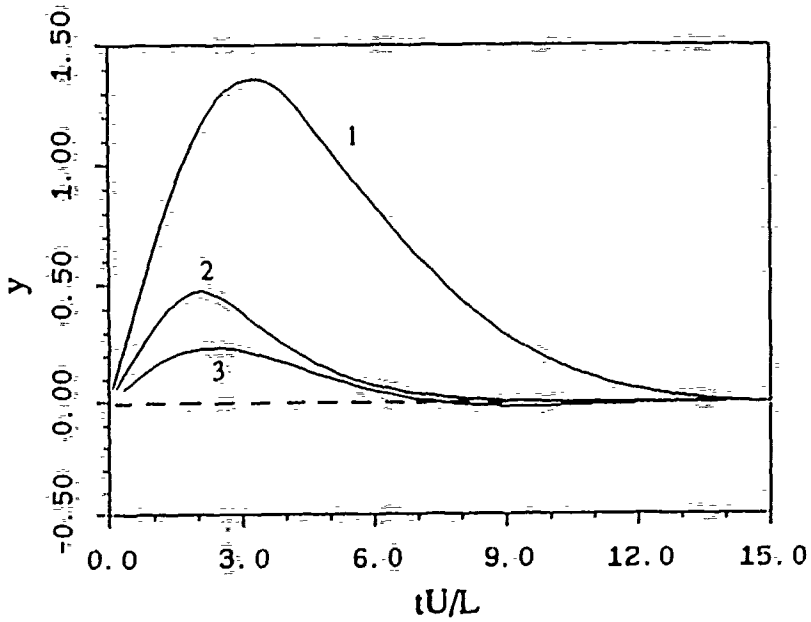

Figure 43. Robustness Test: Forward Speed Effect.

Curve 1 is for u = 3 ft/sec and Curve 3 is for u = 12 ft/sec, with the same gains and sliding plane coefficients as for the nominal case. It can be seen that large deviations in the forward speed can be accomodated by the controller without the need for gain scheduling.

The robustness of the compensator is also evaluated in Figure 44 for a drastically off design case (Curve 2), which is shown along with the response of the nominal design (Curve 1). The same current v_c = 2 ft/sec is present. For Curve 2, the values of the hydrodynamic coefficients Y_v and N_r were reduced in the equations of motion to half of their actual values, and the rudder coefficients Y_δ and N_δ were increased to twice their actual values. Both of these changes correspond to a more responsive and less damped vehicle. The controller and observer were designed for the true values of the coefficients, so that the vehicle is operating with large errors in the knowledge of its dynamics. The results of Figure 44 demonstrate the ability of the controller to meet its mission requirements even under unrealistic errors in the design. The track overshoot for the off design case is attributed to the slower convergence of the current observer to the true current speed, as is also shown in Figure 44.

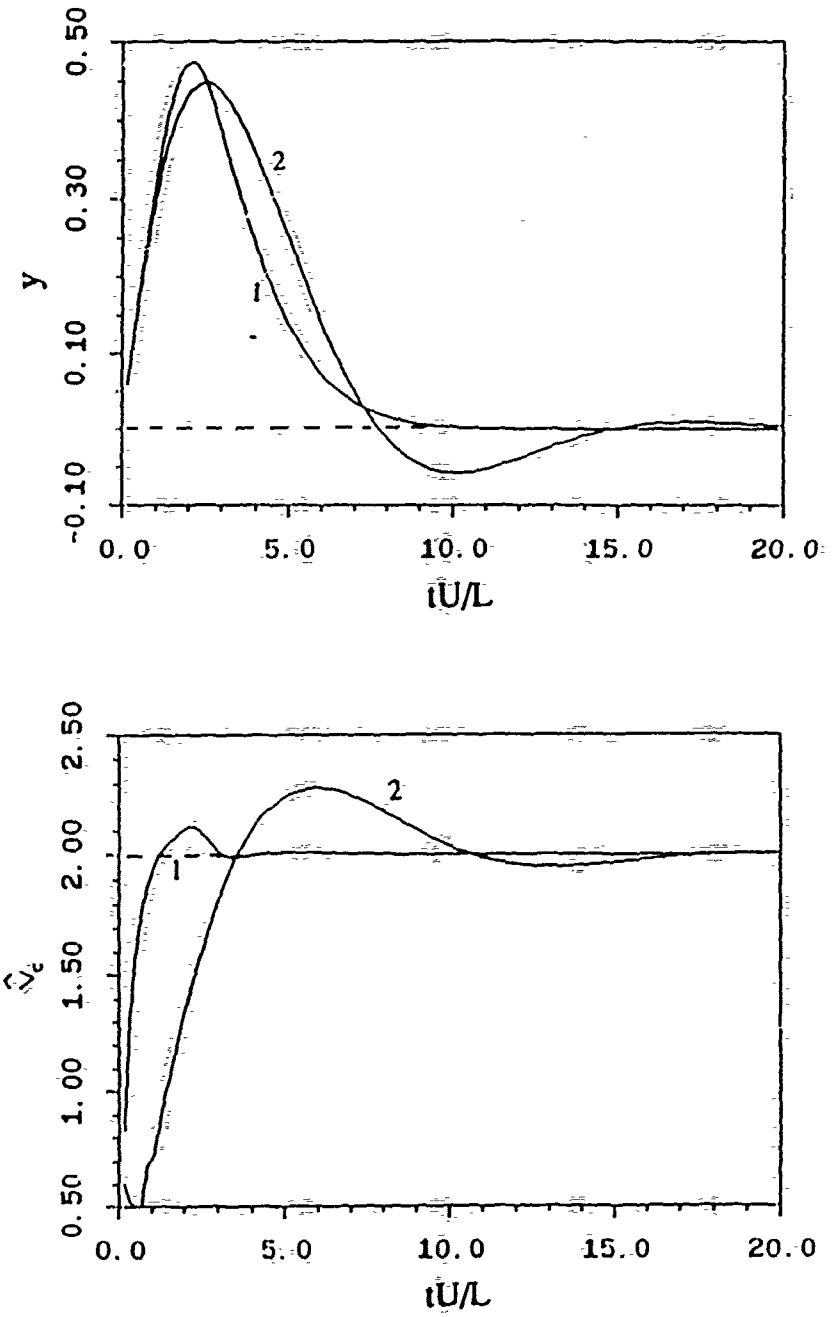

Figure 44. Robustness Test: Effect of Hydrodynamic Coefficients Mismatch.

C. EFFECTS OF SENSOR NOISE

So far, incomplete but perfect state measurement has been assumed. To analyze the effects of sensor noise on the sliding mode track controller with the disturbance estimation and compensation method, the following scenario is considered. The vehicle is moving with u = 6 ft/sec in a lateral current v_c = 2 ft/sec. Controller poles are selected at -0.25 and observer poles at -0.50. The measurable quantities are ψ, r and y, and the noise is simulated by Gaussian distribution with typical standard deviations of 0.1 degrees for ψ, 0.01 degrees/sec for r and 0.1 ft for y. All simulations are performed using Euler integrations with time step Δt = 0.1 seconds. This corresponds to a sample rate of 10 hertz, which is reasonable. All results show time histories of the exact, not the measured, lateral deviation y, in vehicle lengths, and the actual rudder angle δ in degrees. The same scale has been kept for all graphs for comparison.

The results of the simulation for k_n = 2, ϕ = 0.5 and for noise free sensors are presented in Figure 45. When the assumed noise is introduced, as in Figure 46, the actual y does not differ significantly. The rudder angle δ, however, is chattering so that the design cannot be accepted. If the value of ϕ is increased to 5, then the level of rudder chattering is significantly reduced at the expense of a slower vehicle response, as shown in Figure 47. The level of ϕ is ultimately related to the standard deviation of the sliding plane σ. If a faster vehicle response is needed, then ϕ can become a function of σ, so

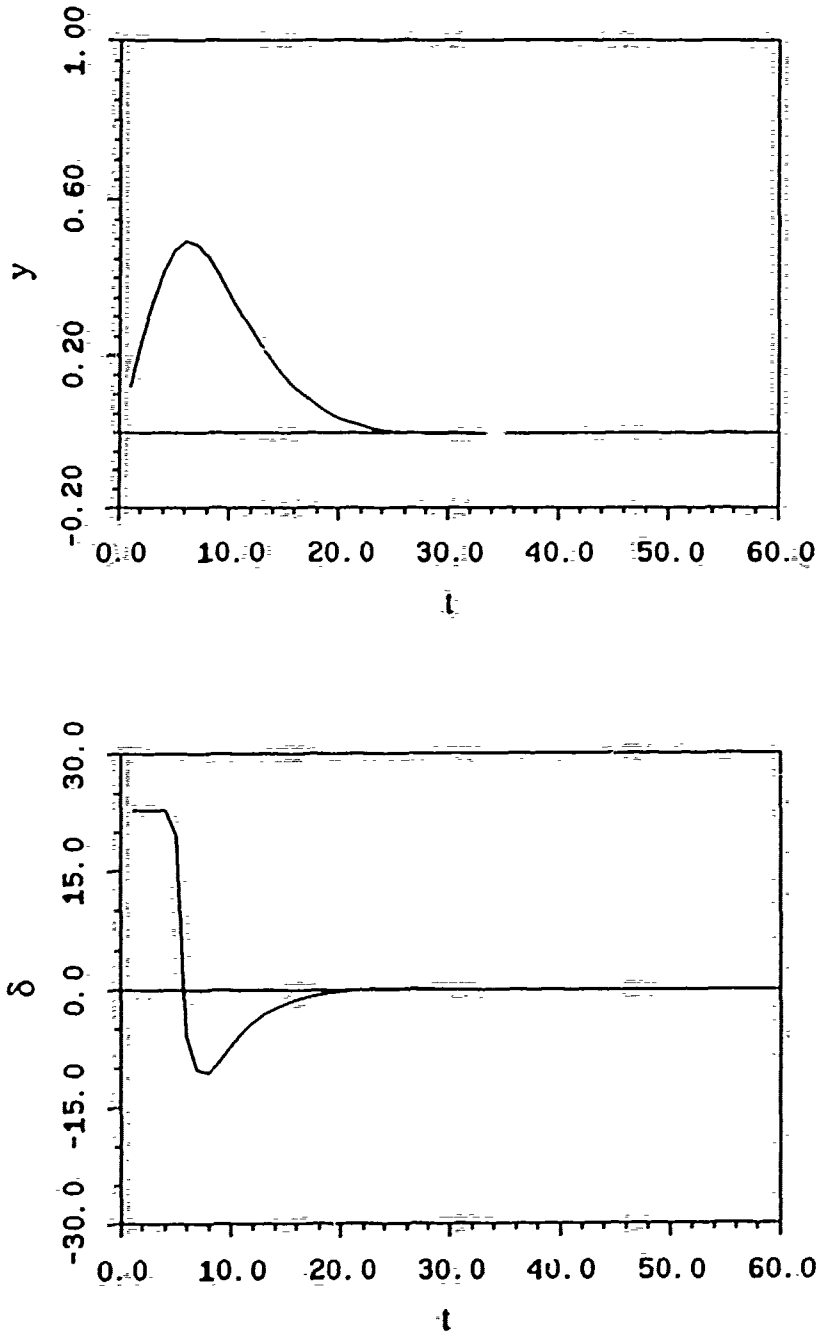

Figure 45. Sensor Noise Effect: Noise Free Sensors, $k_a = 2$, $\phi = 0.5$.

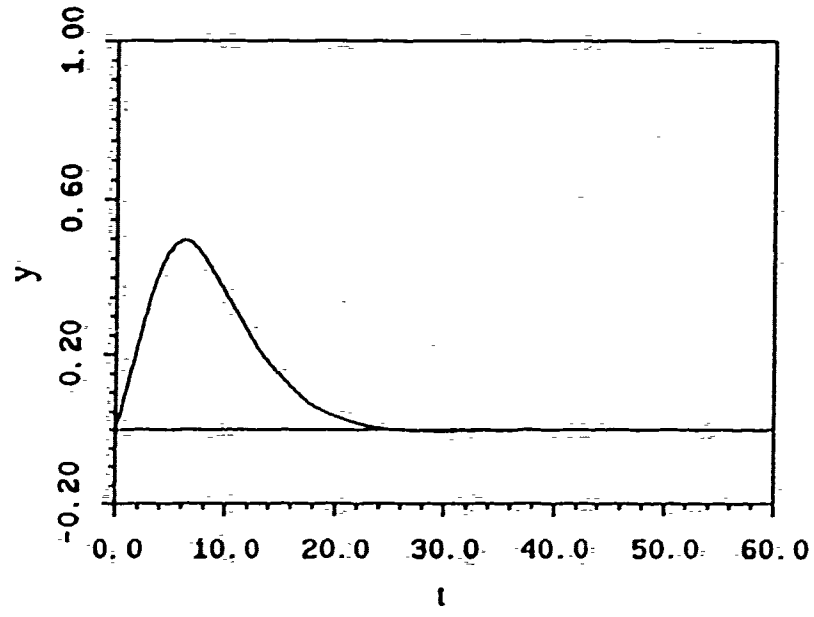

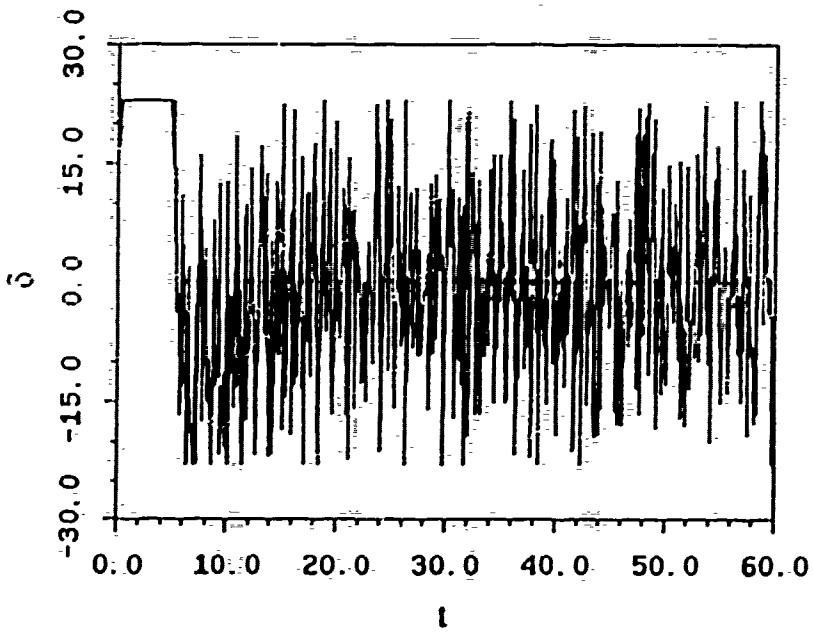

Figure 46. Sensor Noise Effect: $k_n = 2$, $\phi = 0.5$.

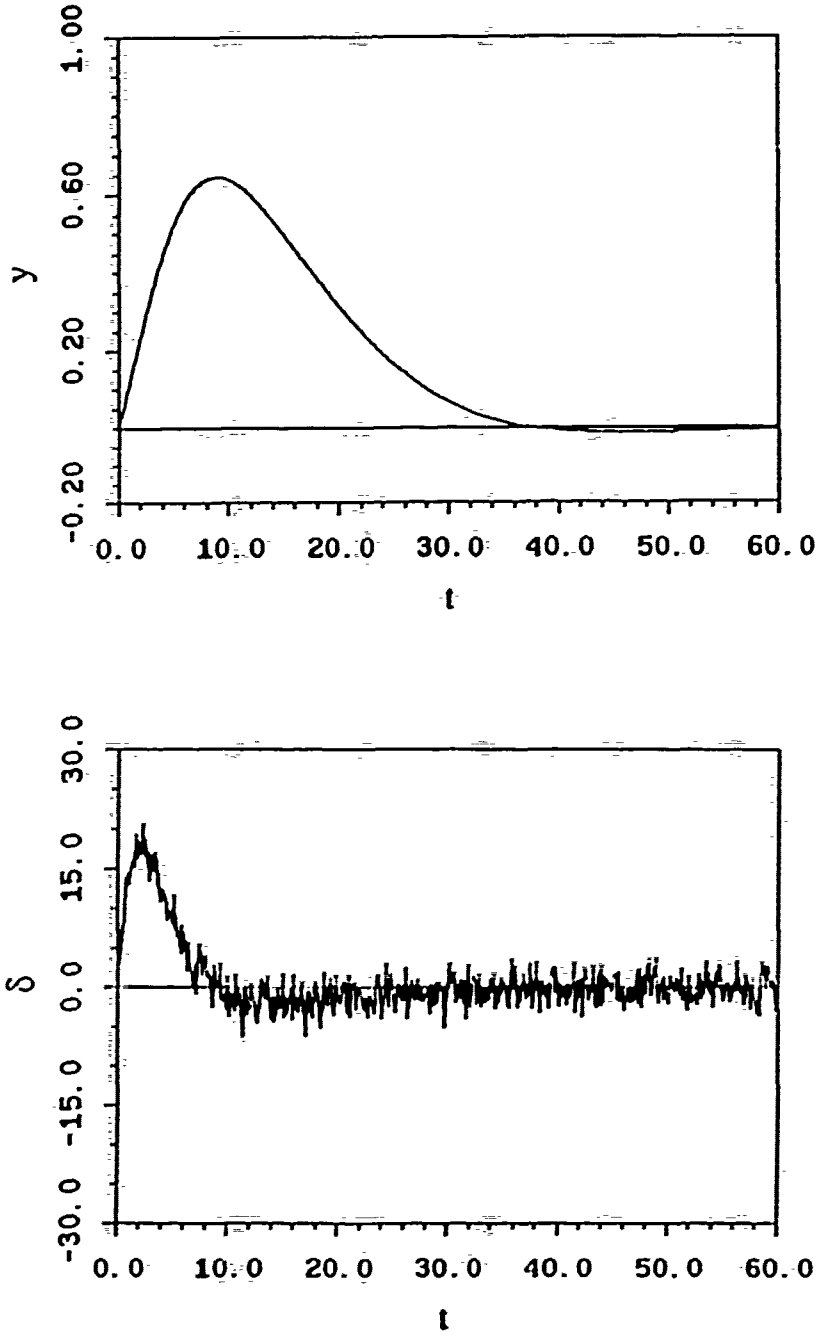

Figure 47. Sensor Noise Effect: $k_a = 2$, $\phi = 5.0$.

that it is small away from the sliding plane and becomes larger as the system approaches $\sigma = 0$. Keeping the same $\phi = 0.5$ and reducing k_a to 0.5 helps to reduce the level of chattering, as shown in Figure 48. This, however, has the effect of possibly sacrificing stability or steady state accuracy, as analyzed in the previous chapters. It follows then, that the first action to suppress the noise effects must be to increase the value of ϕ.

Another way to further improve on the response, in a noisy set of measurements, is to introduce a first order lag between commanded and actual rudder angle. If T_r denotes the artificial (software) steering gear time constant, then

$$T_r\dot{\delta} + \delta = \delta_c \quad , \tag{7.1}$$

where δ_c is the commanded rudder angle and δ the actual rudder angle. A time constant $T_r = 0.5$ seconds, which is five times higher than the integration step, should provide enough noise attenuation, since the corner frequency of (7.1) is 2, while the frequency of the noise is 10. At the same time a value of $T_r = 0.5$ seconds is small enough so that the transient response characteristics of the vehicle are not significantly affected. The results are shown in Figure 49, and for comparison, the response of the identical system, with noise free sensors, is shown in Figure 50. If a faster response is necessary, then the controller has to be redesigned by taking (7.1) as an extra state equation.

Very low values of T_r (of the same order of magnitude as Δt) do not have any visible effects in noise reduction, while large values of T_r can deteriorate the transient

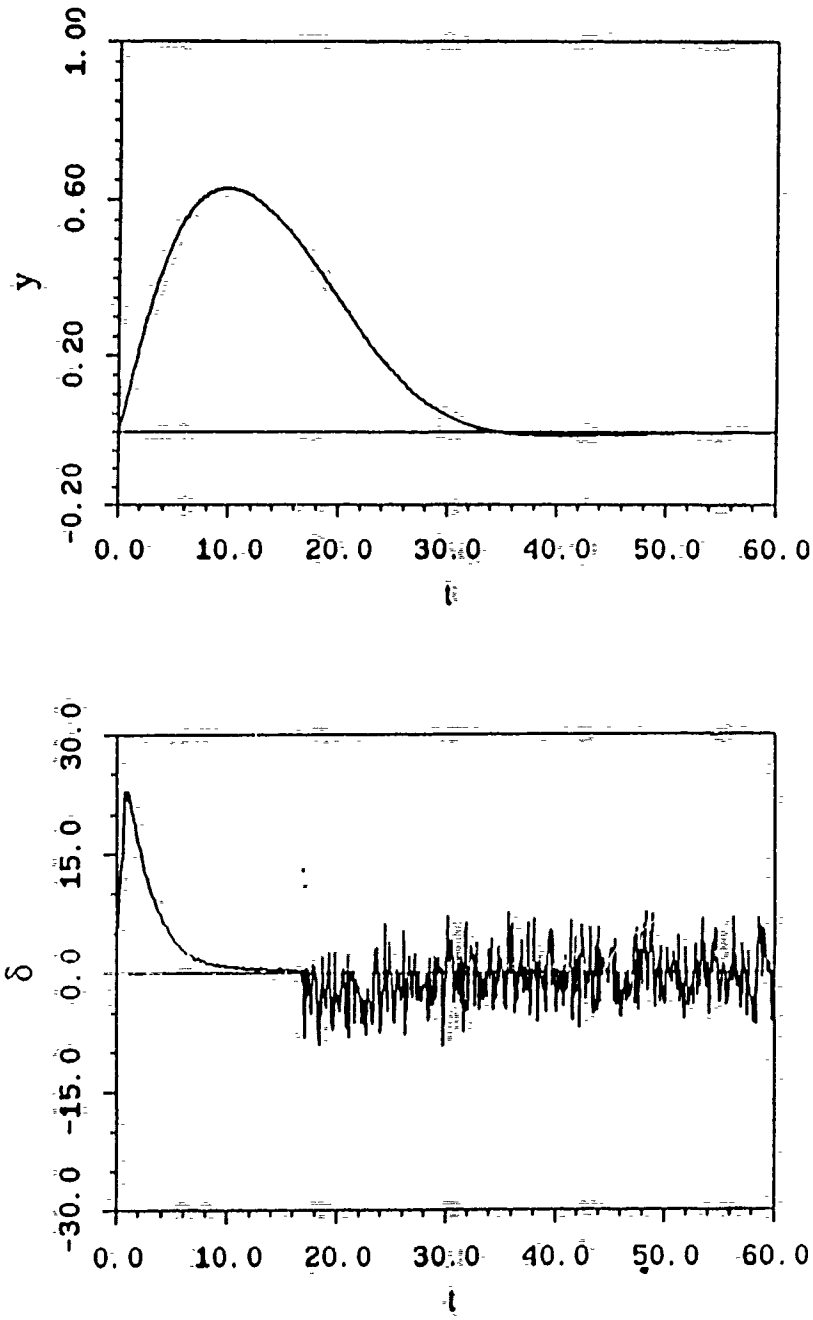

Figure 48. Sensor Noise Effect: $k_n = 0.5$, $\phi = 0.5$.

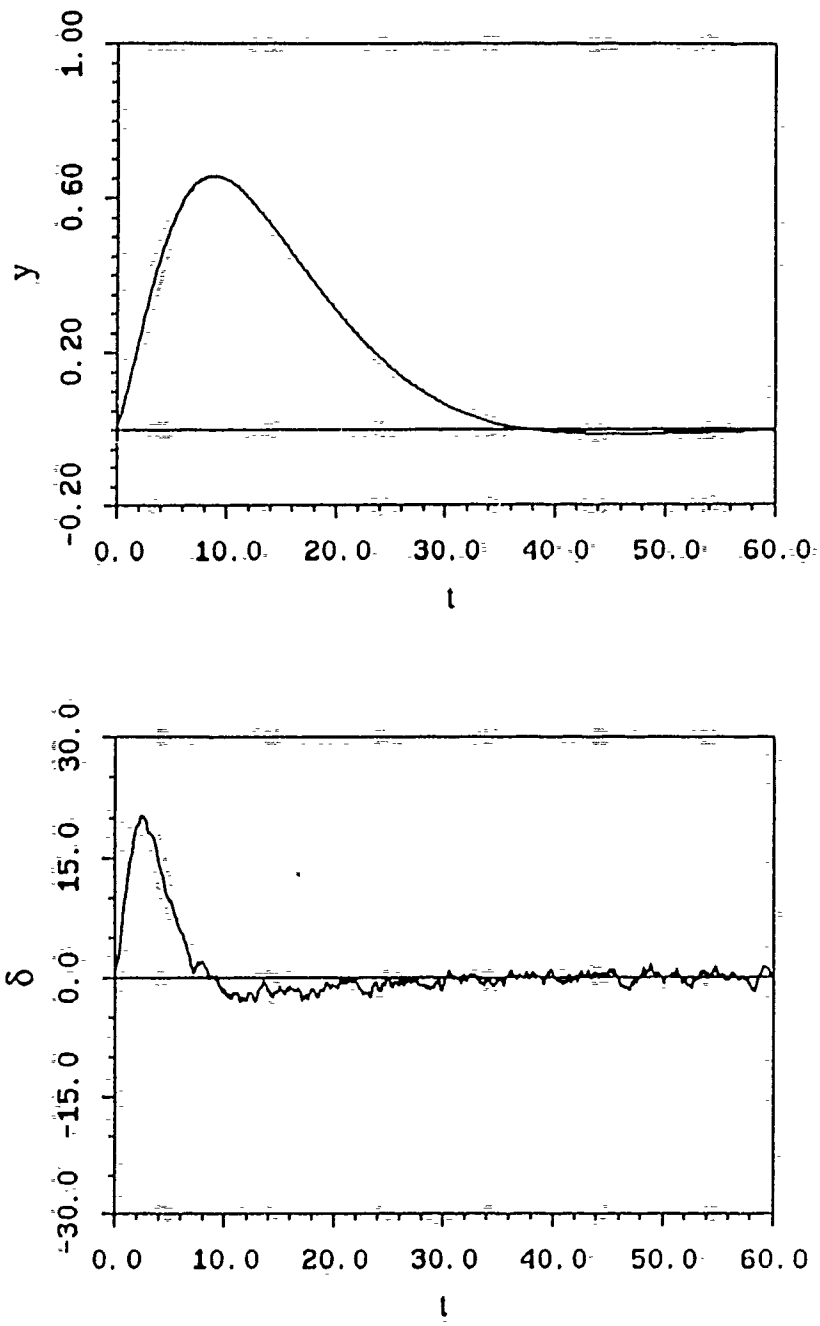

Figure 49. Sensor Noise Effect: $k_n = 2$, $\phi = 5$, $T_r = 0.5$.

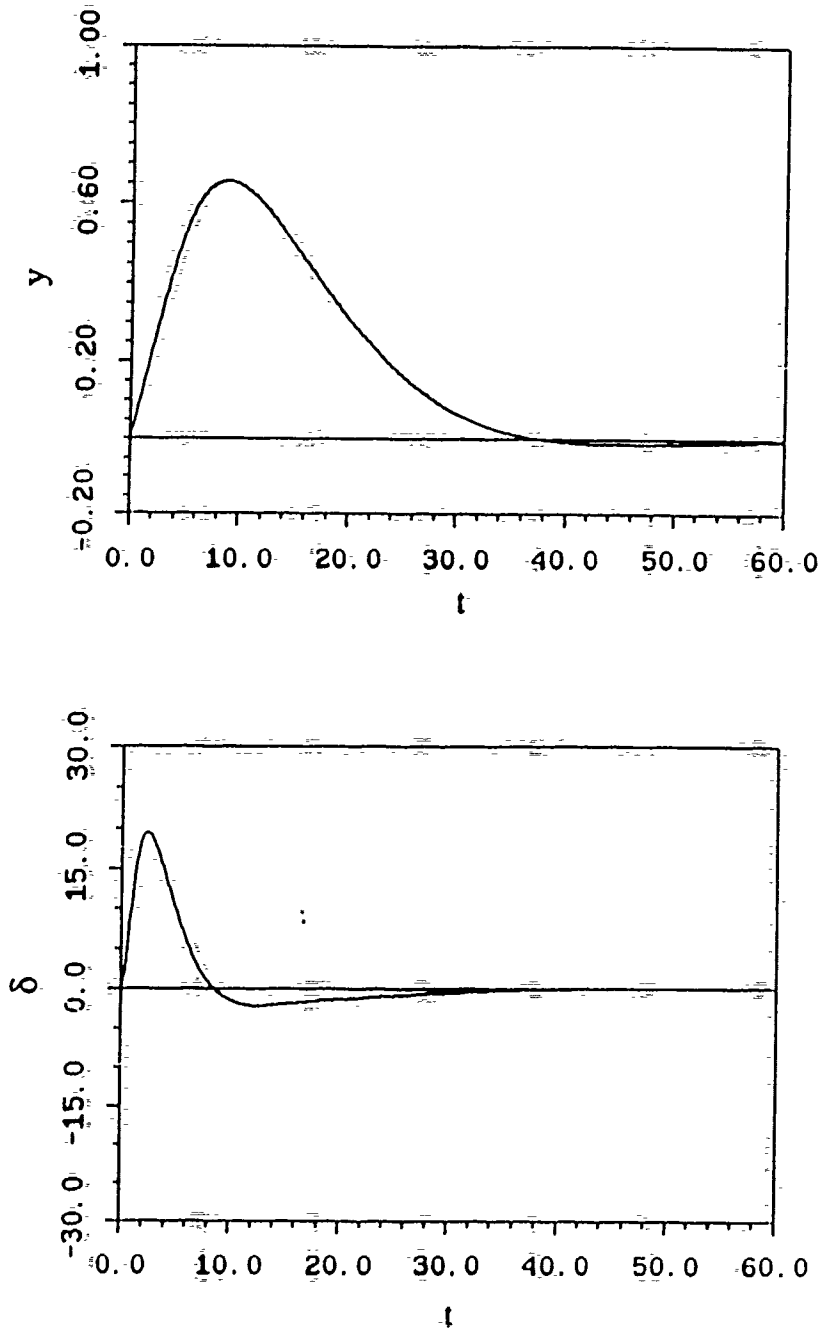

Figure 50. Sensor Noise Effect: Noise Free Sensors, $k_a = 2$, $\phi = 5$, $T_r = 0.5$.

response characteristics significantly. The latter is demonstrated in Figure 51 for T_r = 5 seconds. Finally, even if ϕ is kept at 0.5, introduction of T_r = 0.5 seconds reduces the chattering significantly, as seen in Figure 52.

It follows that increasing the value of ϕ and introducing an appropriate software rudder time constant T_r are two major guidelines for reducing the effects of sensor noise and still keep satisfactory transient response. Of course, observer gains can be established be a Kalman filter design. This should help in minimizing the variance of the control effort and response even further.

D. EFFECTS OF SENSOR DRIFT

Having analyzed the effects of sensor noise, a different aspect of sensor imperfection, namely sensor drift, will now be investigated. The most critical sensor drift for the track keeping problem is the offset or positional drift of the Inertial Navigation System. Along with the simulated noise of the previous section, the offset measurement is assumed to experience a drift of one vehicle length in ten dimensionless seconds before the next exact navigational update comes up. For simulation purposes the drift is assumed to be linear between the two updates. Results for the lateral offset y and rudder angle δ are presented in Figure 53 for u = 6 ft/sec, k_n = 2, ϕ = 5, T_r = 0.5 seconds and lateral current v_c = 2 ft/sec. As expected, the vehicle drifts off the y = 0 track following the sensor read out.

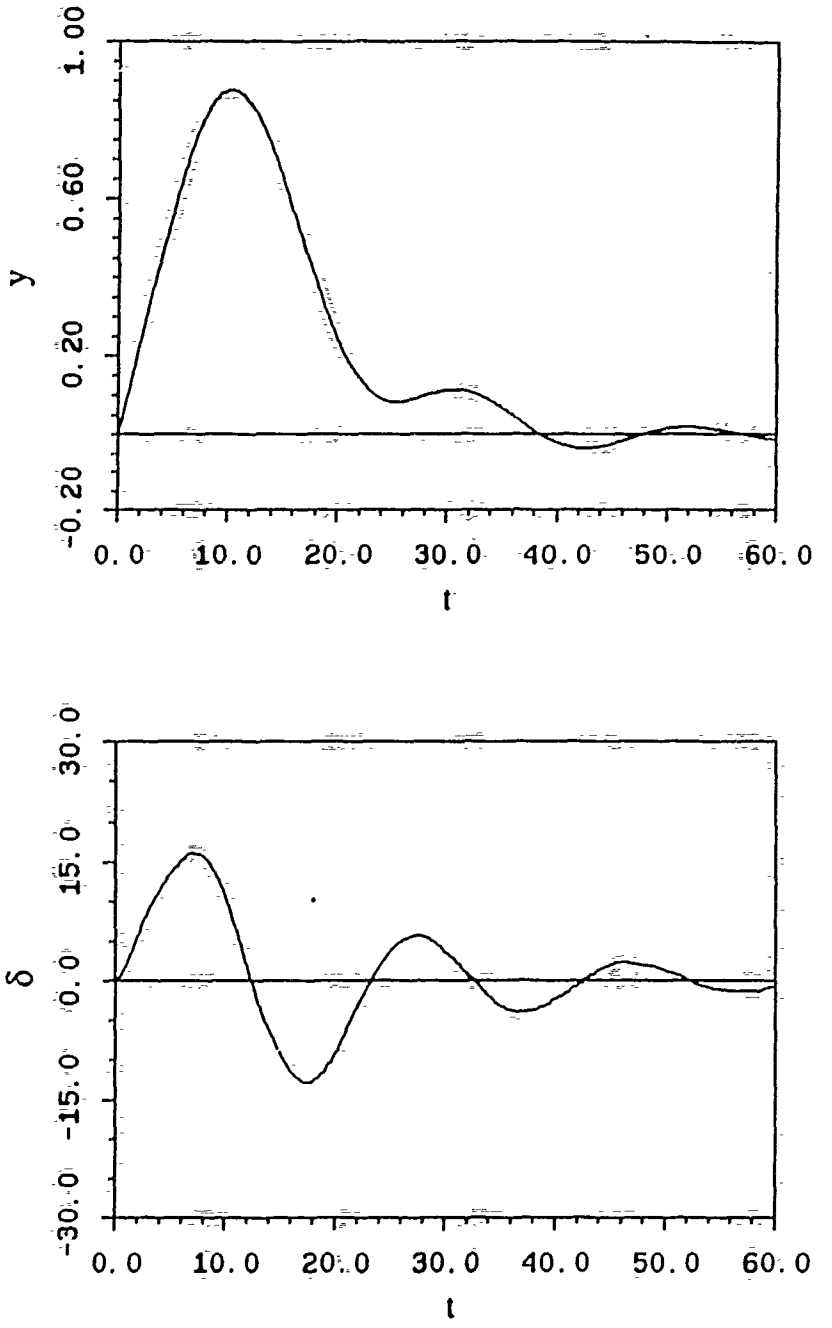

Figure 51. Sensor Noise Effect: $k_a = 2$, $\phi = 5$, $T_r = 5$.

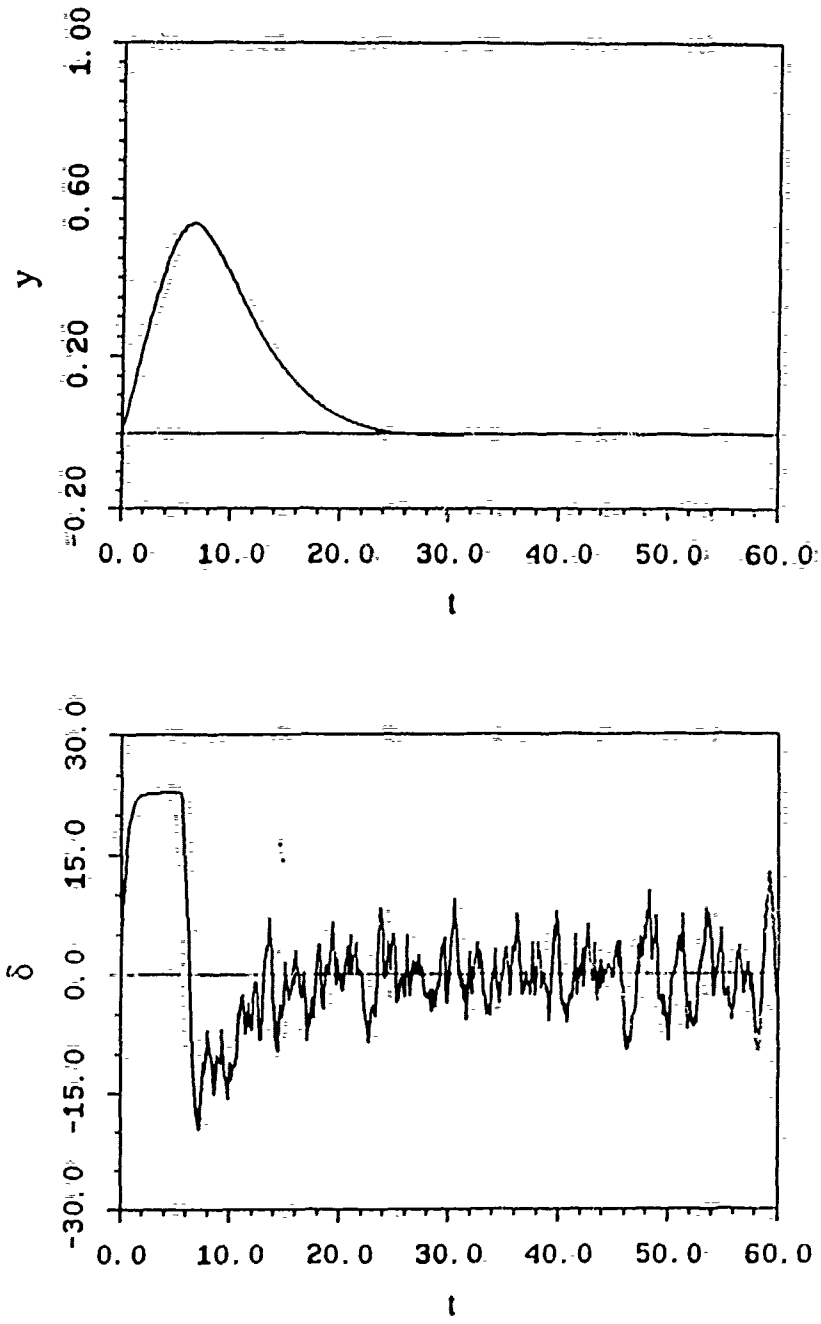

Figure 52. Sensor Noise Effect: $k_a = 2$, $\phi = 0.5$, $T_r = 0.5$.

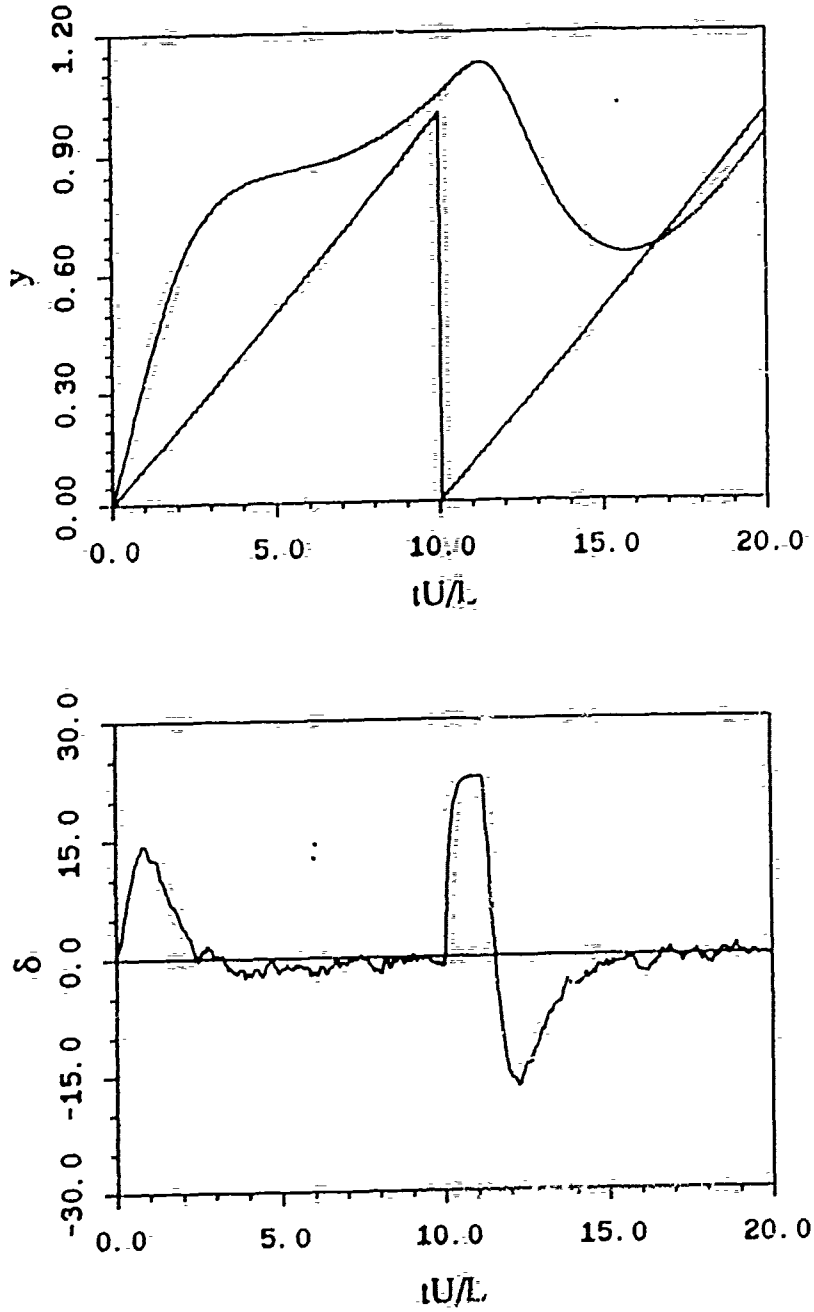

Figure 53. Sensor Drift Effect: Original Design.

This lateral offset drift, or bias, cannot unfortunately be estimated by an observer because the dynamic system is unobservable unless y is measured. One way to improve the response is to record the two most recent navigational updates together with the corresponding sensor readings. Then the sensor drift is assumed to be linear, and this result is extrapolated until the next navigational fix, and the process is repeated. The vehicle response is now satisfactory, as shown in Figure 54, unless the actual sensor drift is significantly different than the extrapolated, such as is the case between 10 and 20, and 30 and 40 dimensionless seconds.

E. NAVIGATIONAL UPDATES EFFECT

So far, knowledge of y is assumed to occur at the same rate as the simulation step, or the autopilot updates in ψ and r. In reality, this will probably not be the case, since measurement of y is more involved than ψ or r, and will thus occur at a slower rate. The effects of updating the cross track error at a slower rate are analyzed in Figures 55 through 61 for u = 6 ft/sec and v_c = 2 ft/sec. The actual path, not the one that is available to the compensator at all times, is plotted versus time using the same scale in all figures for comparison. The response of the nominal design is shown in Figure 55 for k_n = 5 and ϕ = 0.5. The response, when the cross track error y updates are 10, 20 and 30 times slower than the integration step, is presented in Figures 56 through 58. It can be seen that in the latter case, the vehicle is unstable. It should be pointed out, though, that it should not really be expected to apply a cross track error compensator in a strong current

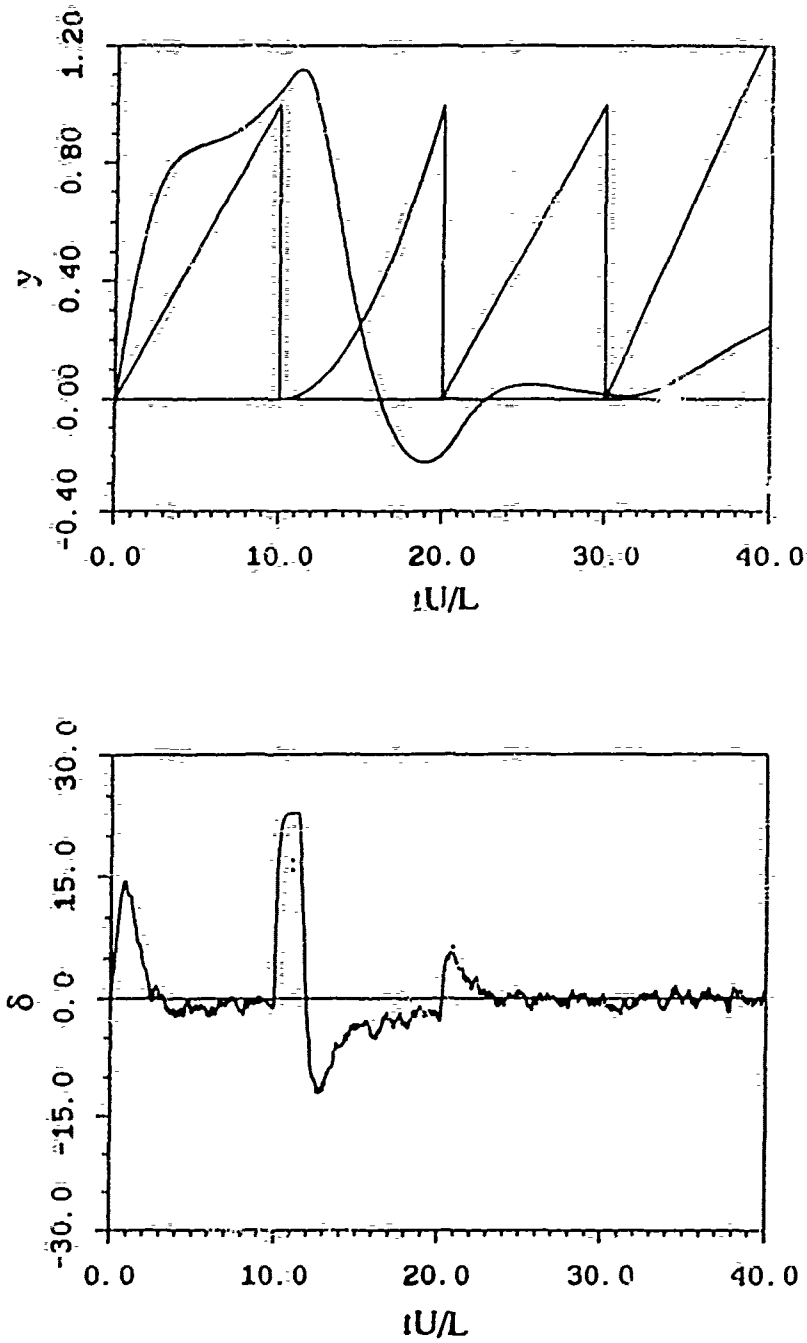

Figure 54. Sensor Drift Effect: Modified Design.

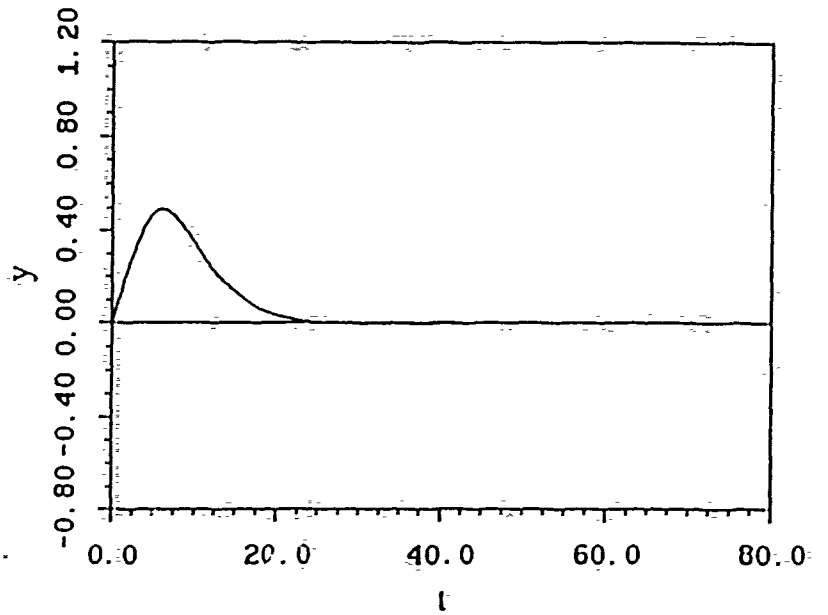

Figure 55. Navigational Updates Effect: Nominal Design.

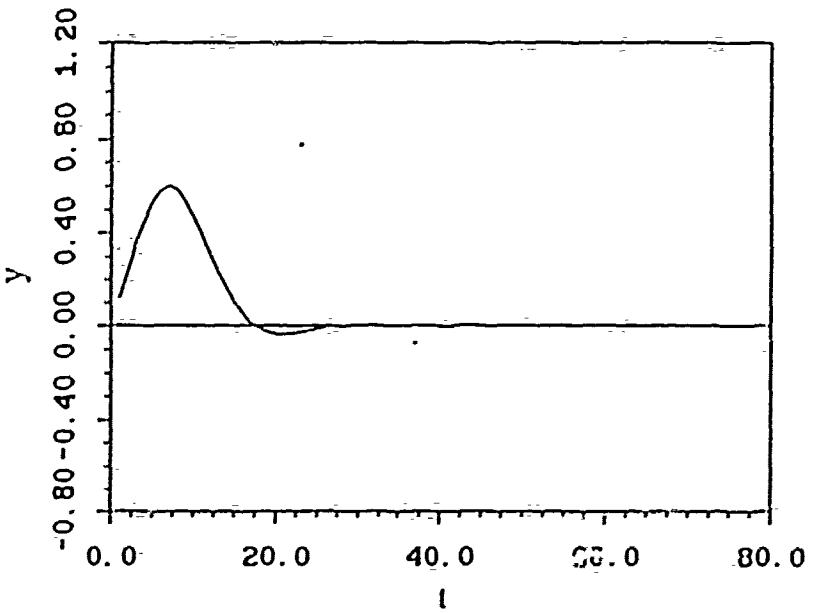

Figure 56. Navigational Updates Effect: Navigational Updates 10 Times Slower Than Autopilot.

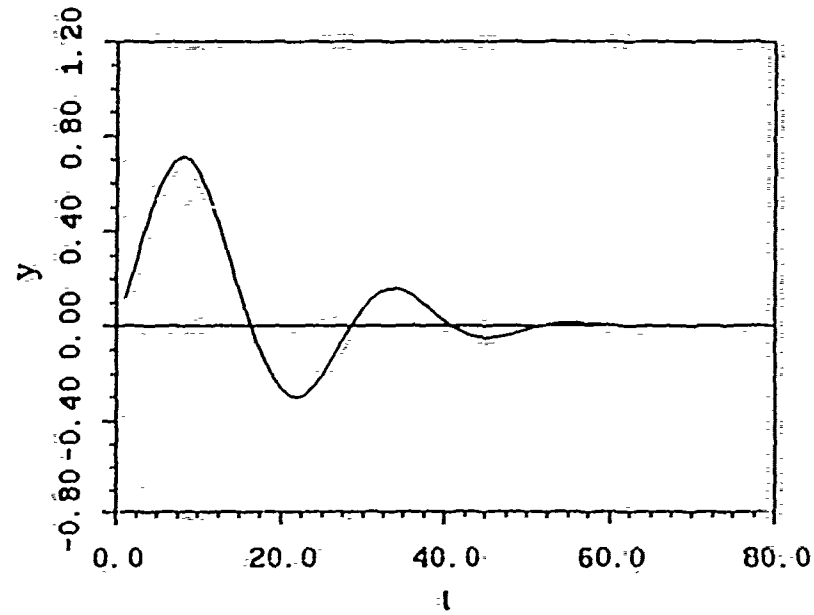

Figure 57. Navigational Updates Effect: Navigational Updates 20 Times Slower Than Autopilot.

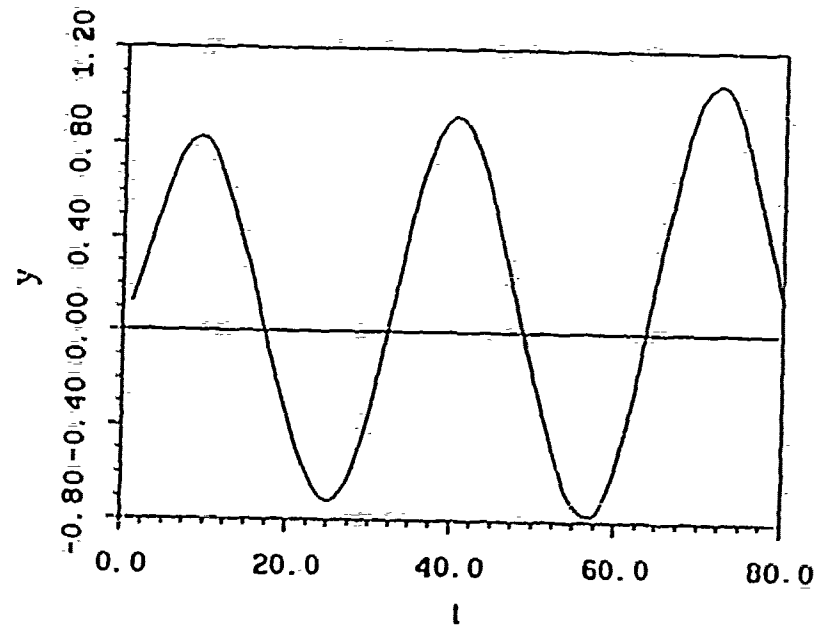

Figure 58. Navigational Updates Effect: Navigational Updates 30 Times Slower Than Autopilot.

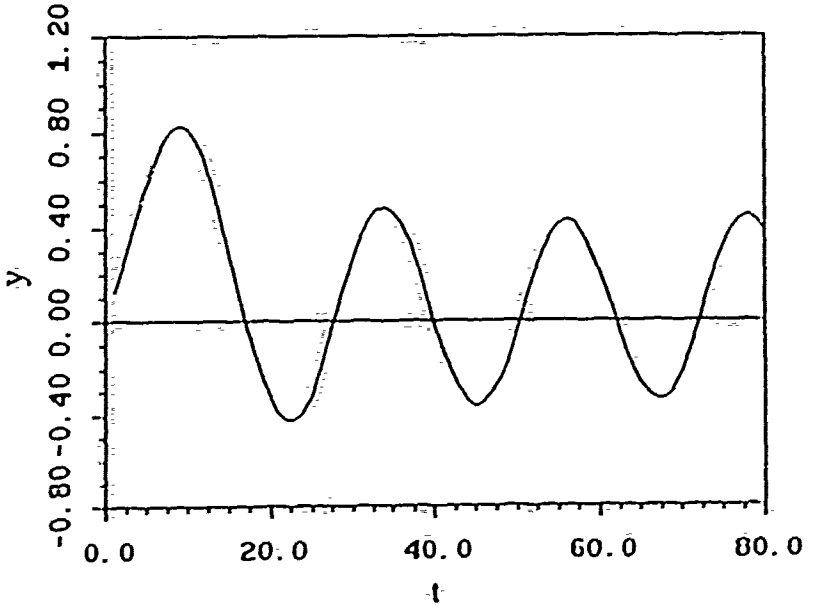

Figure 59. Navigational Updates Effect: Same As Figure 58 with Assumed Linear Variation Between Consecutive Navigational Updates.

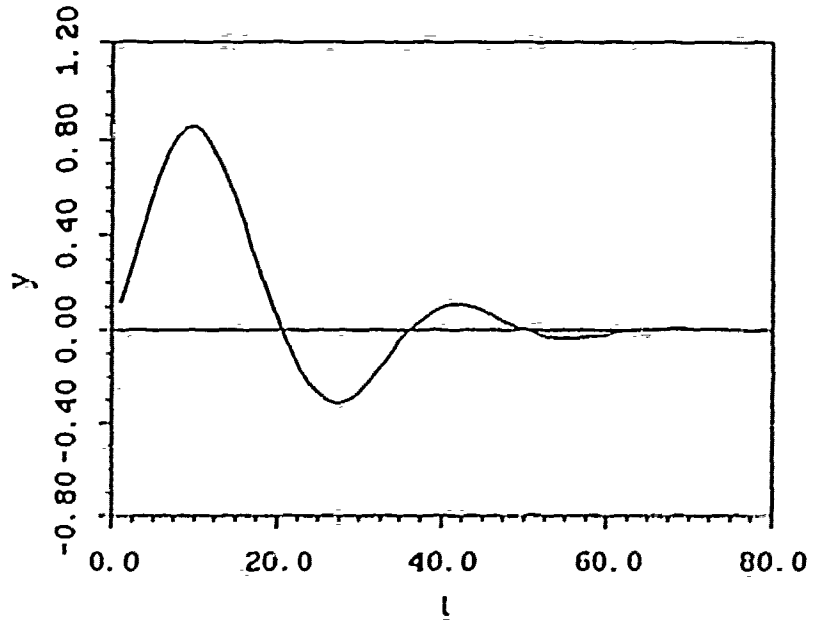

Figure 60. Navigational Updates Effect: Same As Figure 58 with $\phi = 5$.

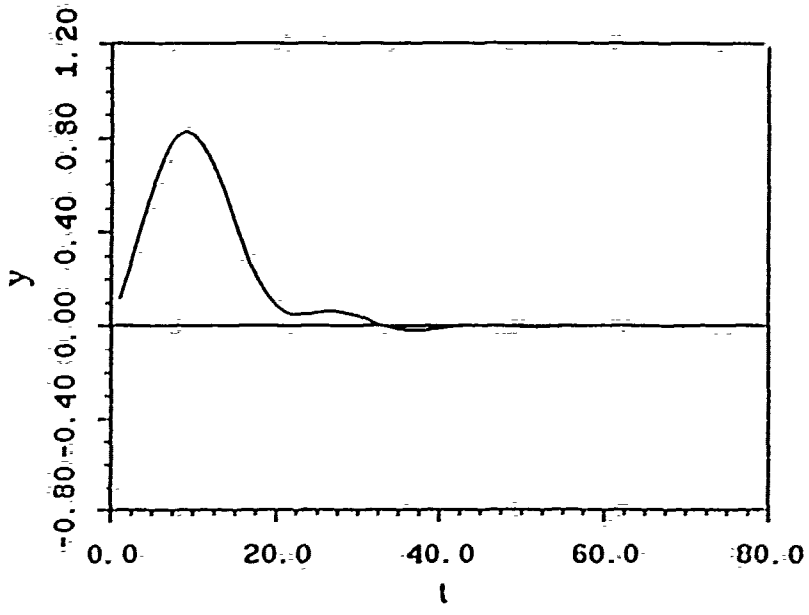

Figure 61. Navigational Updates Effect: Same As Figure 59 with $\phi = 5$.

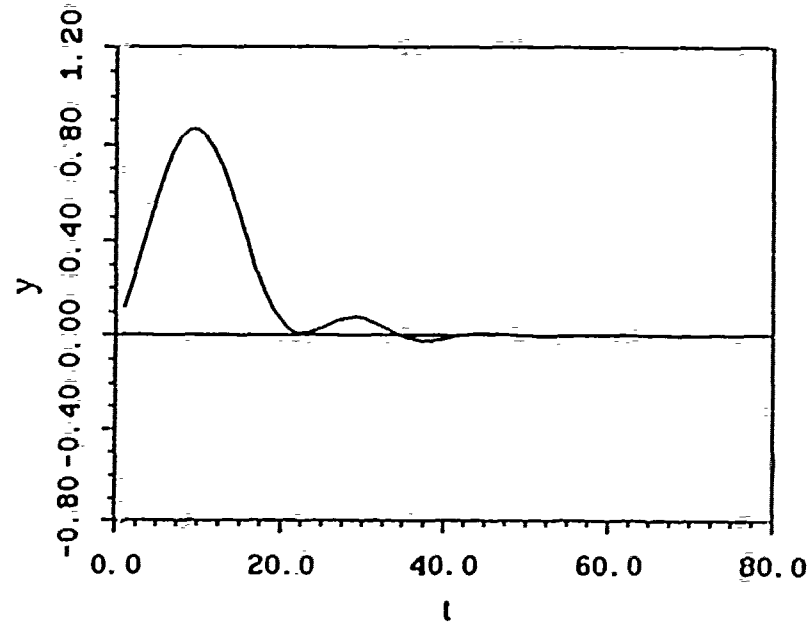

Figure 62. Navigational Updates Effect: Same As Figure 61 with $T_r = 0.5$.

environment when the cross track error is available only once every thirty sample instances!

An improvement can be achieved if the actual track deviation is assumed to vary linearly between two consecutive navigational updates. The results are presented in Figure 59 where the improvement over Figure 58 is evident. The response appears now to be bounded about the y = 0 track. Further improvement can be achieved, if more than two navigational updates are kept and a spline curve is fit among them.

A final improvement is possible if the value of $\dot{\phi}$ is increased. Such an increase was found to be advisable for noise suppression as well. Results for $\dot{\phi}$ = 5 are presented in Figure 60 for a navigational update factor of 30. Unlike the case $\dot{\phi}$ = 0.5 of Figure 58, the response is now stable. When the linear extrapolation technique of the previous paragraph is combined with the above increase in $\dot{\phi}$, the response is faster and less oscillatory, as depicted in Figure 61. Introduction of the software steering gear lag, T_r = 0.5 seconds, does not alter significantly the response, as shown in Figure 62.

CONCLUSIONS AND RECOMMEDATIONS

A. CONCLUSIONS

A methodology for designing sliding mode autopilots for vehicle maneuvering and track following control has been presented. The methods are suitable for a wide variety of related control problems. Also, a technique has been presented to drive the vehicle onto the next track, with no overshoot and minimal rudder use, and which can be used with any of the control methods presented. Finally, noise in the measurable parameters was evaluated and guidelines for suppressing the effects of this noise were presented. In the present case of the AUV track keeping, the principal conclusions of this work can be summarized in the following paragraphs and in Figures 63 and 64.

As seen in Figure 63, it is shown that the cross track error control provides better track keeping characteristics than heading (Line of Sight) control. The premise of this research was the necessity for accurate track keeping of autonomous underwater vehicles for autonomous navigation of a vehicle through confined spaces, and in the presence of obstacles and cross current environments. Thus, it is paramount that AUV's have the ability to follow a track, with minimal cross track error, using the control methods developed in this research. The Line of Sight scheme is very efficient and provides smooth turning characteristics during rapid maneuvering and course changing. For transits along straight line tracks, however, the stability of the scheme is not guaranteed for every way point, target distance combination. This is demonstrated in Figure 63

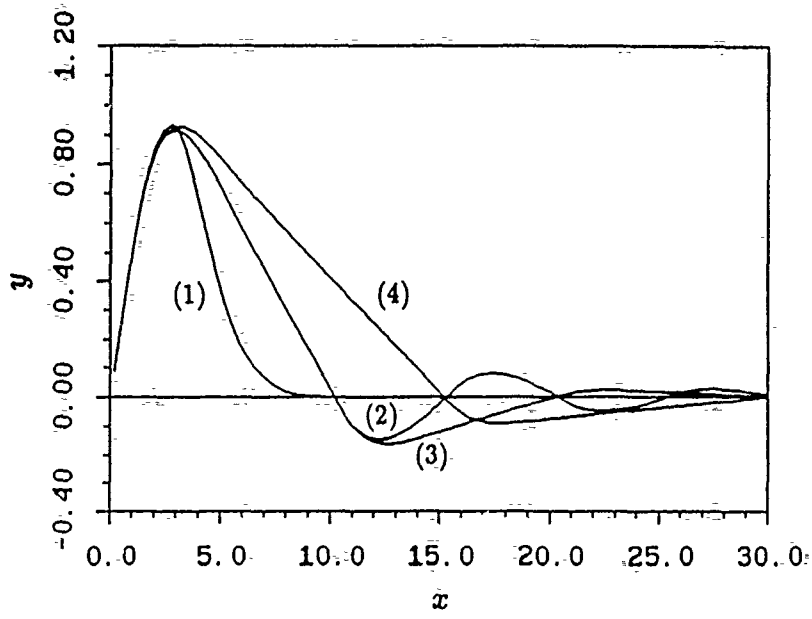

Figure 63. Comparison of Cross Track Error and Line of Sight Control Schemes.

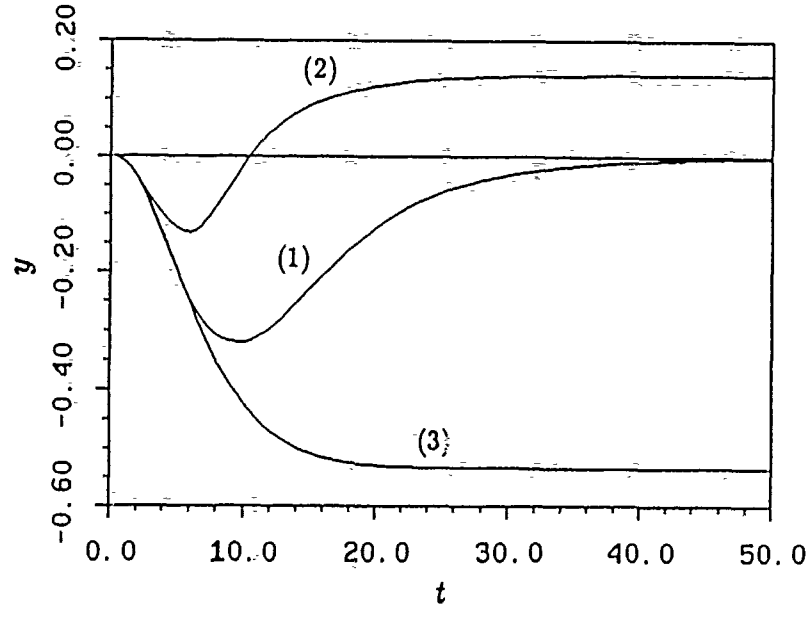

Figure 64. Response of Cross Track Error Controllers Under the Influence of Generic Sway Force and Yaw Moment Disturbances.

where the initial heading is 30°. Curve 1 corresponds to the response of the cross track error design. The rest of the curves correspond to stable responses of Line of Sight designs. Curve 2 corresponds to five way points and target distance d = 2 vehicle lengths, Curve 3 to three way points and d = 0.1 vehicle lengths and Curve 4 to two way points and d = 2 vehicle lengths. As can be seen, Curve 1 is superior to all.

Analytical evaluation of the stability criterion, in the presence of a constant disturbance, was achieved. The cross track error controller developed a steady state track error for this case.

For the integral control method, it was shown that for a nonlinear gain, k_n, greater than or equal to the theoretical critical gain, k_{crit}, there was zero steady state error. However, when the nonlinear gain was less than the theoretical critical gain, there was a finite, but stable steady state error. When the integral control method was modified, a zero steady state error was seen for a nonlinear gain greater than or equal to the theoretical critical gain, as for the integral control method. However, when the nonlinear gain is less than the theoretical critical gain, a zero steady state error results vice the finite, stable steady state error, as in the integral control method. Due to the general oscillatory response of the integral control method, it is best to keep the integrator pole closer to the origin. When utilizing the integral control method, it would be best employed by switching the integrator off, if the oscillatory response is too much during transients, and by switching the integrator on for long, straight transit tracks.

In the disturbance estimation and compensation method, a zero steady state error resulted when the nonlinear gain was greater than or equal to the theoretical critical gain. An unstable response resulted for this control method when the nonlinear gain was less than the theoretical critical gain. For the modified disturbance estimation and compensation method, a zero steady state error again resulted for the nonlinear gain greater than or equal to the theoretical critical gain. Now for the nonlinear gain less than the theoretical critical gain, a stable nonzero steady state error resulted. In general, the response is not oscillatory for the disturbance estimation and compensation method, but this method only controls the cross track error, due to a constant disturbance, when the constant disturbance is a current. On the other hand, the integral control method can control the cross track error, due to any constant disturbance, not only a current. These results are seen in Figure 64. The vehicle was subjected to a sway force disturbance equivalent to a 1 ft/sec current and a yaw moment disturbance equivalent to a 2 ft/sec current, thus the constant disturbances do not correspond to any physically realizable currents. The integral control method (Curve 1) brings the vehicle onto the desired track, whereas, the disturbance estimation and compensation method (Curve 2) and the plain cross track error designs (Curve 3) both experience nonzero steady state errors. Of course, if the disturbance observer is modified to take into account a general sway force and yaw moment, then the response would experience zero steady state error as the integral control method does.

The leading track control technique was seen to improve the turning characteristics of the vehicle, so as not to overshoot the next track and to use minimal rudder. The

distance from the way point to accomplish this was determined automatically by the technique. This technique can be used with all the control methods developed in this research.

The cross track error controller proved to be very robust and was able to handle a wide range of parameter variations without loss of stability.

The effects of sensor noise and sensor drift were numerically evaluated. With appropriate modifications in the control law, it was shown that sensor noise and sensor drift could be minimized. Finally, it was demonstrated that positional updates are very important for accurate track keeping, but they can occur at a slower rate than the rest of the autopilot updates.

B. RECOMMENDATIONS

Some recommendations for further research are as follows:

- Experimental verification using the full scale NPS AUV II after its hydrodynamic coefficients have been reliably established.
- Incorporation of Kalman filter designs to further improve the response and to reduce the effects of sensor noise and random disturbances.
- Simulation of an Inertial Navigation System required for positional updates.

APPENDIX A

```
C ADDED CURRENT AS A DISTURBANCE IN THE CONTROL LAW
C ADDED CURRENT OBSERVER
C ADDED XI TO MODIFY THE DISTURBANCE AND ESTIMATION COMPENSATION
C    METHOD
C
      REAL MASS,LATYAW,NORPIT
      REAL MM(6,6),G4(4),GK4(4),BR(9),HH(9)
      REAL  B(6,6),BB(6,6)
      REAL A(12,12), AA(12,12),INDX(100)
      REAL XPP ,XQQ ,XRR ,XPR
      REAL XUDOT ,XWQ ,XVP ,XVR
      REAL XQDS ,XQDB ,XRDR  ,XVV
      REAL XWW  ,XVDR ,XWDS ,XWDB
      REAL XDSDS,XDBDB ,XDRDR ,XQDSN
      REAL XWDSN ,XDSDSN
      REAL TIME,S,EITA,UBAR,UHAT,COMZ,BAR,SIM,DE,SAT,VHAT,ZZOBS,ZZOBSDOT,SIM1
      REAL SS1,SS2,UD,XD,YD,TD,TNWP,XA,YA,HD,HDMDEG,DAWAY,SATSGN1,SATSGN2
      REAL NAVUPDATE,TNAV,TARGET,FF,GG,HHH,LLL,HDP,HDM,VCUR,UCUR,UCO,VCO,WCO
      REAL UCOOBS,VCOOBS,VCOHAT,UCHAT
      INTEGER DV
C
C     LATERAL HYDRODYNAMIC COEFFICIENTS
C
      REAL YPDOT ,YRDOT,YPQ  ,YQR
      REAL YVDOT ,YP   ,YR   ,YVQ
      REAL YWP  ,YWR ,YV ,YVW
      REAL YDR  ,CDY
C
C     NORMAL HYDRODYNAMIC COEFFICIENTS
C
      REAL ZQDOT ,ZPP,ZPR ,ZRR
      REAL ZWDOT ,ZQ  ,ZVP   ,ZVR
      REAL ZW  ,ZVV   ,ZDS  ,ZDB
      REAL ZQN ,ZWN  ,ZDSN ,CDZ
      REAL ZHADOT,ZHAT
C
C     ROLL HYDRODYNAMIC COEFFICIENTS
C
      REAL KPDOT ,KRDOT ,KPQ ,KQR
      REAL KVDOT , KP  ,KR    ,KVQ
      REAL KWP  , KWR   ,KV     ,KVW
      REAL KPN   , KDB
C
C     PITCH HYDRODYNAMIC COEFFICIENTS
C
      REAL MQDOT ,MPP  ,MPR,MRR
      REAL MWDOT , MQ  ,MVP    ,MVR
      REAL MW  , MVV   ,MDS  ,MDB
      REAL MQN , MWN  ,MDSN
      REAL QHADOT,QHAT,THADOT,THAT
C
C     YAW HYDRODYNAMIC COEFFICIENTS
C
      REAL NPDOT,NRDOT,NPQ ,NQR
      REAL NVDOT  , NP   ,NR     ,NVQ
      REAL NWP  , NWR  ,NV   ,NVW
      REAL NDR
C
C     MASS CHARACTERISTICS OF THE FLOODED VEHICLE
C
```

```
      REAL  WEIGHT , BOY   ,VOL ,XG
      REAL YG   , ZG   ,XB    ,ZB
      REAL IX   , IY   ,IZ    ,IXZ
      REAL IYZ   , IXY    ,YB
      REAL L   , RHO  ,G     ,NU
      REAL A0    ,KPROP ,NPROP ,    X1TEST
      REAL DEGRUD   ,DEGSTN
      COMMON /BLOCK1/ F(12), FP(6), XMMINV(6,6), UCF
      INTEGER N,IA,IDGT,IER,LAST,J,K,M,JJ,KK,I
      REAL VECV1(9),VECV2(9),X(12),VECH1(9),VECH2(9),X1(9)
C
C     RUDDER COEFFICIENTS
C
      PARAMETER ( DSMAX= -0.175)
C
C     LONGITUDINAL HYDRODYNAMIC COEFFICIENTS
C
      PARAMETER(XPP = 7.E-3   ,XQQ = -1.5E-2 ,XRR = 4.E-3   ,XPR =7.5E-4,
     & XUDOT=-7.6E-3   ,XWQ = -2.E-1     ,XVP = -3.E-3    ,XVR = 2.E-2,
     & XQDS=2.5E-2     ,XQDB=-2.6E-3     ,XRDR= -1.E-3    ,XVV =5.3E-2,
     & XWW =1.7E-1     ,XVDR=1.7E-3      ,XWDS=4.6E-2     ,XWDB= 1.E-2,
     & XDSDS= -1.E-2   ,XDBDB= -8.E-3    ,XDRDR= -1.E-2   ,XQDSN= 2.E-3,
     & XWDSN=3.5E-3    ,XDSDSN= -1.6E-3 )
C
C     LATERAL HYDRODYNAMIC COEFFICIENTS
C
      PARAMETER(YPDOT=1.2E-4 ,YRDOT=1.2E-3  ,YPQ = 4.E-3 ,YQR =-6.5E-3,
     & YVDOT=-5.5E-2   ,YP  = 3.E-3      ,YR = 3.E-2      ,YVQ =2.4E-2,
     & YWP =2.3E-1     ,YWR =-1.9E-2     ,YV = -1.E-1     ,YVW =6.8E-2,
     & YDR =2.7E-2     ,CDY =3.5E-1)
C
C     NORMAL HYDRODYNAMIC COEFFICIENTS
C
      PARAMETER(ZQDOT=-6.8E-3 ,ZPP =1.3E-4  ,ZPR =6.7E-3  ,ZRR =-7.4E-3,
     & ZWDOT=-2.4E-1 ,ZQ =-1.4E-1      ,ZVP =-4.8E-2    ,ZVR =4.5E-2,
     & ZW =  -3.E-1    ,ZVV =-6.8E-2     ,ZDS =-7.3E-2    ,ZDB =2.6E-2,
     & ZQN =-2.9E-3    ,ZWN =-5.1E-3     ,ZDSN= -1.E-2    ,CDZ = 1.0)
C
C     ROLL HYDRODYNAMIC COEFFICIENTS
C
      PARAMETER(KPDOT= -1.E-3 ,KRDOT=-3.4E-5 ,KPQ =-6.9E-5 ,KQR =1.7E-2,
     & KVDOT=1.3E-4    , KP =-1.1E-2     ,KR =-8.4E-4     ,KVQ=-5.1E-3,
     & KWP =-1.3E-4    , KWR =1.4E-2     ,KV =3.1E-3      ,KVW =-1.9E-1,
     & KPN =-5.7E-4   , KDB = 0.0 )
C
C     PITCH HYDRODYNAMIC COEFFICIENTS
C
      PARAMETER(MQDOT=-1.7E-2 ,MPP =5.3E-5  ,MPR = 5.E-3 ,MRR =-2.9E-3,
     & MWDOT=-6.8E-3   , MQ =-6.8E-2     ,MVP =1.2E-3     ,MVR =1.7E-2,
     & MW = 1.E-1      , MVV =-2.6E-2    ,MDS =-4.1E-2    ,MDB =6.9E-3,
     & MQN =-1.6E-3    , MWN =-2.9E-3    ,MDSN =-5.2E-3)
C
C     YAW HYDRODYNAMIC COEFFICIENTS
C
      PARAMETER(NPDOT=-3.4E-5 ,NRDOT=-3.4E-3,NPQ =-2.1E-2 ,NQR =2.7E-3,
     & NVDOT=1.2E-3    , NP =-8.4E-4     ,NR =-1.6E-2     ,NVQ = -1.E-2,
     & NWP =-1.7E-2    , NWR =7.4E-3     ,NV =-7.4E-3     ,NVW =-2.7E-2,
     & NDR =-1.3E-2)
C
C     MASS CHARACTERISTICS OF THE FLOODED VEHICLE
```

```
C
      PARAMETER( WEIGHT =12000.  BOY =12000. ,VOL =200. ,XG = 0.   ,
     & YG = 0.0        , ZG = 0.20       ,XB = 0.         ,ZB =  0.0 ,
     & IX = 1500.      , IY = 10000.     ,IZ = 10000.     ,IXZ = -10. ,
     & IYZ = -10.      , IXY = -10.      ,YB =  0.0 ,
     & L = 17.4        , RHO = 1.94      ,G = 32.2        ,NU = 8.47E-4 ,
     & A0 = 2.0        ,KPROP = 0.       ,NPROP = 0. ,    X1TEST= 0.1 ,
     & DEGRUD= 0.0     ,DEGSTN=  0.0)
C
C     INPUT INITIAL CONDITIONS HERE IF REQUIRED
C
      OPEN(20,FILE='MODEL1.DAT',STATUS='NEW')
C
      NUMPTS=0.0
      DV=1.0
C
C**********************OBTAIN INITIAL INFORMATION*****************
C
        OPEN (30,FILE='INITIAL.DAT',STATUS='OLD')
        READ (30,*) U0,RPM
        READ (30,*) UD,NAVUPDATE,SIM1,DELT
        READ (30,*) XD2,YD2,COMZ
C
C... READ IN STEERING AND SLIDING SURFACE GAINS,INITIAL CURRENTS,
C...     AND SATURATION DESIRED
C
      OPEN(21,FILE='SMCINT.DAT',STATUS='OLD')
      READ(21,*) GG1,GG2,GG3,GG4,GG5
      READ(21,*) SP1,SP2,SP3,SP4,SP5
      READ(21,*) UCO,VCO,WCO
      READ(21,*) AKN,SSPHI
      READ(21,*) IPTS,XI
C
      UCOOBS=0.0
      VCOOBS=0.0
      V0 = 0.0
      W0 = 0.0
      P0 = 0.0
      Q0 = 0.0
      R0 = 0.0
      PHI0 = 0.0
      THETA0 = 0.0
      PSI0 = 0.0
      XPOS0=0.0
      YPOS0=0.0
      ZPOS0=0.0
      XD1=0.0
      YD1=0.0
      DB= 0.0
      DS = 0.0
      DR = 0.0
      LATYAW = 0.0
      NORPIT = 0.0
      RE = U0*L/NU
        TNAV=0
        XA=XPOS0
        YA=YPOS0
C
      TIME=0.0
      TIME0=0.0
```

```
      U = U0
      V = V0
      W = W0
      P = P0
      Q = Q0
      R = R0
      XPOS = XPOS0
      YPOS = YPOS0
      ZPOS = ZPOS0
      PSI = PHI0
      THETA = THETA0
      PHI = PHI0
        QHADOT=0.0
        THADOT=0.0
        ZHADOT=0.0
        QHAT=0.0
        THAT=0.0
        ZHAT=0.0
        VHAT=0.0
        ZOBSDOT=0.0
        ZZOBS = 0.0
C
C... DEFINE THE LENGTH X AND HEIGHT HH TERMS FOR THE DRAG INTEGRATION
C
      X1(1) = -105.9/12.
      X1(2) = -99.3/12.
      X1(3) = -87.3/12.
      X1(4) = -66.3/12.
      X1(5) = 72.7/12.
      X1(6) = 83.2/12.
      X1(7) = 91.2/12.
      X1(8) = 99.2/12.
      X1(9) = 103.2/12.
C
      HH(1) = 0.00/12.
      HH(2) = 8.24/12.
      HH(3) = 19.76/12.
      HH(4) = 29.36/12.
      HH(5) = 31.85/12.
      HH(6) = 27.84/12.
      HH(7) = 21.44/12.
      HH(8) = 12.00/12.
      HH(9) = 0.00/12.
C
      BR(1) =    0.00/12.0
      BR(2) =    8.24/12.0
      BR(3) =   19.76/12.0
      BR(4) =   29.36/12.0
      BR(5) =   31.85/12.0
      BR(6) =   27.84/12.0
      BR(7) =   21.44/12.0
      BR(8) =   12.00/12.0
      BR(9) =    0.00/12.0
C
      MASS = WEIGHT/G
C
      N = 6
      DO 15 J = 1,N
         DO 10 K = 1,N
         XMMINV(J,K) = 0.0
```

```
          MM(J,K) = 0.0
10        CONTINUE
15      CONTINUE
C
C       DEFINE MASS MATRIX
C
        MM(1,1) = MASS -((RHO/2)*(L**3)*XUDOT)
        MM(1,5) = MASS*ZG
        MM(1,6) = -MASS*YG
C
        MM(2,2) = MASS -((RHO/2)*(L**3)*YVDOT)
        MM(2,4) = -MASS*ZG -((RHO/2)*(L**4)*YPDOT)
        MM(2,6) = MASS*XG - ((RHO/2)*(L**4)*YRDOT)
C
        MM(3,3) = MASS - ((RHO/2)*(L**3)*ZWDOT)
        MM(3,4) = MASS*YG
        MM(3,5) = -MASS*XG -((RHO/2)*(L**4)*ZQDOT)
C
        MM(4,2) = -MASS*ZG - ((RHO/2)*(L**4)*KVDOT)
        MM(4,3) = MASS*YG
        MM(4,4) = IX - ((RHO/2)*(L**5)*KPDOT)
        MM(4,5) = -IXY
        MM(4,6) = -IXZ -((RHO/2)*(L**5)*KRDOT)
C
        MM(5,1) = MASS*ZG
        MM(5,3) = -MASS*XG -((RHO/2)*(L**4)*MWDOT)
        MM(5,4) = -IXY
        MM(5,5) = IY -((RHO/2)*(L**5)*MQDOT)
        MM(5,6) = -IYZ
C
        MM(6,1) = -MASS*YG
        MM(6,2) = MASS*XG -((RHO/2)*(L**4)*NVDOT)
        MM(6,4) = -IXZ - ((RHO/2)*(L**5)*NPDOT)
        MM(6,5) = -IYZ
        MM(6,6) = IZ - ((RHO/2)*(L**5)*NRDOT)
C
C   OBSERVER POLES
C
        S1=-1.0
        S2=-1.1
        S3=-1.2
C
C   OBSERVER A MATRIX CONSTANTS AND B MATRIX CONSTANTS
C
        A11=-0.04538
        A12=-0.35119
        A21=-0.002795
        A22=-0.09568
        B1 = 0.011432
        B2 =-0.004273
C
C         *****ROUTINE FOR INVERTING THE MM MATRIX*****
C
          DO 12 I=1,N
            DO 11 J=1,N
              XMMINV(I,J)=0.0
11          CONTINUE
            XMMINV(I,I)=1
12        CONTINUE
        CALL INVTA(MM,N,INDX,D)
```

```
        DO 13 J=1,N
      CALL INVTB(MM,N,INDX,XMMINV(1,J))
13      CONTINUE
C
C       *************          INPUTS          **************
C
C      RUDDER AND DIVE PLANE COMMANDS
C
        SIM=SIM1/DELT
        TIME=0.0
        DS= 0.0
        DR= 0.0
        DB= 0.0
        EITA=4.0
        BAR=.4
C
      YINTGR=0.0
      SSPHM=-SSPHI
C
C... DETERMINE THE ANGLE ALPHA;XPOS AND YPOS ARE GLOBAL COORDINATES
C
      XPOS1=XD1
      YPOS1=YD1
      XPOS2=XD2
      YPOS2=YD2
      CALL ANGLE(XPOS1,YPOS1,XPOS2,YPOS2,ALPH)
C
C... DETERMINE THE LENGTH OF INITIAL PATH
C
      XT=SQRT((XPOS2-XPOS1)**2 + (YPOS2-YPOS1)**2)
      XT=XT*L
C
C       ********************SIMULATION BEGINS ****************
C
        DO 100 I=1,SIM
C
C     PROPULSION MODEL
C
      SIGNU = 1.0
      IF (U.LT.0.0) SIGNU = -1.0
      IF (ABS(U).LT.X1TEST) U = X1TEST
      SIGNN = 1.0
      IF (RPM.LT.0.0) SIGNN = -1.0
      ETA = 0.012*RPM/U
      RE = U*L/NU
      CD0 =  .00385 + (1.296E-17)*(RE - 1.2E7)**2
      CT  = ABS(0.008*L**2*ETA*ABS(ETA)/(A0))
      CT1 =ABS( 0.008*L**2/(A0))
      EPS = -1.0+SIGNN/SIGNU*(SQRT(CT+1.0)-1.0)/(SQRT(CT1+1.0)-1.0)
      XPROP = CD0*(ETA*ABS(ETA) - 1.0)
C
C... CALCULATE THE DRAG FORCE, INTEGRATE THE DRAG OVER THE VEHICLE
C
      DO 500 K=1,9
         UCF=(V+X(K)*R)**2+(W-X(K)*Q)**2
         UCF=SQRT(UCF)
         IF (UCF.LT.1.E-6) GO TO 601
         CFLOW   =CDY*HH(K)*(V+X(K)*R)**2+CDZ*BR(K)*(W-X(K)*Q)**2
         VECH1(K)=CFLOW*(V+X(K)*R)/UCF
         VECH2(K)=CFLOW*(V+X(K)*R)*X(K)/UCF
```

```
          VECV1(K)=CFLOW*(W-X(K)*Q)/UCF
          VECV2(K)=CFLOW*(W-X(K)*Q)*X(K)/UCF
  500   CONTINUE
        CALL TRAP(9,VECV1,X,HEAVE)
        CALL TRAP(9,VECV2,X,PITCH)
        CALL TRAP(9,VECH1,X,SWAY )
        CALL TRAP(9,VECH2,X,YAW  )
       SWAY=-0.5*RHO*SWAY
       YAW =-0.5*RHO*YAW
       HEAVE=-0.5*RHO*HEAVE
       PITCH=+0.5*RHO*PITCH
           GO TO 602
  601      HEAVE=0.0
           PITCH=0.0
           SWAY =0.0
           YAW  =0.0
  602      CONTINUE
C
C      FORCE EQUATIONS
C
C
C     LONGITUDINAL FORCE
C
        FP(1) = MASS*V*R - MASS*W*Q + MASS*XG*Q**2 + MASS*XG*R**2-
     &         MASS*YG*P*Q - MASS*ZG*P*R + (RHO/2)*L**4*(XPP*P**2 +
     &         XQQ*Q**2 + XRR*R**2 + XPR*P*R) +(RHO/2)*L**3*(XWQ*W*Q +
     &         XVP*V*P+XVR*V*R+U*Q*(XQDS*DS+XQDB*DB)+XRDR*U*R*DR)+
     &         (RHO/2)*L**2*(XVV*V**2 + XWW*W**2 + XVDR*U*V*DR + U*W*
     &         (XWDS*DS+XWDB*DB)+U**2*(XDSDS*DS**2+XDBDB*DB**2+
     &         XDRDR*DR**2))-(WEIGHT -BOY)*SIN(THETA) +(RHO/2)*L**3*
     &         XQDSN*U*Q*DS*EPS+(RHO/2)*L**2*(XWDSN*U*W*DS+XDSDSN*U**2*
     &         DS**2)*EPS +(RHO/2)*L**2*U**2*XPROP
C
C     LATERAL FORCE
C
        FP(2) = -MASS*U*R - MASS*XG*P*Q + MASS*YG*R**2 - MASS*ZG*Q*R +
     &         (RHO/2)*L**4*(YPQ*P*Q + YQR*Q*R)+(RHO/2)*L**3*(YP*U*P +
     &         YR*U*R + YVQ*V*Q + YWP*W*P + YWR*W*R) + (RHO/2)*L**2*
     &         (YV*U*V + YVW*V*W +YDR*U**2*DR) +SWAY +(WEIGHT-BOY)*
     &         COS(THETA)*SIN(PHI)+MASS*W*P+MASS*YG*P**2
C
C     NORMAL FORCE
C
        FP(3) = MASS*U*Q - MASS*V*P - MASS*XG*P*R - MASS*YG*Q*R +
     &         MASS*ZG*P**2 + MASS*ZG*Q**2 + (RHO/2)*L**4*(ZPP*P**2 +
     &         ZPR*P*R + ZRR*R**2) + (RHO/2)*L**3*(ZQ*U*Q + ZVP*V*P +
     &         ZVR*V*R) +(RHO/2)*L**2*(ZW*U*W + ZVV*V**2 + U**2*(ZDS*
     &         DS+ZDB*DB))+HEAVE+(WEIGHT-BOY)*COS(THETA)*COS(PHI)+
     &         (RHO/2)*L**3*ZQN*U*Q*EPS +(RHO/2)*L**2*(ZWN*U*W +ZDSN*
     &         U**2*DS)*EPS
C
C     ROLL FORCE
C
        FP(4) = -IZ*Q*R +IY*Q*R -IXY*P*R +IYZ*Q**2 -IYZ*R**2 +IXZ*P*Q +
     &         MASS*YG*U*Q -MASS*YG*V*P -MASS*ZG*W*P+(RHO/2)*L**5*(KPQ*
     &         P*Q + KQR*Q*R) +(RHO/2)*L**4*(KP*U*P +KR*U*R + KVQ*V*Q +
     &         KWP*W*P + KWR*W*R) +(RHO/2)*L**3*(KV*U*V + KVW*V*W) +
     &         (YG*WEIGHT - YB*BOY)*COS(THETA)*COS(PHI) - (ZG*WEIGHT -
     &         ZB*BOY)*COS(THETA)*SIN(PHI) + (RHO/2)*L**4*KPN*U*P*EPS+
     &         (RHO/2)*L**3*U**2*KPROP +MASS*ZG*U*R
```

```
C
C     PITCH FORCE
C
      FP(5) = -IX*P*R +IZ*P*R +IXY*Q*R -IYZ*P*Q -IXZ*P**2 +IXZ*R**2 -
     &        MASS*XG*U*Q + MASS*XG*V*P + MASS*ZG*V*R - MASS*ZG*W*Q +
     &        (RHO/2)*L**5*(MPP*P**2 +MPR*P*R +MRR*R**2)+(RHO/2)*L**4*
     &        (MQ*U*Q + MVP*V*P + MVR*V*R) + (RHO/2)*L**3*(MW*U*W +
     &        MVV*V**2+U**2*(MDS*DS+MDB*DB))+ PITCH -(XG*WEIGHT-
     &        XB*BOY)*COS(THETA)*COS(PHI)+(RHO/2)*L**4*MQN*U*Q*EPS +
     &        (RHO/2)*L**3*(MWN*U*W+MDSN*U**2*DS)*EPS-
     &        (ZG*WEIGHT-ZB*BOY)*SIN(THETA)
C
C     YAW FORCE
C
      FP(6) = -IY*P*Q +IX*P*Q +IXY*P**2 -IXY*Q**2 +IYZ*P*R -IXZ*Q*R -
     &        MASS*XG*U*R + MASS*XG*W*P - MASS*YG*V*R + MASS*YG*W*Q +
     &        (RHO/2)*L**5*(NPQ*P*Q + NQR*Q*R) +(RHO/2)*L**4*(NP*U*P+
     &        NR*U*R + NVQ*V*Q +NWP*W*P + NWR*W*R) +(RHO/2)*L**3*(NV*
     &        U*V + NVW*V*W + NDR*U**2*DR) + YAW + (XG*WEIGHT -
     &        XB*BOY)*COS(THETA)*SIN(PHI)+(YG*WEIGHT)*SIN(THETA)
     &        +(RHO/2)*L**3*U**2*NPROP-YB*BOY*SIN(THETA)
C
C     NOW COMPUTE THE F(1-6) FUNCTIONS
C
      DO 600 J = 1,6
             F(J) = 0.0
      DO 600 K = 1,6
             F(J) = XMMINV(J,K)*FP(K) + F(J)
600   CONTINUE
C
C     THE LAST SIX EQUATIONS COME FROM THE KINEMATIC RELATIONS
C
C      INERTIAL POSITION RATES F(7-9)
C
      F(7) = UCO + U*COS(PSI)*COS(THETA) + V*(COS(PSI)*SIN(THETA)*
     &       SIN(PHI) - SIN(PSI)*COS(PHI)) + W*(COS(PSI)*SIN(THETA)*
     &       COS(PHI) + SIN(PSI)*SIN(PHI))
C
      F(8) = VCO + U*SIN(PSI)*COS(THETA) + V*(SIN(PSI)*SIN(THETA)*
     &       SIN(PHI) + COS(PSI)*COS(PHI)) + W*(SIN(PSI)*SIN(THETA)*
     &       COS(PHI) - COS(PSI)*SIN(PHI))
C
      F(9) = WCO - U*SIN(THETA) +V*COS(THETA)*SIN(PHI) +W*COS(THETA)*
     &       COS(PHI)
C
C     EULER ANGLE RATES F(10-12)
C
      F(10) = P + Q*SIN(PHI)*TAN(THETA) + R*COS(PHI)*TAN(THETA)
C
      F(11) = Q*COS(PHI) - R*SIN(PHI)
C
      F(12) = Q*SIN(PHI)/COS(THETA) + R*COS(PHI)/COS(THETA)
C
C
      UDOT = F(1)
      VDOT = F(2)
      WDOT = F(3)
      PDOT = F(4)
      QDOT = F(5)
      RDOT = F(6)
```

```
      XDOT = F(7)
      YDOT = F(8)
      ZDOT = F(9)
      PHIDOT = F(10)
      THETAD = F(11)
      PSIDOT = F(12)
C
C     *******  CREATE OUTPUT DATA FILE *************************
C
       IF (I .EQ. DV ) THEN
       TIMER=FLOAT(I)/2.
       WRITE (20,*) I
       WRITE (20,743)  DR/.01745
       WRITE (20,744)  XPOS/L,YPOS/L,XD2,YD2
       WRITE (20,746)  (PSI-ALPH)/.01745,YLCASE/L
       WRITE (20,746) VCOOBS,UCOOBS
743    FORMAT (E11.3)
744    FORMAT (4E12.4)
746    FORMAT (2E12.4)
C
       NUMPTS=NUMPTS + 1
       DV=DV+1.0/DELT
       ENDIF
C
C*****
C      FIRST ORDER INTEGRATION
C
      U = U + DELT*UDOT
C                                      U = SURGE RATE
      V = V + DELT*VDOT
C                                      V = SWAY RATE
      W = W + DELT*WDOT
C                                      W = HEAVE RATE
      P = P + DELT*PDOT
C                                      P = ROLL RATE
      Q = Q + DELT*QDOT
C                                      Q = PITCH RATE
      R = R + DELT*RDOT
C                                      R = YAW RATE
      XPOS = XPOS + DELT*XDOT
C                                      X = SURGE
      YPOS = YPOS + DELT*YDOT
C                                      Y = SWAY
      ZPOS = ZPOS + DELT*ZDOT
C                                      Z = HEAVE
      PHI = PHI + DELT*PHIDOT
C                                      PHI = ROLL
      THETA = THETA + DELT*THETAD
C                                      THETA = PITCH
      PSI = PSI + DELT*PSIDOT
C                                      PSI = YAW
C
      YINTGR=YINTGR + DELT*YLCASE
C
C       *********SLIDING MODE DEPTH  CONTROL*************
C
        CALL OBSER(QHADOT,THADOT,ZHADOT,QHAT,THAT,ZHAT,DELT,ZPOS,DS,U0)
C
        S=QHAT + 0.52*THAT - 0.0112*(ZHAT-COMZ*L)
        IF(ABS(S) .LT. BAR) SAT=(S/BAR)
```

```
        IF(S .LE. -BAR) SAT=-1.0
        IF(S .GE. BAR) SAT=1.0
        UHAT=-5.1429*QHAT + 1.0714*THAT
        UBAR=EITA*SAT
        DE=UHAT+UBAR
        IF (DE .GE. 0.4) DS=0.4
        IF (DE .LE. -0.4) DS=-0.4
        IF( (DE .LT. 0.4) .AND. (DE .GT. -0.4)) DS=DE
        DB=-DS*1.0
C
C       *********SLIDING MODE STEERING CONTROL************
C
C       *******PLANNER*********
C
C... DETERMINE REQUIRED POSITION
C
        CALL HEAD(L,XPOS,YPOS,XPOS1,YPOS1,ALPH,XLCASE,YLCASE)
C
C... DETERMINE IF XLCASE IS WITHIN L/2 DISTANCE OF D
C
        DAWAY=ABS(XLCASE-XT)
        IF ( DAWAY .LE. 2.0*L ) THEN
           WRITE(*,*) 'CURRENT POSITION IS ',XPOS/L,YPOS/L,ZPOS/L
           WRITE(*,*) 'SIMULATION TIME IS ',I
           XD1=XD2
           YD1=YD2
           READ (30,*) XD2,YD2,COMZ
           IF ((XD2 .EQ. 0.0) .AND.(YD2 .EQ. 0.0) .AND.
     $        (COMZ .EQ. 0.0)) GO TO 3
C
C... CONVERTS LOCAL COORDINATES INTO GLOBAL COORDINATES
C
           XPOS1=XD1
           YPOS1=YD1
           XPOS2=XD2
           YPOS2=YD2
C
C... DETERMINE THE NEW ANGLE ALPHA FOR THE NEW WAY POINT
C
           CALL ANGLE(XPOS1,YPOS1,XPOS2,YPOS2,ALPH)
           VC=VCOOBS*COS(ALPH)-UCOOBS*SIN(ALPH)
           UC=UCOOBS*COS(ALPH)-VCOOBS*SIN(ALPH)
C
C... CALCULATE THE LENGTH OF THE NEW PATH
C
           XT=SQRT((YPOS2-YPOS1)**2 + (XPOS2-XPOS1)**2)
           XT=XT*L
C
C... DETERMINE NEW XLCASE AND YLCASE FOR THE NEW WAY POINT
C
           CALL HEAD(L,XPOS,YPOS,XPOS1,YPOS1,ALPH,XLCASE,YLCASE)
           Z2=VC+S2*YLCASE
           Z3=UC+S3*XLCASE+U*COS(PSI-ALPH)
C
C... RESET YINTGR FOR NEXT WAY POINT
C
        YINTGR=0.0
        ENDIF
C
C       ******NAVIGATOR*******
```

```
        IF ((TIME-TNAV) .GE. NAVUPDATE ) THEN
        XA=XID
        YA=YID
        TNAV=TNAV+NAVUPDATE
        ENDIF
C
C       ****DESIRED SPEED***
C       UD IS SPECIFIED AND HELD CONSTANT
C
C       ********RPM INPUT CALCULATION *********
        SS1=U-UD
        IF(ABS(SS1) .LT. 1.0) SATSGN1=(SS1/1)
        IF(SS1 .LE. -1.0) SATSGN1=-1.0
        IF(SS1 .GE. 1.0) SATSGN1=1.0
        RPM=-1153.9*SATSGN1 + 83.33*U
         IF (RPM .GE. 500.0) RPM= 500.0
         IF (RPM .LE. -500.0) RPM=-500.0
C
C ************************CURRENT OBSERVER*******************************
C
          Z1DOT=S1*Z1+(S1*(A11+A22)/A21+(A12-A11*A22/A21)*U-
     $          S1*S1/(A21*U))*R+(B1*U-B2*(A11*U-S1)/A21)*U*DR
          Z2DOT=S2*Z1+S2*Z2+S2*U*SIN(PSI-ALPH)-S2*S2*YLCASE+
     $          (S2*(A11*U-S1)/(A21*U))*R
          Z3DOT=S3*Z3-S3*S3*XLCASE
          Z1=Z1+Z1DOT*DELT
          Z2=Z2+Z2DOT*DELT
          Z3=Z3+Z3DOT*DELT
          VHAT=Z1+R*(A11*U-S1)/(A21*U)
          VCOHAT=Z2-S2*YLCASE
          UCHAT=Z3-S3*XLCASE
          VCOOBS=VCOHAT
          UCOOBS=UCHAT-U*COS(PSI-ALPH)
C
C ***************************************************************************
C
C
C       *******RUDDER INPUT CALCULATION*******
C
        DANGLE=(PSI-ALPH)
        IF (DANGLE .GE. 6.2832) THEN
           DANGLE=DANGLE-6.2832
        ENDIF
        VC1=VCOOBS/U
        IF (VC1 .GE. 1.0) THEN
           VC1=1.0
        ELSEIF (VC1 .LE. -1.0) THEN
           VC1=-1.0
        ENDIF
        SS2=SP1*(DANGLE)+SP2*VHAT+SP3*R+SP4*YLCASE+
     &      ((SSPHI*GG1)/AKN + SP1)*ASIN(VC1)
C
         IF(ABS(SS2) .LT. SSPHI) SATSGN2=(SS2/SSPHI)
         IF(SS2 .LE. SSPHM) SATSGN2=-1.0
         IF(SS2 .GE. SSPHI) SATSGN2=1.0
C
        DR=AKN*SATSGN2+(GG1+(XI)*SP1)*(DANGLE)+(GG2+(XI)*SP2)*VHAT
     &     +(GG3+(XI)*SP3)*R+(XI)*SP4*YLCASE+GG5*YINTGR
C
         IF (DR .GE. 0.4) DR =  0.4
```

```
          IF (DR .LE. - 0.4) DR = -0.4
C
          TIME=TIME+DELT
C
        PHIANG = PHI/0.0174532925
        THEANG = THETA/0.0174532925
        PSIANG = PSI/0.0174532925
C
        ALPANG=ALPH/0.0174532925
C
        TRAC=-YPOS
        ROLL=PHIANG
        YAW=PSIANG
        DEPTH=-ZPOS
        PITCH=THEANG
        BOWANG=(DB/.01745)
        STNANG=(DS/.01745)
100     CONTINUE
  3     WRITE(*,*) 'NPTS =  ',NUMPTS
        WRITE(*,*) 'TIMEINTERVAL = ',DELT
        WRITE(*,*) 'NAVIGATOR  UPDATE TIME = ',NAVUPDATE
C       WRITE(*,*) 'TARGET RADIUS = ',TARGET
        STOP
        END
C
C     ***************DEPTH CONTROL OBSERVER*****************
          SUBROUTINE OBSER(QHADOT,THADOT,ZHADOT,QHAT,THAT,ZHAT,DELT,ZPOS,D
     ^S,U)
C
          QHADOT=-0.7*QHAT-0.03*THAT-0.035*DS-20.9293*(ZPOS-ZHAT)
          THADOT=QHAT-14.4092*(ZPOS-ZHAT)
          ZHADOT=-6*THAT+16.45*(ZPOS-ZHAT)
C
          QHAT= QHAT+DELT*QHADOT
          THAT= THAT+DELT*THADOT
          ZHAT= ZHAT+DELT*ZHADOT
          RETURN
          END
C
C.... SUBROUTINE FOR THE ANGLE ALPHA
C
          SUBROUTINE ANGLE(X1,Y1,X2,Y2,A)
          REAL X1,Y1,X2,Y2,A,DX,DY
          DX=X2-X1
          DY=Y2-Y1
          A=ATAN2(DY,DX)
          RETURN
          END
C
C.... SUBROUTINE FOR XLCASE AND YLCASE
C
          SUBROUTINE HEAD(L,XPOS,YPOS,XPOS1,YPOS1,ALPH,XLCASE,YLCASE)
          REAL XPOS,YPOS,XPOS1,YPOS1,ALPH,XLCASE,YLCASE,L
          YLCASE=((YPOS-YPOS1*L)*COS(ALPH))-((XPOS-XPOS1*L)*SIN(ALPH))
          XLCASE=((XPOS-XPOS1*L)*COS(ALPH))+((YPOS-YPOS1*L)*SIN(ALPH))
          RETURN
          END
C
C.... SUBROUTINE FOR DETERMINING THE REQUIRED POSITION
C
```

```
      SUBROUTINE POSREQ(TIME,UREQ,XREQ)
      REAL XREQ,UREQ,TIME
      XREQ=UREQ*TIME
      RETURN
      END
C
C... SUBROUTINE FOR NUMERICAL INTEGRATION USING THE TRAPEZOIDAL RULE
C
      SUBROUTINE TRAP(N,A,B,OUT)
      DIMENSION A(1),B(1)
      N1=N-1
      OUT=0.0
      DO 1 I=1,N1
         OUT1=0.5*(A(I)+A(I+1))*(B(I+1)-B(I))
         OUT=OUT+OUT1
 1    CONTINUE
      RETURN
      END
```

APPENDIX B

```
C ADDED CURRENT AS A DISTURBANCE IN THE CONTROL LAW
C ADDED CURRENT OBSERVER
C ADDED MONITORING OF SECOND LEG TO INITIATE TURN
C ****************************************************************
      REAL MASS,LATYAW,NORPIT
      REAL MM(6,6),G4(4),GK4(4),BR(9),HH(9)
      REAL  B(6,6),BB(6,6)
      REAL A(12,12), AA(12,12),INDX(100),XDES(100),YDES(100),ZDES(100)
      REAL XPP ,XQQ ,XRR ,XPR
      REAL XUDOT ,XWQ ,XVP ,XVR
      REAL XQDS ,XQDB ,XRDR  ,XVV
      REAL XWW  ,XVDR ,XWDS ,XWDB
      REAL XDSDS,XDBDB ,XDRDR ,XQDSN
      REAL XWDSN ,XDSDSN
      REAL TIME,S,EITA,UBAR,UHAT,COMZ,BAR,SIM,DE,SAT,VHAT,ZZOBS,ZZOBSDOT,SIM1
      REAL SS1,SS2,UD,XD,YD,TD,TNWP,XA,YA,HD,HDMDEG,DAWAY,SATSGN1,SATSGN2
      REAL NAVUPDATE,TNAV,TARGET,FF,GG,HHH,LLL,HDP,HDM,VCUR,UCUR,UCO,VCO,WCO
      REAL UCOOBS,VCOOBS,VCOHAT,UCHAT
      INTEGER DV
C
C     LATERAL HYDRODYNAMIC COEFFICIENTS
C
      REAL YPDOT ,YRDOT,YPQ  ,YQR
      REAL YVDOT ,YP   ,YR   ,YVQ
      REAL YWP  ,YWR ,YV ,YVW
      REAL YDR  ,CDY
C
C     NORMAL HYDRODYNAMIC COEFFICIENTS
C
      REAL ZQDOT ,ZPP,ZPR ,ZRR
      REAL ZWDOT ,ZQ  ,ZVP   ,ZVR
      REAL ZW  ,ZVV   ,ZDS  ,ZDB
      REAL ZQN ,ZWN  ,ZDSN ,CDZ
      REAL ZHADOT,ZHAT
C
C     ROLL HYDRODYNAMIC COEFFICIENTS
C
      REAL KPDOT ,KRDOT ,KPQ ,KQR
      REAL KVDOT , KP  ,KR    ,KVQ
      REAL KWP  , KWR   ,KV     ,KVW
      REAL KPN   , KDB
C
C     PITCH HYDRODYNAMIC COEFFICIENTS
C
      REAL MQDOT ,MPP  ,MPR,MRR
      REAL MWDOT , MQ  ,MVP    ,MVR
      REAL MW  , MVV   ,MDS  ,MDB
      REAL MQN , MWN  ,MDSN
      REAL QHADOT,QHAT,THADOT,THAT
C
C     YAW HYDRODYNAMIC COEFFICIENTS
C
      REAL NPDOT,NRDOT,NPQ ,NQR
      REAL NVDOT  , NP   ,NR     ,NVQ
      REAL NWP  , NWR  ,NV   ,NVW
      REAL NDR
C
C     MASS CHARACTERISTICS OF THE FLOODED VEHICLE
C
      REAL  WEIGHT , BOY  ,VOL ,XG
```

```
      REAL YG  , ZG  ,XB   ,ZB
      REAL IX  , IY  ,IZ    ,IXZ
      REAL IYZ  , IXY    ,YB
      REAL L  , RHO ,G    ,NU
      REAL A0   ,KPROP ,NPROP ,    X1TEST
      REAL DEGRUD  ,DEGSTN
      COMMON /BLOCK1/ F(12), FP(6), XMMINV(6,6), UCF
      INTEGER N,IA,IDGT,IER,LAST,J,K,M,JJ,KK,I
      REAL VECV1(9),VECV2(9),X(12),VECH1(9),VECH2(9),X1(9)
C
C     RUDDER COEFFICIENTS
C
      PARAMETER ( DSMAX= -0.175)
C
C     LONGITUDINAL HYDRODYNAMIC COEFFICIENTS
C
      PARAMETER(XPP = 7.E-3  ,XQQ = -1.5E-2 ,XRR = 4.E-3  ,XPR =7.5E-4,
     & XUDOT=-7.6E-3  ,XWQ = -2.E-1    ,XVP = -3.E-3   ,XVR = 2.E-2,
     & XQDS=2.5E-2    ,XQDB=-2.6E-3    ,XRDR= -1.E-3   ,XVV =5.3E-2,
     & XWW =1.7E-1    ,XVDR=1.7E-3     ,XWDS=4.6E-2    ,XWDB= 1.E-2,
     & XDSDS= -1.E-2  ,XDBDB= -8.E-3   ,XDRDR= -1.E-2  ,XQDSN= 2.E-3,
     & XWDSN=3.5E-3   ,XDSDSN= -1.6E-3 )
C
C     LATERAL HYDRODYNAMIC COEFFICIENTS
C
      PARAMETER(YPDOT=1.2E-4 ,YRDOT=1.2E-3  ,YPQ = 4.E-3 ,YQR =-6.5E-3,
     & YVDOT=-5.5E-2  ,YP  = 3.E-3     ,YR = 3.E-2     ,YVQ =2.4E-2,
     & YWP =2.3E-1    ,YWR =-1.9E-2    ,YV = -1.E-1    ,YVW =6.8E-2,
     & YDR =2.7E-2    ,CDY =3.5E-1)
C
C     NORMAL HYDRODYNAMIC COEFFICIENTS
C
      PARAMETER(ZQDOT=-6.8E-3 ,ZPP =1.3E-4  ,ZPR =6.7E-3  ,ZRR =-7.4E-3,
     & ZWDOT=-2.4E-1 ,ZQ =-1.4E-1     ,ZVP =-4.8E-2   ,ZVR =4.5E-2,
     & ZW =  -3.E-1   ,ZVV =-6.8E-2    ,ZDS =-7.3E-2   ,ZDB =-2.6E-2,
     & ZQN =-2.9E-3   ,ZWN =-5.1E-3    ,ZDSN= -1.E-2   ,CDZ = 1.0)
C
C     ROLL HYDRODYNAMIC COEFFICIENTS
C
      PARAMETER(KPDOT= -1.E-3 ,KRDOT=-3.4E-5 ,KPQ =-6.9E-5 ,KQR =1.7E-2,
     & KVDOT=1.3E-4   , KP =-1.1E-2    ,KR =-8.4E-4    ,KVQ=-5.1E-3,
     & KWP =-1.3E-4   , KWR =1.4E-2    ,KV =3.1E-3     ,KVW =-1.9E-1,
     & KPN =-5.7E-4   , KDB = 0.0 )
C
C     PITCH HYDRODYNAMIC COEFFICIENTS
C
      PARAMETER(MQDOT=-1.7E-2 ,MPP =5.3E-5  ,MPR = 5.E-3 ,MRR =-2.9E-3,
     & MWDOT=-6.8E-3  , MQ =-6.8E-2    ,MVP =1.2E-3    ,MVR =1.7E-2,
     & MW = 1.E-1     , MVV =-2.6E-2   ,MDS =-4.1E-2   ,MDB =6.9E-3,
     & MQN =-1.6E-3   , MWN =-2.9E-3   ,MDSN =-5.2E-3)
C
C     YAW HYDRODYNAMIC COEFFICIENTS
C
      PARAMETER(NPDOT=-3.4E-5 ,NRDOT=-3.4E-3,NPQ =-2.1E-2 ,NQR =2.7E-3,
     & NVDOT=1.2E-3   , NP =-8.4E-4    ,NR =-1.6E-2    ,NVQ = -1.E-2,
     & NWP =-1.7E-2   , NWR =7.4E-3    ,NV =-7.4E-3    ,NVW =-2.7E-2,
     & NDR =-1.3E-2)
C
C     MASS CHARACTERISTICS OF THE FLOODED VEHICLE
C
```

```
      PARAMETER( WEIGHT =12000., BOY =12000. ,VOL =200. ,XG = 0.   ,
     & YG = 0.0        , ZG = 0.20       ,XB = 0.         ,ZB =  0.0 ,
     & IX = 1500.      , IY = 10000.     ,IZ = 10000.     ,IXZ = -10. ,
     & IYZ = -10.      , IXY = -10.      ,YB =  0.0 ,
     & L = 17.4        , RHO = 1.94      ,G = 32.2        ,NU = 8.47E-4 ,
     & A0 = 2.0        ,KPROP = 0.       ,NPROP = 0. ,     X1TEST= 0.1 ,
     & DEGRUD= 0.0     ,DEGSTN=  0.0)
C
C     INPUT INITIAL CONDITIONS HERE IF REQUIRED
C
      OPEN(20,FILE='MODEL1.DAT',STATUS='NEW')
C
      NUMPTS=0.0
      DV=1.0
C
C*********************OBTAIN INITIAL INFORMATION*****************
C
        OPEN (30,FILE='INITIAL.DAT',STATUS='OLD')
        READ (30,*) U0,RPM
        READ (30,*) UD,NAVUPDATE,SIM1,DELT
C
C... READ IN STEERING AND SLIDING SURFACE GAINS,INITIAL CURRENTS,
C...     AND SATURATION DESIRED
C
      OPEN(21,FILE='SMCINT.DAT',STATUS='OLD')
      READ(21,*) GG1,GG2,GG3,GG4,GG5
      READ(21,*) SP1,SP2,SP3,SP4,SP5
      READ(21,*) UCO,VCO,WCO
      READ(21,*) AKN,SSPHI
      READ(21,*) IPTS
C
C... READ IN WAY POINTS
C
      IF (IPTS .GT. 100) IPTS=100
      DO 200 I=1,IPTS
         READ(30,*) XD,YD,ZD
         XDES(I)=XD*L
         YDES(I)=YD*L
         ZDES(I)=ZD*L
 200  CONTINUE
      PI=4.0*ATAN(1.0)
C
      UC=0.0
      VC=0.0
      UCOOBS=0.0
      VCOOBS=0.0
      V0 = 0.0
      W0 = 0.0
      P0 = 0.0
      Q0 = 0.0
      R0 = 0.0
      PHI0 = 0.0
      THETA0 = 0.0
      PSI0 = 0.0
      XPOS0=0.0
      YPOS0=0.0
      ZPOS0=0.0
      XD1=0.0
      YD1=0.0
      Z1=0.0
```

```
      Z19=0.0
      Z2=0.0
      Z29=0.0
      Z3=0.0
      Z39=0.0
      DB= 0.0
      DS = 0.0
      DR = 0.0
      LATYAW = 0.0
      NORPIT = 0.0
      RE = U0*L/NU
        TNAV=0
        XA=XPOS0
        YA=YPOS0
C
      TIME=0.0
      TIME0=0.0
      U = U0
      V = V0
      W = W0
      P = P0
      Q = Q0
      R = R0
      XPOS = XPOS0
      YPOS = YPOS0
      ZPOS = ZPOS0
      PSI = PHI0
      THETA = THETA0
      PHI = PHI0
        QHADOT=0.0
        THADOT=0.0
        ZHADOT=0.0
        QHAT=0.0
        THAT=0.0
        ZHAT=0.0
        VHAT=0.0
        ZOBSDOT=0.0
        ZZOBS = 0.0
C
C... DEFINE THE LENGTH X AND HEIGHT HH TERMS FOR THE DRAG INTEGRATION
C
      X1(1) = -105.9/12.
      X1(2) = -99.3/12.
      X1(3) = -87.3/12.
      X1(4) = -66.3/12.
      X1(5) = 72.7/12.
      X1(6) = 83.2/12.
      X1(7) = 91.2/12.
      X1(8) = 99.2/12.
      X1(9) = 103.2/12.
C
      HH(1) = 0.00/12.
      HH(2) = 8.24/12.
      HH(3) = 19.76/12.
      HH(4) = 29.36/12.
      HH(5) = 31.85/12.
      HH(6) = 27.84/12.
      HH(7) = 21.44/12.
      HH(8) = 12.00/12.
      HH(9) = 0.00/12.
```

```
C
C
      BR(1) =    0.00/12.0
      BR(2) =    8.24/12.0
      BR(3) =   19.76/12.0
      BR(4) =   29.36/12.0
      BR(5) =   31.85/12.0
      BR(6) =   27.84/12.0
      BR(7) =   21.44/12.0
      BR(8) =   12.00/12.0
      BR(9) =    0.00/12.0
C
      MASS = WEIGHT/G
C
      N = 6
      DO 15 J = 1,N
         DO 10 K = 1,N
         XMMINV(J,K) = 0.0
         MM(J,K) = 0.0
10       CONTINUE
15    CONTINUE
C
      MM(1,1) = MASS -((RHO/2)*(L**3)*XUDOT)
      MM(1,5) = MASS*ZG
      MM(1,6) = -MASS*YG
C
      MM(2,2) = MASS -((RHO/2)*(L**3)*YVDOT)
      MM(2,4) = -MASS*ZG -((RHO/2)*(L**4)*YPDOT)
      MM(2,6) = MASS*XG - ((RHO/2)*(L**4)*YRDOT)
C
      MM(3,3) = MASS - ((RHO/2)*(L**3)*ZWDOT)
      MM(3,4) = MASS*YG
      MM(3,5) = -MASS*XG -((RHO/2)*(L**4)*ZQDOT)
C
      MM(4,2) = -MASS*ZG - ((RHO/2)*(L**4)*KVDOT)
      MM(4,3) = MASS*YG
      MM(4,4) = IX - ((RHO/2)*(L**5)*KPDOT)
      MM(4,5) = -IXY
      MM(4,6) = -IXZ -((RHO/2)*(L**5)*KRDOT)
C
      MM(5,1) = MASS*ZG
      MM(5,3) = -MASS*XG -((RHO/2)*(L**4)*MWDOT)
      MM(5,4) = -IXY
      MM(5,5) = IY -((RHO/2)*(L**5)*MQDOT)
      MM(5,6) = -IYZ
C
      MM(6,1) = -MASS*YG
      MM(6,2) = MASS*XG -((RHO/2)*(L**4)*NVDOT)
      MM(6,4) = -IXZ - ((RHO/2)*(L**5)*NPDOT)
      MM(6,5) = -IYZ
      MM(6,6) = IZ - ((RHO/2)*(L**5)*NRDOT)
C
C  OBSERVER POLES
C
      S1=-1.0
      S2=-1.1
      S3=-1.2
C
C  OBSERVER A MATRIX CONSTANTS AND B MATRIX CONSTANTS
C
```

```
      A11=-0.04538
      A12=-0.35119
      A21=-0.002795
      A22=-0.09568
      B1 = 0.011432
      B2 =-0.004273
C
C       *****ROUTINE FOR INVERTING THE MM MATRIX*****
C
        DO 12 I=1,N
          DO 11 J=1,N
            XMMINV(I,J)=0.0
11        CONTINUE
          XMMINV(I,I)=1
12      CONTINUE
      CALL INVTA(MM,N,INDX,D)
        DO 13 J=1,N
      CALL INVTB(MM,N,INDX,XMMINV(1,J))
13      CONTINUE
C
C       ************        INPUTS          **************
C
C       RUDDER AND DIVE PLANE COMMANDS
C
        SIM=SIM1/DELT
        TIME=0.0
        DS= 0.0
        DR= 0.0
        DB= 0.0
        EITA=4.0
        BAR=.4
C
      YINTGR=0.0
      SSPHM=-SSPHI
C
      ISIM=SIM1/DELT
      ISTART=1
C
C       ********************SIMULATION BEGINS ****************
C
C  LOOP OVER WAY POINTS
C
      DO 210 IP=1,IPTS
         IF (IP .GE. 2) GO TO 211
         XD=XDES(1)
         YD=YDES(1)
         XD1=0.0
         YD1=0.0
         XD2=XD
         YD2=YD
         GO TO 212
 211    XD=XDES(IP)
        YD=YDES(IP)
        XD1=XD2
        YD1=YD2
        XD2=XD
        YD2=YD
 212    YD12=(YD2-YD1)
        XD12=(XD2-XD1)
      ALPH=ATAN(YD12/XD12)
```

```
      ALPH=ABS(ALPH)
      IF ((XD12 .GE. 0.0) .AND. (YD12 .GE. 0.0)) ALPH=   ALPH
      IF ((XD12 .GE. 0.0) .AND. (YD12 .LT. 0.0)) ALPH=  -ALPH
      IF ((XD12 .LT. 0.0) .AND. (YD12 .GE. 0.0)) ALPH=PI-ALPH
      IF ((XD12 .LT. 0.0) .AND. (YD12 .LT. 0.0)) ALPH=PI+ALPH
      VCHAT=VC*COS(ALPH)-UC*SIN(ALPH)
      UCHAT=VC*SIN(ALPH)+UC*COS(ALPH)
      YCTE=(YPOS-YD1)*COS(ALPH)-(XPOS-XD1)*SIN(ALPH)
      XCTE=(YPOS-YD1)*SIN(ALPH)+(XPOS-XD1)*COS(ALPH)
      Z2=VCHAT+S2*YCTE
      Z3=UCHAT+S3*XCTE+U*COS(PSI-ALPH)
    4 WRITE(*,101) XD/L,YD/L
      WRITE(*,102) XD12/L,YD12/L,ALPH*(180/PI),ISTART
  101 FORMAT(' HEADING FOR (X,Y) = (',F9.3,',',F9.3,')')
  102 FORMAT(' XD12= ',F8.3,' YD12= ',F8.3,' ALPH= ',F9.3,' ISTART= ',
     &       I6)
C
        DO 100 M=ISTART,ISIM
           ICOUNT=M
C
C     PROPULSION MODEL
C
      SIGNU = 1.0
      IF (U.LT.0.0) SIGNU = -1.0
      IF (ABS(U).LT.X1TEST) U = X1TEST
      SIGNN = 1.0
      IF (RPM.LT.0.0) SIGNN = -1.0
      ETA = 0.012*RPM/U
      RE = U*L/NU
      CD0 =  .00385 + (1.296E-17)*(RE - 1.2E7)**2
      CT  = ABS(0.008*L**2*ETA*ABS(ETA)/(A0))
      CT1 =ABS( 0.008*L**2/(A0))
      EPS = -1.0+SIGNN/SIGNU*(SQRT(CT+1.0)-1.0)/(SQRT(CT1+1.0)-1.0)
      XPROP = CD0*(ETA*ABS(ETA) - 1.0)
C
C... CALCULATE THE DRAG FORCE, INTEGRATE THE DRAG OVER THE VEHICLE
C
      DO 500 K=1,9
         UCF=(V+X(K)*R)**2+(W-X(K)*Q)**2
         UCF=SQRT(UCF)
         IF (UCF.LT.1.E-6) GO TO 601
         CFLOW   =CDY*HH(K)*(V+X(K)*R)**2+CDZ*BR(K)*(W-X(K)*Q)**2
         VECH1(K)=CFLOW*(V+X(K)*R)/UCF
         VECH2(K)=CFLOW*(V+X(K)*R)*X(K)/UCF
         VECV1(K)=CFLOW*(W-X(K)*Q)/UCF
         VECV2(K)=CFLOW*(W-X(K)*Q)*X(K)/UCF
  500 CONTINUE
       CALL TRAP(9,VECV1,X,HEAVE)
       CALL TRAP(9,VECV2,X,PITCH)
       CALL TRAP(9,VECH1,X,SWAY )
       CALL TRAP(9,VECH2,X,YAW  )
      SWAY=-0.5*RHO*SWAY
      YAW =-0.5*RHO*YAW
      HEAVE=-0.5*RHO*HEAVE
      PITCH=+0.5*RHO*PITCH
          GO TO 602
  601     HEAVE=0.0
          PITCH=0.0
          SWAY =0.0
          YAW  =0.0
```

```
  602     CONTINUE
C
C     FORCE EQUATIONS
C
C
C     LONGITUDINAL FORCE
C
      FP(1) = MASS*V*R - MASS*W*Q + MASS*XG*Q**2 + MASS*XG*R**2-
     &       MASS*YG*P*Q - MASS*ZG*P*R + (RHO/2)*L**4*(XPP*P**2 +
     &       XQQ*Q**2 + XRR*R**2 + XPR*P*R) +(RHO/2)*L**3*(XWQ*W*Q +
     &       XVP*V*P+XVR*V*R+U*Q*(XQDS*DS+XQDB*DB)+XRDR*U*R*DR)+
     &       (RHO/2)*L**2*(XVV*V**2 + XWW*W**2 + XVDR*U*V*DR + U*W*
     &       (XWDS*DS+XWDB*DB)+U**2*(XDSDS*DS**2+XDBDB*DB**2+
     &       XDRDR*DR**2))-(WEIGHT -BOY)*SIN(THETA) +(RHO/2)*L**3*
     &       XQDSN*U*Q*DS*EPS+(RHO/2)*L**2*(XWDSN*U*W*DS+XDSDSN*U**2*
     &       DS**2)*EPS +(RHO/2)*L**2*U**2*XPROP
C
C     LATERAL FORCE
C
      FP(2) = -MASS*U*R - MASS*XG*P*Q + MASS*YG*R**2 - MASS*ZG*Q*R +
     &       (RHO/2)*L**4*(YPQ*P*Q + YQR*Q*R)+(RHO/2)*L**3*(YP*U*P +
     &       YR*U*R + YVQ*V*Q + YWP*W*P + YWR*W*R) + (RHO/2)*L**2*
     &       (YV*U*V + YVW*V*W +YDR*U**2*DR) +SWAY +(WEIGHT-BOY)*
     &       COS(THETA)*SIN(PHI)+MASS*W*P+MASS*YG*P**2
C
C     NORMAL FORCE
C
      FP(3) = MASS*U*Q - MASS*V*P - MASS*XG*P*R - MASS*YG*Q*R +
     &       MASS*ZG*P**2 + MASS*ZG*Q**2 + (RHO/2)*L**4*(ZPP*P**2 +
     &       ZPR*P*R + ZRR*R**2) + (RHO/2)*L**3*(ZQ*U*Q + ZVP*V*P +
     &       ZVR*V*R) +(RHO/2)*L**2*(ZW*U*W + ZVV*V**2 + U**2*(ZDS*
     &       DS+ZDB*DB))+HEAVE+(WEIGHT-BOY)*COS(THETA)*COS(PHI)+
     &       (RHO/2)*L**3*ZQN*U*Q*EPS +(RHO/2)*L**2*(ZWN*U*W +ZDSN*
     &       U**2*DS)*EPS
C
C     ROLL FORCE
C
      FP(4) = -IZ*Q*R +IY*Q*R -IXY*P*R +IYZ*Q**2 -IYZ*R**2 +IXZ*P*Q +
     &       MASS*YG*U*Q -MASS*YG*V*P -MASS*ZG*W*P+(RHO/2)*L**5*(KPQ*
     &       P*Q + KQR*Q*R) +(RHO/2)*L**4*(KP*U*P +KR*U*R + KVQ*V*Q +
     &       KWP*W*P + KWR*W*R) +(RHO/2)*L**3*(KV*U*V + KVW*V*W) +
     &       (YG*WEIGHT - YB*BOY)*COS(THETA)*COS(PHI) - (ZG*WEIGHT -
     &       ZB*BOY)*COS(THETA)*SIN(PHI) + (RHO/2)*L**4*KPN*U*P*EPS+
     &       (RHO/2)*L**3*U**2*KPROP +MASS*ZG*U*R
C
C     PITCH FORCE
C
      FP(5) = -IX*P*R +IZ*P*R +IXY*Q*R -IYZ*P*Q -IXZ*P**2 +IXZ*R**2 -
     &       MASS*XG*U*Q + MASS*XG*V*P + MASS*ZG*V*R - MASS*ZG*W*Q +
     &       (RHO/2)*L**5*(MPP*P**2 +MPR*P*R +MRR*R**2)+(RHO/2)*L**4*
     &       (MQ*U*Q + MVP*V*P + MVR*V*R) + (RHO/2)*L**3*(MW*U*W +
     &       MVV*V**2+U**2*(MDS*DS+MDB*DB))+ PITCH -(XG*WEIGHT-
     &       XB*BOY)*COS(THETA)*COS(PHI)+(RHO/2)*L**4*MQN*U*Q*EPS +
     &       (RHO/2)*L**3*(MWN*U*W+MDSN*U**2*DS)*EPS-
     &       (ZG*WEIGHT-ZB*BOY)*SIN(THETA)
C
C     YAW FORCE
C
      FP(6) = -IY*P*Q +IX*P*Q +IXY*P**2 -IXY*Q**2 +IYZ*P*R -IXZ*Q*R -
     &       MASS*XG*U*R + MASS*XG*W*P - MASS*YG*V*R + MASS*YG*W*Q +
```

```
     &        (RHO/2)*L**5*(NPQ*P*Q + NQR*Q*R) +(RHO/2)*L**4*(NP*U*P+
     &        NR*U*R + NVQ*V*Q +NWP*W*P + NWR*W*R) +(RHO/2)*L**3*(NV*
     &        U*V + NVW*V*W + NDR*U**2*DR) + YAW + (XG*WEIGHT -
     &        XB*BOY)*COS(THETA)*SIN(PHI)+(YG*WEIGHT)*SIN(THETA)
     &        +(RHO/2)*L**3*U**2*NPROP-YB*BOY*SIN(THETA)
C
C
C    NOW COMPUTE THE F(1-6) FUNCTIONS
C
      DO 600 J = 1,6
             F(J) = 0.0
      DO 600 K = 1,6
             F(J) = XMMINV(J,K)*FP(K) + F(J)
600   CONTINUE
C
C    THE LAST SIX EQUATIONS COME FROM THE KINEMATIC RELATIONS
C
C     INERTIAL POSITION RATES F(7-9)
C
      F(7) = UCO + U*COS(PSI)*COS(THETA) + V*(COS(PSI)*SIN(THETA)*
     &        SIN(PHI) - SIN(PSI)*COS(PHI)) + W*(COS(PSI)*SIN(THETA)*
     &        COS(PHI) + SIN(PSI)*SIN(PHI))
C
      F(8) = VCO + U*SIN(PSI)*COS(THETA) + V*(SIN(PSI)*SIN(THETA)*
     &        SIN(PHI) + COS(PSI)*COS(PHI)) + W*(SIN(PSI)*SIN(THETA)*
     &        COS(PHI) - COS(PSI)*SIN(PHI))
C
      F(9) = WCO - U*SIN(THETA) +V*COS(THETA)*SIN(PHI) +W*COS(THETA)*
     &        COS(PHI)
C
C     EULER ANGLE RATES F(10-12)
C
      F(10) = P + Q*SIN(PHI)*TAN(THETA) + R*COS(PHI)*TAN(THETA)
C
      F(11) = Q*COS(PHI) - R*SIN(PHI)
C
      F(12) = Q*SIN(PHI)/COS(THETA) + R*COS(PHI)/COS(THETA)
C
C
      UDOT = F(1)
      VDOT = F(2)
      WDOT = F(3)
      PDOT = F(4)
      QDOT = F(5)
      RDOT = F(6)
      XDOT = F(7)
      YDOT = F(8)
      ZDOT = F(9)
      PHIDOT = F(10)
      THETAD = F(11)
      PSIDOT = F(12)
C
C     *******  CREATE OUTPUT DATA FILE ************************
C
      IF (M .EQ. DV ) THEN
      TIMER=FLOAT(M)/2.
C
      WRITE (20,*) M
C
      IF (DR .GT. 0.4) THEN
```

```
            DR = 0.4
          ELSEIF (DR .LT. -0.4) THEN
            DR = -0.4
          ENDIF
C
          WRITE (20,743)  DR/.01745
          WRITE (20,744)  XPOS/L,YPOS/L,XDES(IP)/L,YDES(IP)/L
          WRITE (20,746)  (PSI-ALPH)/.01745,YCTE/L
C
          IF (DR99 .GT. 0.4) THEN
            DR99 = 0.4
          ELSEIF (DR99 .LT. -0.4) THEN
            DR99 = -0.4
          ENDIF
C
          WRITE (20,744) YCTE99/L,DR99/0.01745,SS99,PROD
743       FORMAT (E11.3)
744       FORMAT (4E12.4)
746       FORMAT (2E12.4)
C
          NUMPTS=NUMPTS + 1
          DV=DV+1.0/DELT
          ENDIF
C
C*****
C         FIRST ORDER INTEGRATION
C
        U = U + DELT*UDOT
C                                       U = SURGE RATE
        V = V + DELT*VDOT
C                                       V = SWAY RATE
        W = W + DELT*WDOT
C                                       W = HEAVE RATE
        P = P + DELT*PDOT
C                                       P = ROLL RATE
        Q = Q + DELT*QDOT
C                                       Q = PITCH RATE
        R = R + DELT*RDOT
C                                       R = YAW RATE
        XPOS = XPOS + DELT*XDOT
C                                       X = SURGE
        YPOS = YPOS + DELT*YDOT
C                                       Y = SWAY
        ZPOS = ZPOS + DELT*ZDOT
C                                       Z = HEAVE
        PHI = PHI + DELT*PHIDOT
C                                       PHI = ROLL
        THETA = THETA + DELT*THETAD
C                                       THETA = PITCH
        PSI = PSI + DELT*PSIDOT
C                                       PSI = YAW
C
        YINTGR=YINTGR + DELT*YLCASE
C                 INTEGRAL OF LATERAL DEVIATION ERROR
C
C         *********SLIDING MODE DEPTH  CONTROL************
          CALL OBSER(QHADOT,THADOT,ZHADOT,QHAT,THAT,ZHAT,DELT,ZPOS,DS,UO)
C
          S=QHAT + 0.52*THAT - 0.0112*(ZHAT-COMZ*L)
          IF(ABS(S) .LT. BAR) SAT=(S/BAR)
```

```
        IF(S .LE. -BAR) SAT=-1.0
        IF(S .GE. BAR) SAT=1.0
        UHAT=-5.1429*QHAT + 1.0714*THAT
        UBAR=EITA*SAT
        DE=UHAT+UBAR
        IF (DE .GE. 0.4) DS=0.4
        IF (DE .LE. -0.4) DS=-0.4
        IF( (DE .LT. 0.4) .AND. (DE .GT. -0.4)) DS=DE
        DB=-DS*1.0
C
C       *********SLIDING MODE STEERING CONTROL************
C
C       *******PLANNER*********
C
C... DETERMINE REQUIRED POSITION
C
        YCTE=(YPOS-YD1)*COS(ALPH)-(XPOS-XD1)*SIN(ALPH)
        XCTE=(YPOS-YD1)*SIN(ALPH)+(XPOS-XD1)*COS(ALPH)
C
C... DETERMINE IF XLCASE IS WITHIN L/2 DISTANCE OF D
C
        XT=SQRT((XD2-XD1)**2 + (YD2-YD1)**2)
        XAWAY=(XT-XCTE)
        DAWAY=ABS(XAWAY)
C
C ************************CURRENT OBSERVER*******************************
C
          Z1DOT=S1*Z1+(S1*(A11+A22)/A21+(A12-A11*A22/A21)*U-
     $          S1*S1/(A21*U))*R+(B1*U-B2*(A11*U-S1)/A21)*U*DR
          Z2DOT=S2*Z1+S2*Z2+S2*U*SIN(PSI-ALPH)-S2*S2*YCTE+
     $          (S2*(A11*U-S1)/(A21*U))*R
          Z3DOT=S3*Z3-S3*S3*XCTE
          Z1=Z1+Z1DOT*DELT
          Z2=Z2+Z2DOT*DELT
          Z3=Z3+Z3DOT*DELT
          VHAT=Z1+R*(A11*U-S1)/(A21*U)
          VCHAT=Z2-S2*YCTE
          UCHAT=Z3-S3*XCTE
          VCOOBS=VCHAT
          UCOOBS=UCHAT-U*COS(PSI-ALPH)
C
          VC=UCOOBS*SIN(ALPH)+VCOOBS*COS(ALPH)
          UC=UCOOBS*COS(ALPH)-VCOOBS*SIN(ALPH)
C
      IF (IP .LT. IPTS) GO TO 250
      IF (DAWAY .LT. 0.1) GO TO 201
      GO TO 230
C
C  MONITOR CONTROL LAW FOR NEXT SEGMENT
C
 250  YN12=YDES(IP+1)-YDES(IP)
      XN12=XDES(IP+1)-XDES(IP)
      BETA=ATAN(YN12/XN12)
      BETA=ABS(BETA)
      IF ((XN12 .GE. 0.0) .AND. (YN12 .GE. 0.0)) BETA=   BETA
      IF ((XN12 .GE. 0.0) .AND. (YN12 .LT. 0.0)) BETA=  -BETA
      IF ((XN12 .LT. 0.0) .AND. (YN12 .GE. 0.0)) BETA=PI-BETA
      IF ((XN12 .LT. 0.0) .AND. (YN12 .LT. 0.0)) BETA=PI+BETA
C
C... CURRENT OBSERVER FOR NEXT PATH
```

```
C
      YCTE99=(YPOS-YDES(IP))*COS(BETA)-(XPOS-XDES(IP))*SIN(BETA)
      VC99=VC*COS(BETA)-UC*SIN(BETA)
      VC2=VC99/U
      IF (VC2 .GE. 1.0) THEN
          VC2=1.0
      ELSEIF (VC2 .LE. -1.0) THEN
          VC2=-1.0
      ENDIF
C
      SS99=SP1*(PSI-BETA)+SP2*VHAT+SP3*R+SP4*YCTE99+
     ?     ((SSPHI*GG1)/AKN+SP1)*ASIN(VC2)
      IF (ABS(SS99) .LT. SSPHI) SPHI99=SS99/SSPHI
      IF (SS99 .LE. SSPHM) SPHI99=-1.0
      IF (SS99 .GE. SSPHI) SPHI99= 1.0
      DR98=GG1*(PSI-BETA)+GG2*VHAT+GG3*R+GG4*YCTE99
      DR97=AKN*SPHI99
      DR99=DR97+DR98
      IF (DR99 .GE. 0.4) DR99=0.4
      IF (DR99 .LE. -0.4) DR99=-0.4
      DRNEW=DR99
C
      IF (M .EQ. 1) GO TO 230
      PROD=DROLD*DRNEW
C
      IF (XAWAY .LE. 0.0) GO TO 201
      IF (XAWAY .GT. (0.5*XT)) GO TO 230
      IF (PROD .LE. 0.0) GO TO 201
C
 230  DROLD=DRNEW
C
C       ******NAVIGATOR*******
C
        IF ((TIME-TNAV) .GE. NAVUPDATE ) THEN
        XA=XID
        YA=YID
        TNAV=TNAV+NAVUPDATE
        ENDIF
C
C       ****HEADING*********
C
C       ****DESIRED SPEED***
C       UD IS SPECIFIED AND HELD CONSTANT
C
C       ********RPM INPUT CALCULATION *********
        SS1=U-UD
        IF(ABS(SS1) .LT. 1.0) SATSGN1=(SS1/SSPHI)
        IF(SS1 .LE. SSPHM) SATSGN1=-1.0
        IF(SS1 .GE. SSPHI) SATSGN1= 1.0
        RPM=-1153.9*SATSGN1 + 83.33*U
         IF (RPM .GE. 500.0) RPM= 500.0
         IF (RPM .LE. -500.0) RPM=-500.0
C
C       *******RUDDER INPUT CALCULATION*******
C
C       ************BEGIN SMC CALCULATIONS **********************
C
        DANGLE=(PSI-ALPH)
        VC1=VCOOBS/U
        IF (VC1 .GE. 1.0) THEN
```

```
            VC1=1.0
          ELSEIF (VC1 .LE. -1.0) THEN
            VC1=-1.0
          ENDIF
C
          SS2=SP1*(DANGLE)+SP2*VHAT+SP3*R+SP4*YCTE+
     &        ((SSPHI*GG1)/AKN + SP1)*ASIN(VC1)
C
           IF(ABS(SS2) .LT. SSPHI) SATSGN2=(SS2/SSPHI)
           IF(SS2 .LE. SSPHM) SATSGN2=-1.0
           IF(SS2 .GE. SSPHI) SATSGN2=1.0
C
          DR=AKN*SATSGN2+GG1*(DANGLE)+GG2*VHAT+GG3*R+GG4*YCTE+GG5*YINTGR
C
           IF (DR .GE. 0.4) DR =  0.4
           IF (DR .LE. - 0.4) DR = -0.4
C
          TIME=TIME+DELT
C
        PHIANG = PHI/0.0174532925
        THEANG = THETA/0.0174532925
        PSIANG = PSI/0.0174532925
C
        ALPANG=ALPH/0.0174532925
C
        TRAC=-YPOS
        ROLL=PHIANG
        YAW=PSIANG
        DEPTH=-ZPOS
        PITCH=THEANG
        BOWANG=(DB/.01745)
        STNANG=(DS/.01745)
100     CONTINUE
        GO TO 300
 201    ISTART=ICOUNT
        WRITE(*,103) YCTE99
 103    FORMAT(' YCTE99= ',F9.3)
        WRITE(*,104) SS99
 104    FORMAT(' SS99= ',F9.3)
        WRITE(*,105) DR99
 105    FORMAT(' DR99= ',F9.3)
        WRITE(*,106) DRNEW
 106    FORMAT(' DRNEW= ',F9.3)
        WRITE(*,107) DROLD
 107    FORMAT(' DROLD= ',F9.3)
        WRITE(*,108) PROD
 108    FORMAT(' PROD= ',F9.3)
 210    CONTINUE
C 400   CONTINUE
  300   WRITE(*,*) 'NPTS =  ',NUMPTS
        WRITE(*,*) 'TIMEINTERVAL = ',DELT
        WRITE(*,*) 'NAVIGATOR  UPDATE TIME = ',NAVUPDATE
C       WRITE(*,*) 'TARGET RADIUS = ',TARGET
        STOP
        END
C
C     ***************DEPTH CONTROL OBSERVER*****************
        SUBROUTINE OBSER(QHADOT,THADOT,ZHADOT,QHAT,THAT,ZHAT,DELT,ZPOS,D
     ^S,U)
C
```

```
      QHADOT=-0.7*QHAT-0.03*THAT-0.035*DS-20.9293*(ZPOS-ZHAT)
      THADOT=QHAT-14.4092*(ZPOS-ZHAT)
      ZHADOT=-6*THAT+16.45*(ZPOS-ZHAT)
C
      QHAT= QHAT+DELT*QHADOT
      THAT= THAT+DELT*THADOT
      ZHAT= ZHAT+DELT*ZHADOT
      RETURN
      END
C
C... SUBROUTINE FOR THE ANGLE ALPHA
C
      SUBROUTINE ANGLE(X1,Y1,X2,Y2,A)
      REAL X1,Y1,X2,Y2,A,DX,DY
      DX=X2-X1
      DY=Y2-Y1
      A=ATAN2(DY,DX)
      RETURN
      END
C
C... SUBROUTINE FOR XLCASE AND YLCASE
C
      SUBROUTINE HEAD(L,XPOS,YPOS,XPOS1,YPOS1,ALPH,XLCASE,YLCASE)
      REAL XPOS,YPOS,XPOS1,YPOS1,ALPH,XLCASE,YLCASE,L
      YLCASE=((YPOS-YPOS1*L)*COS(ALPH))-((XPOS-XPOS1*L)*SIN(ALPH))
      XLCASE=((XPOS-XPOS1*L)*COS(ALPH))+((YPOS-YPOS1*L)*SIN(ALPH))
      RETURN
      END
C
C... SUBROUTINE FOR NUMERICAL INTEGRATION USING THE TRAPEZOIDAL RULE
C
      SUBROUTINE TRAP(N,A,B,OUT)
      DIMENSION A(1),B(1)
      N1=N-1
      OUT=0.0
      DO 1 I=1,N1
         OUT1=0.5*(A(I)+A(I+1))*(B(I+1)-B(I))
         OUT=OUT+OUT1
1     CONTINUE
      RETURN
      END
```

LIST OF REFERENCES

1. Jacobsen, M., "The US Navy and Remotely Operated Vehicles, 1962-1966", ASME Paper No. 86-WA/HH-2, 1986 ASME Winter Annual Meeting, CA, December 7-12, 1986.

2. Boncal, R.J., "A Study of Model Based Maneuvering Controls for Autonomous Underwater Vehicles", M.S. Thesis, Naval Postgraduate School, Monterey, CA, December, 1987.

3. Brunner, G., "Experimental Verification of AUV Performances", M.E. Thesis, Naval Postgraduate School, Monerey, CA, March 1988.

4. Goheen, K.R., Jeffreys, E.R., Broome, D.R., "Robust Self Desiging Controllers for Underwater Vehicles", Trans. ASME Journal of Offshore Mechanics and Arctic Engineering, Vol. 109, May 1987, pp. 170-178.

5. Blidberg, D.R., Chappel, S.G., "Guidance and Control Architecture for the EAVE Vehicle", IEEE Journal of Oceanic Engineering, Vol. OE-11 No. 4, October 1986, pp. 447-467.

6. Abkowitz, M.A., "Stability and Motion Control of Oceacn Vehicles", M.I.T. Press, 1969.

7. Lindgren, A.G., Cretella, D.B., Bessacini, A.F., "Dynamics and Control of Submerged Vehicles", Trans. Instrument Society of America, Vol. 6, Issue 4, December 1967, pp. 335-346.

8. Humphries, D., "Dynamics and Hydrodynamics of Ocean Vehicles", IEEE OCEANS '81 Conference Proceedings, Vol. 1, 1981, pp. 88-91.

9. Gertler, M., Hagen, G.R., "Standard Equations of Motion for Submarine Simulations", NSRDC Report No. 2510, 1967.

10. Smith, N.S., Crane, J.W., Summey, D.C., "SDV Simulator Hydrodynamic Coefficients", NCSC Report No. TM-231-78, June 1978.

11. Yoerger, D., Slotine, J.J.E., "Robust Tracking Control of Underwater Vehicles", IEEE Journal of Oceanic Systems, OE-10, n 4, October 1985, pp. 462-470.

12. Lienard, D.E., "Autopilot Design for Autonomous Underwater Vehicles Based on Sliding Mode Control", M.E. Thesis, Naval Postgraduate School, Monterey, CA, June 1990.

13. Papoulias, F.A., Christi, R., Marco, D., Healey, A.J., "Modeling, Sliding Mode, Control Design, and Visual Simulation of AUV Dive Plane Dynamics Response", Proceeding, Sixth International Symposium on Unmanned Untethered Submersible Technology, Washington D.C., June 1989.

14. Dorling, C.M., Zinober, A.S., "Two Approaches to Hyperplane Design in Multivariable Variable Structure Control Systems", Int. J. Control, 1986, Vol. 44, No. 1, pp. 65-82.

15. Utkin, V.I., Yang, K.D., "Methods for Constructing Discontinuity Planes in Multidimensional Variable Structure Systems", Automation and Remote Control, Vol. 39, No. 10, Part 1, October 1978, pp. 1466-1470.

16. Koyama, T., Shimizu, K., "Fundamentals of Automatic Harbour Manoeuvering", Proceedings, Seventh Ship Control Systems Symposium, Bath, U.K., 1984.

INITIAL DISTRIBUTION LIST

1.	Defense Technical Information Center Cameron Station Alexandria, VA 22304-6145	2
2.	Library, Code 52 Naval Postgraduate School Monterey, CA 93940-5002	2
3.	Chairman, Code MEHy Department of Mechanical Engineering Naval Postgraduate School Monterey, CA 93940-5000	1
4.	Dr. G. Dobeck, Code 4210 Naval Coastal Systems Command Panama City, FL 32407-5000	1
5.	Dr. Richard Nadolink Head, Weapon Technology Division Chair in Hydrodynamics Naval Underwater Systems Center Newport, RI 02841-5047	1
6.	RADM Evans, Code SEA-92 Naval Sea Systems Command Washington, DC 20362	1
7.	Dan Steiger Marine Systems Group Naval Research Laboratory Washington, DC 20032	1
8.	Technical Library Branch, Code E23 Naval Surface Warfare Center Silver Spring, MD 20903-5000	1

9. Naval Engineering Curricular Office, Code 34 — 1
Naval Postgraduate School
Monterey, CA 93943-5000

10. Dr. Dana Yoerger — 1
Woods Hole Oceanographic Institute
Woods Hole, MA 02543

11. LT Steven R. Chism — 1
Supervisor of Shipbuilding,
Conversion and Repair, USN
Groton, CT 06340-4990

12. Professor F. A. Papoulias, Code MEPa — 1
Department of Mechanical Engineering
Naval Postgraduate School
Monterey, CA 93943-5000

13. Professor R. Christi, Code 62Cx — 1
Department of Electrical & Computer Engineering
Naval Postgraduate School
Monterey, CA 93943-5000